

# 10. ELECTROWEAK MODEL AND CONSTRAINTS ON NEW PHYSICS

Revised November 2013 by J. Erler (U. Mexico) and A. Freitas (Pittsburgh U.).

- 10.1 Introduction
- 10.2 Renormalization and radiative corrections
- 10.3 Low energy electroweak observables
- 10.4  $W$  and  $Z$  boson physics
- 10.5 Precision flavor physics
- 10.6 Experimental results
- 10.7 Constraints on new physics

## 10.1. Introduction

The standard model of the electroweak interactions (SM) [1] is based on the gauge group  $SU(2) \times U(1)$ , with gauge bosons  $W_\mu^i$ ,  $i = 1, 2, 3$ , and  $B_\mu$  for the  $SU(2)$  and  $U(1)$  factors, respectively, and the corresponding gauge coupling constants  $g$  and  $g'$ . The left-handed fermion fields of the  $i^{\text{th}}$  fermion family transform as doublets  $\Psi_i = \begin{pmatrix} \nu_i \\ \ell_i^- \end{pmatrix}$  and  $\begin{pmatrix} u_i \\ d_i \end{pmatrix}$  under  $SU(2)$ , where  $d_i' \equiv \sum_j V_{ij} d_j$ , and  $V$  is the Cabibbo-Kobayashi-Maskawa mixing matrix. [Constraints on  $V$  and tests of universality are discussed in Ref. 2 and in the Section on “The CKM Quark-Mixing Matrix”. The extension of the formalism to allow an analogous leptonic mixing matrix is discussed in the Section on “Neutrino Mass, Mixing, and Oscillations”.] The right-handed fields are  $SU(2)$  singlets. In the minimal model there are three fermion families.

A complex scalar Higgs doublet,  $\phi \equiv \begin{pmatrix} \phi^+ \\ \phi^0 \end{pmatrix}$ , is added to the model for mass generation through spontaneous symmetry breaking with potential\* given by,

$$V(\phi) = \mu^2 \phi^\dagger \phi + \frac{\lambda^2}{2} (\phi^\dagger \phi)^2. \quad (10.1)$$

For  $\mu^2$  negative,  $\phi$  develops a vacuum expectation value,  $v/\sqrt{2} = \mu/\lambda$ , where  $v \approx 246$  GeV, breaking part of the electroweak (EW) gauge symmetry, after which only one neutral Higgs scalar,  $H$ , remains in the physical particle spectrum. In non-minimal models there are additional charged and neutral scalar Higgs particles [3].

After the symmetry breaking the Lagrangian for the fermion fields,  $\psi_i$ , is

$$\mathcal{L}_F = \sum_i \bar{\psi}_i \left( i \not{\partial} - m_i - \frac{m_i H}{v} \right) \psi_i$$

---

\* There is no generally accepted convention to write the quartic term. Our numerical coefficient simplifies Eq. (10.3a) below and the squared coupling preserves the relation between the number of external legs and the power counting of couplings at a given loop order. This structure also naturally emerges from physics beyond the SM, such as supersymmetry.

## 2 10. Electroweak model and constraints on new physics

$$\begin{aligned}
& - \frac{g}{2\sqrt{2}} \sum_i \bar{\Psi}_i \gamma^\mu (1 - \gamma^5) (T^+ W_\mu^+ + T^- W_\mu^-) \Psi_i \\
& - e \sum_i Q_i \bar{\psi}_i \gamma^\mu \psi_i A_\mu \\
& - \frac{g}{2 \cos \theta_W} \sum_i \bar{\psi}_i \gamma^\mu (g_V^i - g_A^i \gamma^5) \psi_i Z_\mu .
\end{aligned} \tag{10.2}$$

Here  $\theta_W \equiv \tan^{-1}(g'/g)$  is the weak angle;  $e = g \sin \theta_W$  is the positron electric charge; and  $A \equiv B \cos \theta_W + W^3 \sin \theta_W$  is the photon field ( $\gamma$ ).  $W^\pm \equiv (W^1 \mp iW^2)/\sqrt{2}$  and  $Z \equiv -B \sin \theta_W + W^3 \cos \theta_W$  are the charged and neutral weak boson fields, respectively. The Yukawa coupling of  $H$  to  $\psi_i$  in the first term in  $\mathcal{L}_F$ , which is flavor diagonal in the minimal model, is  $gm_i/2M_W$ . The boson masses in the EW sector are given (at tree level, *i.e.*, to lowest order in perturbation theory) by,

$$M_H = \lambda v, \tag{10.3a}$$

$$M_W = \frac{1}{2} g v = \frac{e v}{2 \sin \theta_W}, \tag{10.3b}$$

$$M_Z = \frac{1}{2} \sqrt{g^2 + g'^2} v = \frac{e v}{2 \sin \theta_W \cos \theta_W} = \frac{M_W}{\cos \theta_W}, \tag{10.3c}$$

$$M_\gamma = 0. \tag{10.3d}$$

The second term in  $\mathcal{L}_F$  represents the charged-current weak interaction [4–7], where  $T^+$  and  $T^-$  are the weak isospin raising and lowering operators. For example, the coupling of a  $W$  to an electron and a neutrino is

$$- \frac{e}{2\sqrt{2} \sin \theta_W} \left[ W_\mu^- \bar{e} \gamma^\mu (1 - \gamma^5) \nu + W_\mu^+ \bar{\nu} \gamma^\mu (1 - \gamma^5) e \right]. \tag{10.4}$$

For momenta small compared to  $M_W$ , this term gives rise to the effective four-fermion interaction with the Fermi constant given by  $G_F/\sqrt{2} = 1/2v^2 = g^2/8M_W^2$ .  $CP$  violation is incorporated into the EW model by a single observable phase in  $V_{ij}$ .

The third term in  $\mathcal{L}_F$  describes electromagnetic interactions (QED) [8–10], and the last is the weak neutral-current interaction [5–7]. The vector and axial-vector couplings are

$$g_V^i \equiv t_{3L}(i) - 2Q_i \sin^2 \theta_W, \tag{10.5a}$$

$$g_A^i \equiv t_{3L}(i), \tag{10.5b}$$

where  $t_{3L}(i)$  is the weak isospin of fermion  $i$  ( $+1/2$  for  $u_i$  and  $\nu_i$ ;  $-1/2$  for  $d_i$  and  $e_i$ ) and  $Q_i$  is the charge of  $\psi_i$  in units of  $e$ .

The first term in Eq. (10.2) also gives rise to fermion masses, and in the presence of right-handed neutrinos to Dirac neutrino masses. The possibility of Majorana masses is discussed in the Section on “Neutrino Mass, Mixing, and Oscillations”.

## 10.2. Renormalization and radiative corrections

In addition to the Higgs boson mass,  $M_H$ , the fermion masses and mixings, and the strong coupling constant,  $\alpha_s$ , the SM has three parameters. The set with the smallest experimental errors contains the  $Z$  mass\*\*, the Fermi constant, and the fine structure constant, which will be discussed in turn (if not stated otherwise, the numerical values quoted in Sec. 10.2–10.5 correspond to the main fit result in Table 10.6):

The  $Z$  boson mass,  $M_Z = 91.1876 \pm 0.0021$  GeV, has been determined from the  $Z$  lineshape scan at LEP 1 [11].

The Fermi constant,  $G_F = 1.1663787(6) \times 10^{-5}$  GeV<sup>-2</sup>, is derived from the muon lifetime formula\*\*\*,

$$\frac{\hbar}{\tau_\mu} = \frac{G_F^2 m_\mu^5}{192\pi^3} F(\rho) \left[ 1 + H_1(\rho) \frac{\hat{\alpha}(m_\mu)}{\pi} + H_2(\rho) \frac{\hat{\alpha}^2(m_\mu)}{\pi^2} \right], \quad (10.6)$$

where  $\rho = m_e^2/m_\mu^2$ , and where

$$F(\rho) = 1 - 8\rho + 8\rho^3 - \rho^4 - 12\rho^2 \ln \rho = 0.99981295, \quad (10.7a)$$

$$H_1(\rho) = \frac{25}{8} - \frac{\pi^2}{2} - \left( 9 + 4\pi^2 + 12 \ln \rho \right) \rho + 16\pi^2 \rho^{3/2} + \mathcal{O}(\rho^2) = -1.80793, \quad (10.7b)$$

$$H_2(\rho) = \frac{156815}{5184} - \frac{518}{81} \pi^2 - \frac{895}{36} \zeta(3) + \frac{67}{720} \pi^4 + \frac{53}{6} \pi^2 \ln 2 - (0.042 \pm 0.002)_{\text{had}} - \frac{5}{4} \pi^2 \sqrt{\rho} + \mathcal{O}(\rho) = 6.64, \quad (10.7c)$$

$$\hat{\alpha}(m_\mu)^{-1} = \alpha^{-1} + \frac{1}{3\pi} \ln \rho + \mathcal{O}(\alpha) = 135.901 \quad (10.7d)$$

$H_1$  and  $H_2$  capture the QED corrections within the Fermi model. The results for  $\rho = 0$  have been obtained in Refs. 13 and 14, respectively, where the term in parentheses is from the hadronic vacuum polarization [14]. The mass corrections to  $H_1$  have been known for some time [15], while those to  $H_2$  are more recent [16]. Notice the term linear in  $m_e$  whose appearance was unforeseen and can be traced to the use of the muon pole mass in the prefactor [16]. The remaining uncertainty in  $G_F$  is experimental and has recently been reduced by an order of magnitude by the MuLan collaboration [12] at the PSI.

---

\*\* We emphasize that in the fits described in Sec. 10.6 and Sec. 10.7 the values of the SM parameters are affected by all observables that depend on them. This is of no practical consequence for  $\alpha$  and  $G_F$ , however, since they are very precisely known.

\*\*\* In the spirit of the Fermi theory, we incorporated the small propagator correction,  $3/5 m_\mu^2/M_W^2$ , into  $\Delta r$  (see below). This is also the convention adopted by the MuLan collaboration [12]. While this breaks with historical consistency, the numerical difference was negligible in the past.

## 4 10. Electroweak model and constraints on new physics

The experimental determination of the fine structure constant,  $\alpha = 1/137.035999074(44)$ , is currently dominated by the  $e^\pm$  anomalous magnetic moment [10]. In most EW renormalization schemes, it is convenient to define a running  $\alpha$  dependent on the energy scale of the process, with  $\alpha^{-1} \sim 137$  appropriate at very low energy, *i.e.* close to the Thomson limit. (The running has also been observed [17] directly.) For scales above a few hundred MeV this introduces an uncertainty due to the low energy hadronic contribution to vacuum polarization. In the modified minimal subtraction ( $\overline{\text{MS}}$ ) scheme [18] (used for this *Review*), and with  $\alpha_s(M_Z) = 0.1193 \pm 0.0016$  we have  $\widehat{\alpha}(m_\tau)^{-1} = 133.465 \pm 0.013$  and  $\widehat{\alpha}(M_Z)^{-1} = 127.940 \pm 0.014$ . (In this Section we denote quantities defined in the modified minimal subtraction ( $\overline{\text{MS}}$ ) scheme by a caret; the exception is the strong coupling constant,  $\alpha_s$ , which will always correspond to the  $\overline{\text{MS}}$  definition and where the caret will be dropped.) The latter corresponds to a quark sector contribution (without the top) to the conventional (on-shell) QED coupling,  $\alpha(M_Z) = \frac{\alpha}{1 - \Delta\alpha(M_Z)}$ , of  $\Delta\alpha_{\text{had}}^{(5)}(M_Z) = 0.02771 \pm 0.00011$ . These values are updated from Ref. 19 with  $\Delta\alpha_{\text{had}}^{(5)}(M_Z)$  moved downwards and its uncertainty halved (partly due to a more precise charm quark mass). Its correlation with the  $\mu^\pm$  anomalous magnetic moment (see Sec. 10.5), as well as the non-linear  $\alpha_s$  dependence of  $\widehat{\alpha}(M_Z)$  and the resulting correlation with the input variable  $\alpha_s$ , are fully taken into account in the fits. This is done by using as actual input (fit constraint) instead of  $\Delta\alpha_{\text{had}}^{(5)}(M_Z)$  the analogous low energy contribution by the three light quarks,  $\Delta\alpha_{\text{had}}^{(3)}(1.8 \text{ GeV}) = (55.50 \pm 0.78) \times 10^{-4}$  [20], and by calculating the perturbative and heavy quark contributions to  $\widehat{\alpha}(M_Z)$  in each call of the fits according to Ref. 19. Part of the uncertainty ( $\pm 0.49 \times 10^{-4}$ ) is from  $e^+e^-$  annihilation data below 1.8 GeV and  $\tau$  decay data (including uncertainties from isospin breaking effects), but uncalculated higher order perturbative ( $\pm 0.41 \times 10^{-4}$ ) and non-perturbative ( $\pm 0.44 \times 10^{-4}$ ) QCD corrections and the  $\overline{\text{MS}}$  quark mass values (see below) also contribute. Various evaluations of  $\Delta\alpha_{\text{had}}^{(5)}$  are summarized in Table 10.1 where the relation<sup>†</sup> between the  $\overline{\text{MS}}$  and on-shell definitions is given by [22]

$$\begin{aligned} \Delta\widehat{\alpha}(M_Z) - \Delta\alpha(M_Z) &= \frac{\alpha}{\pi} \left[ \left( \frac{100}{27} - \frac{1}{6} - \frac{7}{4} \ln \frac{M_Z^2}{M_W^2} \right) + \frac{\alpha_s(M_Z)}{\pi} \left( \frac{605}{108} - \frac{44}{9} \zeta(3) \right) \right. \\ &\quad \left. + \frac{\alpha_s^2(M_Z)}{\pi^2} \left( \frac{976481}{23328} - \frac{781}{18} \zeta(3) + \frac{275}{27} \zeta(5) \right) \right] = 0.007165, \end{aligned} \quad (10.8)$$

and where the first entry of the lowest order term is from fermions and the other two are from  $W^\pm$  loops, which are usually excluded from the on-shell definition. The most recent results typically assume the validity of perturbative QCD (PQCD) at scales of 1.8 GeV and above, and are in reasonable agreement with each other. There is, however,

---

<sup>†</sup> In practice,  $\alpha(M_Z)$  is directly evaluated in the  $\overline{\text{MS}}$  scheme using the FORTRAN package GAPP [21], including the QED contributions of both leptons and quarks. The leptonic three-loop contribution in the on-shell scheme has been obtained in Ref. 23.

**Table 10.1:** Evaluations of the on-shell  $\Delta\alpha_{\text{had}}^{(5)}(M_Z)$  by different groups (for a more complete list of evaluations see the 2012 edition of this *Review*). For better comparison we adjusted central values and errors to correspond to a common and fixed value of  $\alpha_s(M_Z) = 0.120$ . References quoting results without the top quark decoupled are converted to the five flavor definition. Ref. [28] uses  $\Lambda_{\text{QCD}} = 380 \pm 60$  MeV; for the conversion we assumed  $\alpha_s(M_Z) = 0.118 \pm 0.003$ .

Reference	Result	Comment
Geshkenbein, Morgunov [24]	$0.02780 \pm 0.00006$	$\mathcal{O}(\alpha_s)$ resonance model
Swartz [25]	$0.02754 \pm 0.00046$	use of fitting function
Krasnikov, Rodenberg [26]	$0.02737 \pm 0.00039$	PQCD for $\sqrt{s} > 2.3$ GeV
Kühn & Steinhauser [27]	$0.02778 \pm 0.00016$	full $\mathcal{O}(\alpha_s^2)$ for $\sqrt{s} > 1.8$ GeV
Erlar [19]	$0.02779 \pm 0.00020$	conv. from $\overline{\text{MS}}$ scheme
Groote <i>et al.</i> [28]	$0.02787 \pm 0.00032$	use of QCD sum rules
Martin <i>et al.</i> [29]	$0.02741 \pm 0.00019$	incl. new BES data
de Troconiz, Yndurain [30]	$0.02754 \pm 0.00010$	PQCD for $s > 2$ GeV <sup>2</sup>
Jegerlehner [31]	$0.02755 \pm 0.00013$	Adler function approach
Davier <i>et al.</i> [20]	$0.02750 \pm 0.00010$	incl. new $e^+e^-$ data, PQCD for $\sqrt{s} > 1.8$ GeV
Davier <i>et al.</i> [20]	$0.02762 \pm 0.00011$	incl. $\tau$ decay data
Burkhardt, Pietrzyk [32]	$0.02750 \pm 0.00033$	incl. BES/BABAR data, PQCD for $\sqrt{s} > 12$ GeV
Hagiwara <i>et al.</i> [33]	$0.02764 \pm 0.00014$	incl. new $e^+e^-$ data, PQCD for $\sqrt{s} = 2.6\text{--}3.7, >11.1$ GeV

some discrepancy between analyses based on  $e^+e^- \rightarrow$  hadrons cross-section data and those based on  $\tau$  decay spectral functions [20]. The latter utilize data from OPAL [34], CLEO [35], ALEPH [36], and Belle [37] and imply lower central values for the extracted  $M_H$  from a global fit to the indirect precision data of about 6%. This discrepancy is smaller than in the past and at least some of it appears to be experimental. The dominant  $e^+e^- \rightarrow \pi^+\pi^-$  cross-section was measured with the CMD-2 [38] and SND [39] detectors at the VEPP-2M  $e^+e^-$  collider at Novosibirsk and the results are (after an initial discrepancy due to a flaw in the Monte Carlo event generator used by SND) in good agreement with each other. As an alternative to cross-section scans, one can use the high statistics radiative return events at  $e^+e^-$  accelerators operating at resonances such as the  $\Phi$  or the  $\Upsilon(4S)$ . The method [40] is systematics limited but dominates over the Novosibirsk data throughout. The BaBar collaboration [41] studied multi-hadron events

radiatively returned from the  $\Upsilon(4S)$ , reconstructing the radiated photon and normalizing to  $\mu^\pm\gamma$  final states. Their result is higher compared to VEPP-2M and in fact agrees quite well with the  $\tau$  analysis including the energy dependence (shape). In contrast, the shape and smaller overall cross-section from the  $\pi^+\pi^-$  radiative return results from the  $\Phi$  obtained by the KLOE collaboration [42] differs significantly from what is observed by BaBar. The discrepancy originates from the kinematic region  $\sqrt{s} \gtrsim 0.6$  GeV, and is most pronounced for  $\sqrt{s} \gtrsim 0.85$  GeV. All measurements including older data [43] and multi-hadron final states (there are also discrepancies in the  $e^+e^- \rightarrow 2\pi^+2\pi^-$  channel [20]) are accounted for and corrections have been applied for missing channels [20]. Further improvement of this dominant theoretical uncertainty in the interpretation of precision data will require better measurements of the cross-section for  $e^+e^- \rightarrow$  hadrons below the charmonium resonances including multi-pion and other final states. To improve the precisions in  $\widehat{m}_c(\widehat{m}_c)$  and  $\widehat{m}_b(\widehat{m}_b)$  it would help to remeasure the threshold regions of the heavy quarks as well as the electronic decay widths of the narrow  $c\bar{c}$  and  $b\bar{b}$  resonances.

Further free parameters entering into Eq. (10.2) are the quark and lepton masses, where  $m_i$  is the mass of the  $i^{\text{th}}$  fermion  $\psi_i$ . For the light quarks, as described in the note on “Quark Masses” in the Quark Listings,  $\widehat{m}_u = 2.3_{-0.5}^{+0.7}$  MeV,  $\widehat{m}_d = 4.8_{-0.3}^{+0.5}$  MeV, and  $\widehat{m}_s = 95 \pm 5$  MeV. These are running  $\overline{\text{MS}}$  masses evaluated at the scale  $\mu = 2$  GeV. For the heavier quarks we use QCD sum rule [44] constraints [45] and recalculate their masses in each call of our fits to account for their direct  $\alpha_s$  dependence. We find<sup>¶</sup>,  $\widehat{m}_c(\mu = \widehat{m}_c) = 1.274_{-0.035}^{+0.030}$  GeV and  $\widehat{m}_b(\mu = \widehat{m}_b) = 4.199 \pm 0.024$  GeV, with a correlation of 33%.

The top quark “pole” mass (the quotation marks are a reminder that quarks do not form asymptotic states),  $m_t = 173.24 \pm 0.81$  GeV, is an average based on the combination,  $m_t = 173.20 \pm 0.51_{\text{stat.}} \pm 0.71_{\text{syst.}}$  GeV, of published and preliminary CDF and DØ results from the Tevatron [48], with the combination,  $m_t = 173.29 \pm 0.23_{\text{stat.}} \pm 0.92_{\text{syst.}}$  GeV, obtained by the LHC Top Working Group [49]. Our average<sup>§</sup> differs slightly from the value,  $m_t = 173.07 \pm 0.52_{\text{stat.}} \pm 0.72_{\text{syst.}}$  GeV, which appears in the top quark Listings in this *Review* and which is based exclusively on published Tevatron results. We are working, however, with  $\overline{\text{MS}}$  masses in all expressions to minimize theoretical uncertainties. Such a short distance mass definition (unlike the pole mass) is free from non-perturbative

---

<sup>¶</sup> Other authors [46] advocate to evaluate and quote  $\widehat{m}_c(\mu = 3 \text{ GeV})$  instead. We use  $\widehat{m}_c(\mu = \widehat{m}_c)$  because in the global analysis it is convenient to nullify any explicitly  $m_c$  dependent logarithms. Note also that our uncertainty for  $m_c$  (and to a lesser degree for  $m_b$ ) is larger than in Refs. 46 and 47, for example. The reason is that we determine the continuum contribution for charm pair production using only resonance data and theoretical consistency across various sum rule moments, and then use any difference to the experimental continuum data as an additional uncertainty. We also include an uncertainty for the condensate terms which grows rapidly for higher moments in the sum rule analysis.

<sup>§</sup> At the time of writing this review, the efforts to establish a top quark averaging group involving both the Tevatron and the LHC were still in progress. Therefore we perform a simplified average ourselves, conservatively assuming that the entire Tevatron systematics is common to both colliders (ignoring correlations yields the same central value).

and renormalon [50] uncertainties. We therefore convert to the top quark  $\overline{\text{MS}}$  mass,

$$\widehat{m}_t(\mu = \widehat{m}_t) = m_t \left[ 1 - \frac{4}{3} \frac{\alpha_s}{\pi} + \mathcal{O}(\alpha_s^2) \right], \quad (10.9)$$

using the three-loop formula [51]. This introduces an additional uncertainty which we estimate to 0.5 GeV (the size of the three-loop term) and add in quadrature to the experimental pole mass error. This is convenient because we use the pole mass as an external constraint while fitting to the  $\overline{\text{MS}}$  mass. We are assuming that the kinematic mass extracted from the collider events corresponds within this uncertainty to the pole mass. In summary, we will use the fit constraint,  $m_t = 173.24 \pm 0.81_{\text{exp.}} \pm 0.5_{\text{QCD}}$  GeV =  $173.24 \pm 0.95$  GeV.

$\sin^2 \theta_W$  and  $M_W$  can be calculated from  $M_Z$ ,  $\widehat{\alpha}(M_Z)$ , and  $G_F$ , when values for  $m_t$  and  $M_H$  are given, or conversely,  $M_H$  can be constrained by  $\sin^2 \theta_W$  and  $M_W$ . The value of  $\sin^2 \theta_W$  is extracted from neutral-current processes (see Sec. 10.3) and  $Z$  pole observables (see Sec. 10.4) and depends on the renormalization prescription. There are a number of popular schemes [52–58] leading to values which differ by small factors depending on  $m_t$  and  $M_H$ . The notation for these schemes is shown in Table 10.2.

**Table 10.2:** Notations used to indicate the various schemes discussed in the text. Each definition of  $\sin^2 \theta_W$  leads to values that differ by small factors depending on  $m_t$  and  $M_H$ . Numerical values are also given for illustration.

Scheme	Notation	Value
On-shell	$s_W^2$	0.22333
$\overline{\text{MS}}$	$\widehat{s}_Z^2$	0.23126
$\overline{\text{MS}}$ ND	$\widehat{s}_{\text{ND}}^2$	0.23144
$\overline{\text{MS}}$	$\widehat{s}_0^2$	0.23864
Effective angle	$\overline{s}_\ell^2$	0.23155

- (i) The on-shell scheme [52] promotes the tree-level formula  $\sin^2 \theta_W = 1 - M_W^2/M_Z^2$  to a definition of the renormalized  $\sin^2 \theta_W$  to all orders in perturbation theory, *i.e.*,  $\sin^2 \theta_W \rightarrow s_W^2 \equiv 1 - M_W^2/M_Z^2$ :

$$M_W = \frac{A_0}{s_W(1 - \Delta r)^{1/2}}, \quad M_Z = \frac{M_W}{c_W}, \quad (10.10)$$

where  $c_W \equiv \cos \theta_W$ ,  $A_0 = (\pi\alpha/\sqrt{2}G_F)^{1/2} = 37.28039(1)$  GeV, and  $\Delta r$  includes the radiative corrections relating  $\alpha$ ,  $\alpha(M_Z)$ ,  $G_F$ ,  $M_W$ , and  $M_Z$ . One finds  $\Delta r \sim \Delta r_0 - \rho_t/\tan^2 \theta_W$ , where  $\Delta r_0 = 1 - \alpha/\widehat{\alpha}(M_Z) = 0.06637(11)$  is due to the

running of  $\alpha$ , and  $\rho_t = 3G_F m_t^2 / 8\sqrt{2}\pi^2 = 0.00940 (m_t/173.24 \text{ GeV})^2$  represents the dominant (quadratic)  $m_t$  dependence. There are additional contributions to  $\Delta r$  from bosonic loops, including those which depend logarithmically on  $M_H$  and higher-order corrections<sup>§§</sup>. One has  $\Delta r = 0.03639 \mp 0.00036 \pm 0.00011$ , where the first uncertainty is from  $m_t$  and the second is from  $\alpha(M_Z)$ . Thus the value of  $s_W^2$  extracted from  $M_Z$  includes an uncertainty ( $\mp 0.00012$ ) from the currently allowed range of  $m_t$ . This scheme is simple conceptually. However, the relatively large ( $\sim 3\%$ ) correction from  $\rho_t$  causes large spurious contributions in higher orders.

$s_W^2$  depends not only on the gauge couplings but also on the spontaneous-symmetry breaking, and it is awkward in the presence of any extension of the SM which perturbs the value of  $M_Z$  (or  $M_W$ ). Other definitions are motivated by the tree-level coupling constant definition  $\theta_W = \tan^{-1}(g'/g)$ :

(ii) In particular, the modified minimal subtraction ( $\overline{\text{MS}}$ ) scheme introduces the quantity  $\sin^2 \hat{\theta}_W(\mu) \equiv \hat{g}'^2(\mu) / [\hat{g}^2(\mu) + \hat{g}'^2(\mu)]$ , where the couplings  $\hat{g}$  and  $\hat{g}'$  are defined by modified minimal subtraction and the scale  $\mu$  is conveniently chosen to be  $M_Z$  for many EW processes. The value of  $\hat{s}_Z^2 = \sin^2 \hat{\theta}_W(M_Z)$  extracted from  $M_Z$  is less sensitive than  $s_W^2$  to  $m_t$  (by a factor of  $\tan^2 \theta_W$ ), and is less sensitive to most types of new physics. It is also very useful for comparing with the predictions of grand unification. There are actually several variant definitions of  $\sin^2 \hat{\theta}_W(M_Z)$ , differing according to whether or how finite  $\alpha \ln(m_t/M_Z)$  terms are decoupled (subtracted from the couplings). One cannot entirely decouple the  $\alpha \ln(m_t/M_Z)$  terms from all EW quantities because  $m_t \gg m_b$  breaks SU(2) symmetry. The scheme that will be adopted here decouples the  $\alpha \ln(m_t/M_Z)$  terms from the  $\gamma$ - $Z$  mixing [18,53], essentially eliminating any  $\ln(m_t/M_Z)$  dependence in the formulae for asymmetries at the  $Z$  pole when written in terms of  $\hat{s}_Z^2$ . (A similar definition is used for  $\hat{\alpha}$ .) The on-shell and  $\overline{\text{MS}}$  definitions are related by

$$\hat{s}_Z^2 = c(m_t, M_H) s_W^2 = (1.0355 \pm 0.0004) s_W^2. \quad (10.11)$$

The quadratic  $m_t$  dependence is given by  $c \sim 1 + \rho_t / \tan^2 \theta_W$ . The expressions for  $M_W$  and  $M_Z$  in the  $\overline{\text{MS}}$  scheme are

$$M_W = \frac{A_0}{\hat{s}_Z (1 - \Delta \hat{r}_W)^{1/2}}, \quad M_Z = \frac{M_W}{\hat{\rho}^{1/2} \hat{c}_Z}, \quad (10.12)$$

and one predicts  $\Delta \hat{r}_W = 0.06943 \pm 0.00011$ .  $\Delta \hat{r}_W$  has no quadratic  $m_t$  dependence, because shifts in  $M_W$  are absorbed into the observed  $G_F$ , so that the error in  $\Delta \hat{r}_W$  is almost entirely due to  $\Delta r_0 = 1 - \alpha/\hat{\alpha}(M_Z)$ . The quadratic  $m_t$  dependence has been shifted into  $\hat{\rho} \sim 1 + \rho_t$ , where including bosonic loops,  $\hat{\rho} = 1.01031 \pm 0.00011$ .

(iii) A variant  $\overline{\text{MS}}$  quantity  $\hat{s}_{\text{ND}}^2$  (used in the 1992 edition of this *Review*) does not decouple the  $\alpha \ln(m_t/M_Z)$  terms [54]. It is related to  $\hat{s}_Z^2$  by

$$\hat{s}_Z^2 = \hat{s}_{\text{ND}}^2 / \left(1 + \frac{\hat{\alpha}}{\pi} d\right), \quad (10.13a)$$

---

<sup>§§</sup> All explicit numbers quoted here and below include the two- and three-loop corrections described near the end of Sec. 10.2.



$$d = \frac{1}{3} \left( \frac{1}{\hat{s}^2} - \frac{8}{3} \right) \left[ \left( 1 + \frac{\alpha_s}{\pi} \right) \ln \frac{m_t}{M_Z} - \frac{15\alpha_s}{8\pi} \right], \quad (10.13b)$$

Thus,  $\hat{s}_Z^2 - \hat{s}_{\text{ND}}^2 \approx -0.0002$ .

(iv) Some of the low-energy experiments discussed in the next section are sensitive to the weak mixing angle at almost vanishing momentum transfer (for a review, see Ref. 55). Thus, Table 10.2 also includes  $\hat{s}_0^2 \equiv \sin^2 \hat{\theta}_W(0)$ .

(v) Yet another definition, the effective angle [56–58]  $\bar{\alpha}_f^2 = \sin^2 \theta_{\text{eff}}^f$  for the  $Z$  vector coupling to fermion  $f$ , is based on  $Z$  pole observables and described in Sec. 10.4.

Experiments are at such level of precision that complete one-loop, dominant two-loop, and partial three-loop radiative corrections must be applied. For neutral-current and  $Z$  pole processes, these corrections are conveniently divided into two classes:

1. QED diagrams involving the emission of real photons or the exchange of virtual photons in loops, but not including vacuum polarization diagrams. These graphs often yield finite and gauge-invariant contributions to observable processes. However, they are dependent on energies, experimental cuts, *etc.*, and must be calculated individually for each experiment.
2. EW corrections, including  $\gamma\gamma$ ,  $\gamma Z$ ,  $ZZ$ , and  $WW$  vacuum polarization diagrams, as well as vertex corrections, box graphs, *etc.*, involving virtual  $W$  and  $Z$  bosons. The one-loop corrections are included for all processes, and many two-loop corrections are also important. In particular, two-loop corrections involving the top quark modify  $\rho_t$  in  $\hat{\rho}$ ,  $\Delta r$ , and elsewhere by

$$\rho_t \rightarrow \rho_t [1 + R(M_H, m_t) \rho_t / 3]. \quad (10.14)$$

$R(M_H, m_t)$  can be described as an expansion in  $M_Z^2/m_t^2$ , for which the leading  $m_t^4/M_Z^4$  [59] and next-to-leading  $m_t^2/M_Z^2$  [60] terms are known. The complete two-loop calculation of  $\Delta r$  (without further approximation) has been performed in Refs. 61 and 62 for fermionic and purely bosonic diagrams, respectively. Similarly, the EW two-loop calculation for the relation between  $\bar{\alpha}_\ell^2$  and  $s_{W}^2$  is complete [63,64].

Mixed QCD-EW contributions to gauge boson self-energies of order  $\alpha\alpha_s m_t^2$  [65],  $\alpha\alpha_s^2 m_t^2$  [66], and  $\alpha\alpha_s^3 m_t^2$  [67] increase the predicted value of  $m_t$  by 6%. This is, however, almost entirely an artifact of using the pole mass definition for  $m_t$ . The equivalent corrections when using the  $\overline{\text{MS}}$  definition  $\hat{m}_t(\hat{m}_t)$  increase  $m_t$  by less than 0.5%. The subleading  $\alpha\alpha_s$  corrections [68] are also included. Further three-loop corrections of order  $\alpha\alpha_s^2$  [69,70],  $\alpha^3 m_t^6$ , and  $\alpha^2 \alpha_s m_t^4$  [71], are rather small. The same is true for  $\alpha^3 M_H^4$  [72] corrections unless  $M_H$  approaches 1 TeV.

The theoretical uncertainty from unknown higher-order corrections is estimated to amount to 4 MeV for the prediction of  $M_W$  [73] and  $4.5 \times 10^{-5}$  for  $\bar{\alpha}_\ell^2$  [74].

Throughout this *Review* we utilize EW radiative corrections from the program GAPP [21], which works entirely in the  $\overline{\text{MS}}$  scheme, and which is independent of the package ZFITTER [58]. Another resource is the recently developed modular fitting toolkit Gfitter [75].

### 10.3. Low energy electroweak observables

In the following we discuss EW precision observables obtained at low momentum transfers [6], *i.e.*  $Q^2 \ll M_Z^2$ . It is convenient to write the four-fermion interactions relevant to  $\nu$ -hadron,  $\nu$ - $e$ , as well as parity violating  $e$ -hadron and  $e$ - $e$  neutral-current processes in a form that is valid in an arbitrary gauge theory (assuming massless left-handed neutrinos). One has<sup>★</sup>

$$-\mathcal{L}^{\nu e} = \frac{G_F}{\sqrt{2}} \bar{\nu} \gamma_\mu (1 - \gamma^5) \nu \bar{e} \gamma^\mu (g_{LV}^{\nu e} - g_{LA}^{\nu e} \gamma^5) e, \quad (10.15)$$

$$-\mathcal{L}^{\nu h} = \frac{G_F}{\sqrt{2}} \bar{\nu} \gamma_\mu (1 - \gamma^5) \nu \sum_q [g_{LL}^{\nu q} \bar{q} \gamma^\mu (1 - \gamma^5) q + g_{LR}^{\nu q} \bar{q} \gamma^\mu (1 + \gamma^5) q], \quad (10.16)$$

$$-\mathcal{L}^{ee} = -\frac{G_F}{\sqrt{2}} g_{AV}^{ee} \bar{e} \gamma_\mu \gamma^5 e \bar{e} \gamma^\mu e, \quad (10.17)$$

$$-\mathcal{L}^{eh} = -\frac{G_F}{\sqrt{2}} \sum_q \left[ g_{AV}^{eq} \bar{e} \gamma_\mu \gamma^5 e \bar{q} \gamma^\mu q + g_{VA}^{eq} \bar{e} \gamma_\mu e \bar{q} \gamma^\mu \gamma^5 q \right], \quad (10.18)$$

where one must include the charged-current contribution for  $\nu_e$ - $e$  and  $\bar{\nu}_e$ - $e$  and the parity-conserving QED contribution for electron scattering.

The SM tree level expressions for the four-Fermi couplings are given in Table 10.3. Note that they differ from the respective products of the gauge couplings in Eq. (10.5) in the radiative corrections and in the presence of possible physics beyond the SM.

**10.3.1. Neutrino scattering :** For a general review on  $\nu$ -scattering we refer to Ref. 77 (nonstandard neutrino scattering interactions are surveyed in Ref. 78).

The cross-section in the laboratory system for  $\nu_\mu e \rightarrow \nu_\mu e$  or  $\bar{\nu}_\mu e \rightarrow \bar{\nu}_\mu e$  elastic scattering [79] is (in this subsection we drop the redundant index  $L$  in the effective neutrino couplings)

$$\frac{d\sigma_{\nu, \bar{\nu}}}{dy} = \frac{G_F^2 m_e E_\nu}{2\pi} \left[ (g_V^{\nu e} \pm g_A^{\nu e})^2 + (g_V^{\nu e} \mp g_A^{\nu e})^2 (1 - y)^2 - (g_V^{\nu e 2} - g_A^{\nu e 2}) \frac{y m_e}{E_\nu} \right], \quad (10.19)$$

where the upper (lower) sign refers to  $\nu_\mu$  ( $\bar{\nu}_\mu$ ), and  $y \equiv T_e/E_\nu$  (which runs from 0 to  $(1 + m_e/2E_\nu)^{-1}$ ) is the ratio of the kinetic energy of the recoil electron to the incident  $\nu$  or  $\bar{\nu}$  energy. For  $E_\nu \gg m_e$  this yields a total cross-section

$$\sigma = \frac{G_F^2 m_e E_\nu}{2\pi} \left[ (g_V^{\nu e} \pm g_A^{\nu e})^2 + \frac{1}{3} (g_V^{\nu e} \mp g_A^{\nu e})^2 \right]. \quad (10.20)$$

---

<sup>★</sup> We use here slightly different definitions (and to avoid confusion also a different notation) for the coefficients of these four-Fermi operators than we did in previous editions of this *Review*. The new couplings [76] are defined in the static limit,  $Q^2 \rightarrow 0$ , with specific radiative corrections included, while others (more experiment specific ones) are assumed to be removed by the experimentalist. They are convenient in that their determinations from very different types of processes can be straightforwardly combined.

**Table 10.3:** SM tree level expressions for the neutral-current parameters for  $\nu$ -hadron,  $\nu$ - $e$ , and  $e^-$ -scattering processes. To obtain the SM values in the last column, the tree level expressions have to be multiplied by the low-energy neutral-current  $\rho$  parameter,  $\rho_{\text{NC}} = 1.00066$ , and further vertex and box corrections need to be added as detailed in Ref. 76. The dominant  $m_t$  dependence is again given by  $\rho_{\text{NC}} \sim 1 + \rho_t$ .

Quantity	SM tree level	SM value
$g_{LV}^{\nu\mu e}$	$-\frac{1}{2} + 2 \widehat{s}_0^2$	-0.0396
$g_{LA}^{\nu\mu e}$	$-\frac{1}{2}$	-0.5064
$g_{LL}^{\nu\mu u}$	$\frac{1}{2} - \frac{2}{3} \widehat{s}_0^2$	0.3457
$g_{LL}^{\nu\mu d}$	$-\frac{1}{2} + \frac{1}{3} \widehat{s}_0^2$	-0.4288
$g_{LR}^{\nu\mu u}$	$-\frac{2}{3} \widehat{s}_0^2$	-0.1553
$g_{LR}^{\nu\mu d}$	$\frac{1}{3} \widehat{s}_0^2$	0.0777
$g_{AV}^{ee}$	$\frac{1}{2} - 2 \widehat{s}_0^2$	0.0225
$g_{AV}^{eu}$	$-\frac{1}{2} + \frac{4}{3} \widehat{s}_0^2$	-0.1887
$g_{AV}^{ed}$	$\frac{1}{2} - \frac{2}{3} \widehat{s}_0^2$	0.3419
$g_{VA}^{eu}$	$-\frac{1}{2} + 2 \widehat{s}_0^2$	-0.0351
$g_{VA}^{ed}$	$\frac{1}{2} - 2 \widehat{s}_0^2$	0.0248

The most accurate measurements [79–84] of  $\sin^2 \theta_W$  from  $\nu$ -lepton scattering (see Sec. 10.6) are from the ratio  $R \equiv \sigma_{\nu\mu e} / \sigma_{\bar{\nu}\mu e}$ , in which many of the systematic uncertainties cancel. Radiative corrections (other than  $m_t$  effects) are small compared to the precision of present experiments and have negligible effect on the extracted  $\sin^2 \theta_W$ . The most precise experiment (CHARM II) [82] determined not only  $\sin^2 \theta_W$  but  $g_{V,A}^{\nu e}$  as well, which are shown in Fig. 10.1. The cross-sections for  $\nu_e$ - $e$  and  $\bar{\nu}_e$ - $e$  may be obtained from Eq. (10.19) by replacing  $g_{V,A}^{\nu e}$  by  $g_{V,A}^{\nu e} + 1$ , where the 1 is due to the charged-current contribution.

A precise determination of the on-shell  $s_W^2$ , which depends only very weakly on  $m_t$  and  $M_H$ , is obtained from deep inelastic scattering (DIS) of neutrinos from (approximately) isoscalar targets [85]. The ratio  $R_\nu \equiv \sigma_{\nu N}^{\text{NC}} / \sigma_{\nu N}^{\text{CC}}$  of neutral-to-charged-current cross-sections has been measured to 1% accuracy by CDHS [86] and CHARM [87] at CERN. CCFR [88] at Fermilab has obtained an even more precise result, so it is important

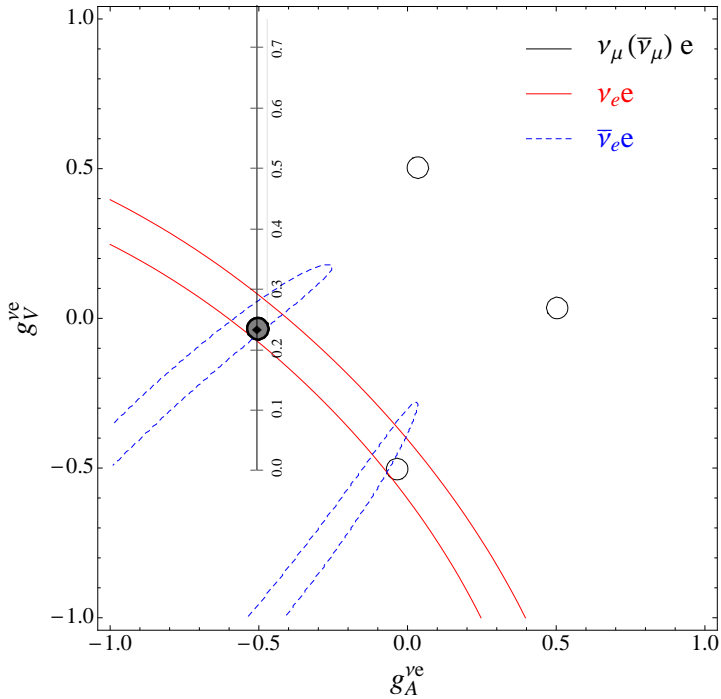


**Figure 10.1:** Allowed contours in  $g_A^{\nu e}$  vs.  $g_V^{\nu e}$  from neutrino-electron scattering and the SM prediction as a function of  $\hat{s}_Z^2$ . (The SM best fit value  $\hat{s}_Z^2 = 0.23126$  is also indicated.) The  $\nu_e e$  [83] and  $\bar{\nu}_e e$  [84] constraints are at  $1\sigma$ , while each of the four equivalent  $\nu_\mu(\bar{\nu}_\mu)e$  [79–82] solutions ( $g_{V,A} \rightarrow -g_{V,A}$  and  $g_{V,A} \rightarrow g_{A,V}$ ) are at the 90% C.L. The global best fit region (shaded) almost exactly coincides with the corresponding  $\nu_\mu(\bar{\nu}_\mu)e$  region. The solution near  $g_A = 0, g_V = -0.5$  is eliminated by  $e^+e^- \rightarrow \ell^+\ell^-$  data under the weak additional assumption that the neutral current is dominated by the exchange of a single  $Z$  boson.

to obtain theoretical expressions for  $R_\nu$  and  $R_{\bar{\nu}} \equiv \sigma_{\bar{\nu}N}^{NC}/\sigma_{\bar{\nu}N}^{CC}$  to comparable accuracy. Fortunately, many of the uncertainties from the strong interactions and neutrino spectra cancel in the ratio. A large theoretical uncertainty is associated with the  $c$ -threshold, which mainly affects  $\sigma^{CC}$ . Using the slow rescaling prescription [89] the central value of  $\sin^2\theta_W$  from CCFR varies as  $0.0111(m_c/\text{GeV} - 1.31)$ , where  $m_c$  is the effective mass which is numerically close to the  $\overline{\text{MS}}$  mass  $\hat{m}_c(\hat{m}_c)$ , but their exact relation is unknown at higher orders. For  $m_c = 1.31 \pm 0.24$  GeV (determined from  $\nu$ -induced dimuon production [90]) this contributes  $\pm 0.003$  to the total uncertainty  $\Delta \sin^2\theta_W \sim \pm 0.004$ . (The experimental uncertainty is also  $\pm 0.003$ .) This uncertainty largely cancels, however, in the Paschos-Wolfenstein ratio [91],

$$R^- = \frac{\sigma_{\nu N}^{NC} - \sigma_{\bar{\nu}N}^{NC}}{\sigma_{\nu N}^{CC} - \sigma_{\bar{\nu}N}^{CC}}. \quad (10.21)$$

It was measured by Fermilab’s NuTeV collaboration [92] for the first time, and required a high-intensity and high-energy anti-neutrino beam.

A simple zero<sup>th</sup>-order approximation is

$$R_\nu = g_L^2 + g_R^2 r, \quad R_{\bar{\nu}} = g_L^2 + \frac{g_R^2}{r}, \quad R^- = g_L^2 - g_R^2, \quad (10.22)$$

where

$$g_L^2 \equiv (g_{LL}^{\nu\mu u})^2 + (g_{LL}^{\nu\mu d})^2 \approx \frac{1}{2} - \sin^2 \theta_W + \frac{5}{9} \sin^4 \theta_W, \quad (10.23a)$$

$$g_R^2 \equiv (g_{LR}^{\nu\mu u})^2 + (g_{LR}^{\nu\mu d})^2 \approx \frac{5}{9} \sin^4 \theta_W, \quad (10.23b)$$

and  $r \equiv \sigma_{\bar{\nu}N}^{CC}/\sigma_{\nu N}^{CC}$  is the ratio of  $\bar{\nu}$  to  $\nu$  charged-current cross-sections, which can be measured directly. [In the simple parton model, ignoring hadron energy cuts,  $r \approx (\frac{1}{3} + \epsilon)/(1 + \frac{1}{3}\epsilon)$ , where  $\epsilon \sim 0.125$  is the ratio of the fraction of the nucleon's momentum carried by anti-quarks to that carried by quarks.] In practice, Eq. (10.22) must be corrected for quark mixing, quark sea effects,  $c$ -quark threshold effects, non-isoscalarity,  $W$ - $Z$  propagator differences, the finite muon mass, QED and EW radiative corrections. Details of the neutrino spectra, experimental cuts,  $x$  and  $Q^2$  dependence of structure functions, and longitudinal structure functions enter only at the level of these corrections and therefore lead to very small uncertainties. CCFR quotes  $s_W^2 = 0.2236 \pm 0.0041$  for  $(m_t, M_H) = (175, 150)$  GeV with very little sensitivity to  $(m_t, M_H)$ .

The NuTeV collaboration found  $s_W^2 = 0.2277 \pm 0.0016$  (for the same reference values), which was  $3.0 \sigma$  higher than the SM prediction [92]. The deviation was in  $g_L^2$  (initially  $2.7 \sigma$  low) while  $g_R^2$  was consistent with the SM. Since then a number of experimental and theoretical developments changed the interpretation of the measured cross section ratios, affecting the extracted  $g_{L,R}^2$  (and thus  $s_W^2$ ) including their uncertainties and correlation. In the following paragraph we give a semi-quantitative and preliminary discussion of these effects, but we stress that the precise impact of them needs to be evaluated carefully by the collaboration with a new and self-consistent set of PDFs, including new radiative corrections, while simultaneously allowing isospin breaking and asymmetric strange seas. This is an effort which is currently on its way and until it is completed we do not include the  $\nu$ DIS constraints in our default set of fits.

(i) In the original analysis NuTeV worked with a symmetric strange quark sea but subsequently measured [93] the difference between the strange and antistrange momentum distributions,  $S^- \equiv \int_0^1 dx x [s(x) - \bar{s}(x)] = 0.00196 \pm 0.00143$ , from dimuon events utilizing the first complete next-to-leading order QCD description [94] and parton distribution functions (PDFs) according to Ref. 95. The global PDF fits in Ref. 96 give somewhat smaller values,  $S^- = 0.0013(9)$  [ $S^- = 0.0010(13)$ ], where the semi-leptonic charmed-hadron branching ratio,  $B_\mu = 8.8 \pm 0.5\%$ , has [not] been used as an external constraint. The resulting  $S^-$  also depends on the PDF model used and on whether theoretical arguments (see Ref. 97 and references therein) are invoked favoring a zero crossing of  $x[s(x) - \bar{s}(x)]$  at values much larger than seen by NuTeV and suggesting

an effect of much smaller and perhaps negligible size. (ii) The measured branching ratio for  $K_{e3}$  decays enters crucially in the determination of the  $\nu_e(\bar{\nu}_e)$  contamination of the  $\nu_\mu(\bar{\nu}_\mu)$  beam. This branching ratio has moved from  $4.82 \pm 0.06\%$  at the time of the original publication [92] to the current value of  $5.07 \pm 0.04\%$ , *i.e.* a change by more than  $4\sigma$ . This moves  $s_W^2$  about one standard deviation further away from the SM prediction while reducing the  $\nu_e(\bar{\nu}_e)$  uncertainty. (iii) PDFs seem to violate isospin symmetry at levels much stronger than generally expected [98]. A minimum  $\chi^2$  set of PDFs [99] allowing charge symmetry violation for both valence quarks [ $d_V^p(x) \neq u_V^n(x)$ ] and sea quarks [ $\bar{d}^p(x) \neq \bar{u}^n(x)$ ] shows a reduction in the NuTeV discrepancy by about  $1\sigma$ . But isospin symmetry violating PDFs are currently not well constrained phenomenologically and within uncertainties the NuTeV anomaly could be accounted for in full or conversely made larger [99]. Still, the leading contribution from quark mass differences turns out to be largely model-independent [100] (at least in sign) and a shift,  $\delta s_W^2 = -0.0015 \pm 0.0003$  [97], has been estimated. (iv) QED splitting effects also violate isospin symmetry with an effect on  $s_W^2$  whose sign (reducing the discrepancy) is model-independent. The corresponding shift of  $\delta s_W^2 = -0.0011$  has been calculated in Ref. 101 but has a large uncertainty. (v) Nuclear shadowing effects [102] are likely to affect the interpretation of the NuTeV result at some level, but the NuTeV collaboration argues that their data are dominated by values of  $Q^2$  at which nuclear shadowing is expected to be relatively small. However, another nuclear effect, known as the isovector EMC effect [103], is much larger (because it affects all neutrons in the nucleus, not just the excess ones) and model-independently works to reduce the discrepancy. It is estimated to lead to a shift of  $\delta s_W^2 = -0.0019 \pm 0.0006$  [97]. It would be important to verify and quantify this kind of effect experimentally, *e.g.*, in polarized electron scattering. (vi) The extracted  $s_W^2$  may also shift at the level of the quoted uncertainty when analyzed using the most recent QED and EW radiative corrections [104,105], as well as QCD corrections to the structure functions [106]. However, these are scheme-dependent and in order to judge whether they are significant they need to be adapted to the experimental conditions and kinematics of NuTeV, and have to be obtained in terms of observable variables and for the differential cross-sections. In addition, there is the danger of double counting some of the QED splitting effects. (vii) New physics could also affect  $g_{L,R}^2$  [107] but it is difficult to convincingly explain the entire effect that way.

### 10.3.2. *Parity violation :*

The SLAC polarized electron-deuteron DIS (eDIS) experiment [108] measured the right-left asymmetry,

$$A = \frac{\sigma_R - \sigma_L}{\sigma_R + \sigma_L}, \quad (10.24)$$

where  $\sigma_{R,L}$  is the cross-section for the deep-inelastic scattering of a right- or left-handed electron:  $e_{R,L}N \rightarrow eX$ . In the quark parton model,

$$\frac{A}{Q^2} = a_1 + a_2 \frac{1 - (1 - y)^2}{1 + (1 - y)^2}, \quad (10.25)$$

where  $Q^2 > 0$  is the momentum transfer and  $y$  is the fractional energy transfer from the electron to the hadrons. For the deuteron or other isoscalar targets, one has, neglecting

the  $s$ -quark and anti-quarks,

$$a_1 = \frac{3G_F}{5\sqrt{2}\pi\alpha} \left( g_{AV}^{eu} - \frac{1}{2}g_{AV}^{ed} \right) \approx \frac{3G_F}{5\sqrt{2}\pi\alpha} \left( -\frac{3}{4} + \frac{5}{3}\hat{s}_0^2 \right), \quad (10.26a)$$

$$a_2 = \frac{3G_F}{5\sqrt{2}\pi\alpha} \left( g_{VA}^{eu} - \frac{1}{2}g_{VA}^{ed} \right) \approx \frac{9G_F}{5\sqrt{2}\pi\alpha} \left( \hat{s}_0^2 - \frac{1}{4} \right). \quad (10.26b)$$

The Jefferson Lab Hall A Collaboration [109] improved on the SLAC result by determining  $A$  at  $Q^2 = 1.085$  GeV and  $1.901$  GeV, and determined the weak mixing angle to 2% precision. In another polarized-electron scattering experiment on deuterons, but in the quasi-elastic kinematic regime, the SAMPLE experiment [110] at MIT-Bates extracted the combination  $g_{VA}^{eu} - g_{VA}^{ed}$  at  $Q^2$  values of  $0.1$  GeV<sup>2</sup> and  $0.038$  GeV<sup>2</sup>. What was actually determined were nucleon form factors from which the quoted results were obtained by the removal of a multi-quark radiative correction [111]. Other linear combinations of the effective couplings have been determined in polarized-lepton scattering at CERN in  $\mu$ -C DIS, at Mainz in  $e$ -Be (quasi-elastic), and at Bates in  $e$ -C (elastic). See the review articles in Refs. 112 and 113 for more details. Recent polarized electron asymmetry experiments, *i.e.*, SAMPLE, the PVA4 experiment at Mainz, and the HAPPEX and G0 experiments at Jefferson Lab, have focussed on the strange quark content of the nucleon. These are reviewed in Refs. 114 and 115.

The parity violating asymmetry,  $A_{PV}$ , in fixed target polarized Møller scattering,  $e^-e^- \rightarrow e^-e^-$ , is defined as in Eq. (10.24) and reads [116],

$$\frac{A_{PV}}{Q^2} = -2g_{AV}^{ee} \frac{G_F}{\sqrt{2}\pi\alpha} \frac{1-y}{1+y^4+(1-y)^4}, \quad (10.27)$$

where  $y$  is again the energy transfer. It has been measured at low  $Q^2 = 0.026$  GeV<sup>2</sup> in the SLAC E158 experiment [117], with the result  $A_{PV} = (-1.31 \pm 0.14_{\text{stat.}} \pm 0.10_{\text{syst.}}) \times 10^{-7}$ . Expressed in terms of the weak mixing angle in the  $\overline{\text{MS}}$  scheme, this yields  $\hat{s}^2(Q^2) = 0.2403 \pm 0.0013$ , and established the scale dependence of the weak mixing angle (see  $Q_W(e)$  in Fig. 10.2) at the level of  $6.4 \sigma$ . One can also extract the model-independent effective coupling,  $g_{AV}^{ee} = 0.0190 \pm 0.0027$  [76] (the implications are discussed in Ref. 119).

In a similar experiment and at about the same  $Q^2 = 0.025$  GeV<sup>2</sup>, Qweak at Jefferson Lab [122] will be able to measure the weak charge of the proton (which is proportional to  $2g_{AV}^{eu} + g_{AV}^{ed}$ ) and  $\sin^2 \theta_W$  in polarized  $ep$  scattering with relative precisions of 4% and 0.3%, respectively. The result based on the collaborations commissioning run [123] and about 4% of the data corresponds to the constraint  $2g_{AV}^{eu} + g_{AV}^{ed} = 0.064 \pm 0.012$ .

There are precise experiments measuring atomic parity violation (APV) [124] in cesium [125,126] (at the 0.4% level [125]), thallium [127], lead [128], and bismuth [129]. The EW physics is contained in the nuclear weak charges  $Q_W^{Z,N}$ , where  $Z$  and  $N$  are the numbers of protons and neutrons in the nucleus. In terms of the nucleon vector couplings,

$$g_{AV}^{ep} \equiv 2g_{AV}^{eu} + g_{AV}^{ed} \approx -\frac{1}{2} + 2\hat{s}_0^2, \quad (10.28)$$

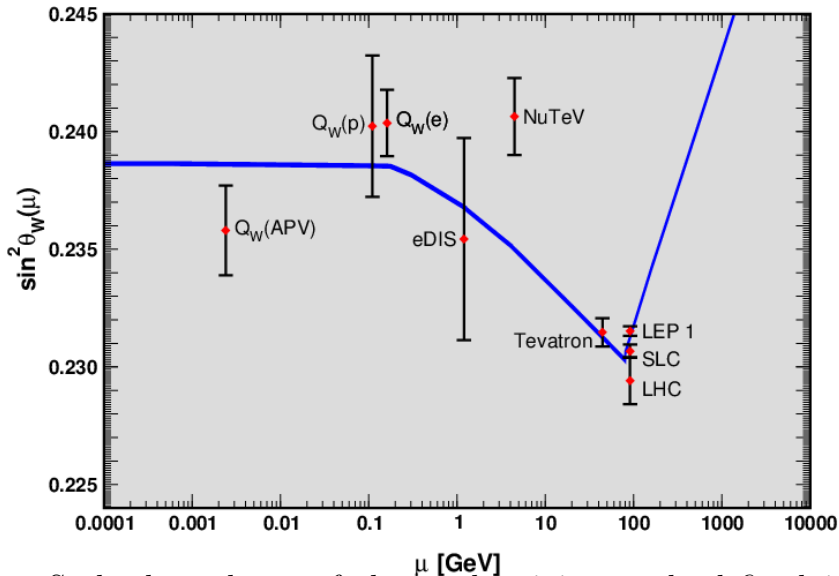


**Figure 10.2:** Scale dependence of the weak mixing angle defined in the  $\overline{\text{MS}}$  scheme [118] (for the scale dependence of the weak mixing angle defined in a mass-dependent renormalization scheme, see Ref. 119). The minimum of the curve corresponds to  $\mu = M_W$ , below which we switch to an effective theory with the  $W^\pm$  bosons integrated out, and where the  $\beta$ -function for the weak mixing angle changes sign. At the location of the  $W$  boson mass and each fermion mass there are also discontinuities arising from scheme dependent matching terms which are necessary to ensure that the various effective field theories within a given loop order describe the same physics. However, in the  $\overline{\text{MS}}$  scheme these are very small numerically and barely visible in the figure provided one decouples quarks at  $\mu = \hat{m}_q(\hat{m}_q)$ . The width of the curve reflects the theory uncertainty from strong interaction effects which at low energies is at the level of  $\pm 7 \times 10^{-5}$  [118]. Following the estimate [121] of the typical momentum transfer for parity violation experiments in Cs, the location of the APV data point is given by  $\mu = 2.4$  MeV. For NuTeV we display the updated value from Ref. 120 and chose  $\mu = \sqrt{20}$  GeV which is about half-way between the averages of  $\sqrt{Q^2}$  for  $\nu$  and  $\bar{\nu}$  interactions at NuTeV. The Tevatron and LHC measurements are strongly dominated by invariant masses of the final state dilepton pair of  $\mathcal{O}(M_Z)$  and can thus be considered as additional  $Z$  pole data points. For clarity we displayed the Tevatron point horizontally to the left.

$$g_{AV}^{en} \equiv g_{AV}^{eu} + 2g_{AV}^{ed} \approx \frac{1}{2}, \quad (10.29)$$

one has,

$$Q_W^{Z,N} \equiv -2 [Z(g_{AV}^{ep} + 0.00005) + N(g_{AV}^{en} + 0.00006)] \left(1 - \frac{\alpha}{2\pi}\right), \quad (10.30)$$

where the numerically small adjustments are discussed in Ref. 76 and include the result of the  $\gamma Z$ -box correction from Ref. 130. *E.g.*,  $Q_W(^{133}\text{Cs})$  is extracted by measuring experimentally the ratio of the parity violating amplitude,  $E_{\text{PNC}}$ , to the Stark vector



transition polarizability,  $\beta$ , and by calculating theoretically  $E_{\text{PNC}}$  in terms of  $Q_W$ . One can then write,

$$Q_W = N \left( \frac{\text{Im } E_{\text{PNC}}}{\beta} \right)_{\text{exp.}} \left( \frac{|e| a_B}{\text{Im } E_{\text{PNC}}} \frac{Q_W}{N} \right)_{\text{th.}} \left( \frac{\beta}{a_B^3} \right)_{\text{exp.+th.}} \left( \frac{a_B^2}{|e|} \right),$$

where  $a_B$  is the Bohr radius. The uncertainties associated with atomic wave functions are quite small for cesium [131]. The semi-empirical value of  $\beta$  used in early analyses added another source of theoretical uncertainty [132]. However, the ratio of the off-diagonal hyperfine amplitude to the polarizability was subsequently measured directly by the Boulder group [133]. Combined with the precisely known hyperfine amplitude [134] one finds  $\beta = (26.991 \pm 0.046) a_B^3$ , in excellent agreement with the earlier results, reducing the overall theory uncertainty (while slightly increasing the experimental error). Utilizing the state-of-the-art many-body calculation in Ref. 135 yields  $\text{Im } E_{\text{PNC}} = (0.8906 \pm 0.0026) \times 10^{-11} |e| a_B Q_W / N$ , while the two measurements [125,126] combine to give  $\text{Im } E_{\text{PNC}} / \beta = -1.5924 \pm 0.0055$  mV/cm, and we would obtain  $Q_W(^{133}\text{Cs}) = -73.20 \pm 0.35$ , or equivalently  $55g_{AV}^{ep} + 78g_{AV}^{en} = 36.64 \pm 0.18$  which is in excellent agreement with the SM prediction of 36.66. However, a very recent atomic structure calculation [136] found significant corrections to two non-dominating terms, changing the result to  $\text{Im } E_{\text{PNC}} = (0.8977 \pm 0.0040) \times 10^{-11} |e| a_B Q_W / N$ , and yielding the constraint,  $55g_{AV}^{ep} + 78g_{AV}^{en} = 36.35 \pm 0.21$  [ $Q_W(^{133}\text{Cs}) = -72.62 \pm 0.43$ ], *i.e.* a 1.5  $\sigma$  SM deviation. Thus, the various theoretical efforts in [135–137] together with an update of the SM calculation [138] reduced an earlier 2.3  $\sigma$  discrepancy from the SM (see the year 2000 edition of this *Review*), but there still appears to remain a small deviation. The theoretical uncertainties are 3% for thallium [139] but larger for the other atoms. The Boulder experiment in cesium also observed the parity-violating weak corrections to the nuclear electromagnetic vertex (the anapole moment [140]).

In the future it could be possible to further reduce the theoretical wave function uncertainties by taking the ratios of parity violation in different isotopes [124,141]. There would still be some residual uncertainties from differences in the neutron charge radii, however [142]. Experiments in hydrogen and deuterium are another possibility for reducing the atomic theory uncertainties [143], while measurements of single trapped radium ions are promising [144] because of the much larger parity violating effect.

#### 10.4. Physics of the massive electroweak bosons

If the CM energy  $\sqrt{s}$  is large compared to the fermion mass  $m_f$ , the unpolarized Born cross-section for  $e^+e^- \rightarrow f\bar{f}$  can be written as

$$\frac{d\sigma}{d\cos\theta} = \frac{\pi\alpha^2(s)}{2s} \left[ F_1(1 + \cos^2\theta) + 2F_2\cos\theta \right] + B, \quad (10.31a)$$

where

$$F_1 = Q_e^2 Q_f^2 - 2\chi Q_e Q_f \bar{g}_V^e \bar{g}_V^f \cos\delta_R + \chi^2 (\bar{g}_V^e{}^2 + \bar{g}_A^e{}^2) (\bar{g}_V^f{}^2 + \bar{g}_A^f{}^2) \quad (10.31b)$$

$$F_2 = -2\chi Q_e Q_f \bar{g}_A^e \bar{g}_A^f \cos \delta_R + 4\chi^2 \bar{g}_V^e \bar{g}_A^e \bar{g}_V^f \bar{g}_A^f \quad (10.31c)$$

$$\tan \delta_R = \frac{M_Z \Gamma_Z}{M_Z^2 - s}, \quad \chi = \frac{G_F}{2\sqrt{2}\pi\alpha(s)} \frac{sM_Z^2}{[(M_Z^2 - s)^2 + M_Z^2 \Gamma_Z^2]^{1/2}}, \quad (10.32)$$

and  $B$  accounts for box graphs involving virtual  $Z$  and  $W$  bosons, and  $\bar{g}_{V,A}^f$  are defined in Eq. (10.33) below. The differential cross-section receives important corrections from QED effects in the initial and final state, and interference between the two, see *e.g.* Ref. 145. For  $q\bar{q}$  production, there are additional final-state QCD corrections, which are relatively large. Note also that the equations above are written in the CM frame of the incident  $e^+e^-$  system, which may be boosted due to the initial-state QED radiation.

Some of the leading virtual EW corrections are captured by the running QED coupling  $\alpha(s)$  and the Fermi constant  $G_F$ . The remaining corrections to the  $Zf\bar{f}$  interaction are absorbed by replacing the tree-level couplings Eq. (10.5) with the  $s$ -dependent *effective couplings* [146]

$$\bar{g}_V^f = \sqrt{\rho_f} (t_{3L}^{(f)} - 2Q_f \kappa_f \sin^2 \theta_W), \quad \bar{g}_A^f = \sqrt{\rho_f} t_{3L}^{(f)}. \quad (10.33)$$

In these equations, the effective couplings are to be taken at the scale  $\sqrt{s}$ , but for notational simplicity we do not show this explicitly. At tree-level  $\rho_f = \kappa_f = 1$ , but inclusion of EW radiative corrections leads to non-zero  $\rho_f - 1$  and  $\kappa_f - 1$ , which depend on the fermion  $f$  and on the renormalization scheme. In the on-shell scheme, the quadratic  $m_t$  dependence is given by  $\rho_f \sim 1 + \rho_t$ ,  $\kappa_f \sim 1 + \rho_t / \tan^2 \theta_W$ , while in  $\overline{\text{MS}}$ ,  $\hat{\rho}_f \sim \hat{\kappa}_f \sim 1$ , for  $f \neq b$  ( $\hat{\rho}_b \sim 1 - \frac{4}{3}\rho_t$ ,  $\hat{\kappa}_b \sim 1 + \frac{2}{3}\rho_t$ ). In the  $\overline{\text{MS}}$  scheme the normalization is changed according to  $G_F M_Z^2 / 2\sqrt{2}\pi \rightarrow \hat{\alpha} / 4\hat{s}^2 \hat{c}_Z^2$  in Eq. (10.32).

For the high-precision  $Z$ -pole observables discussed below, additional bosonic and fermionic loops, vertex corrections, and higher order contributions, *etc.*, must be included [60,63,64,147,148]. For example, in the  $\overline{\text{MS}}$  scheme one has  $\hat{\rho}_\ell = 0.9982$ ,  $\hat{\kappa}_\ell = 1.0013$ ,  $\hat{\rho}_b = 0.9870$ , and  $\hat{\kappa}_b = 1.0068$ .

To connect to measured quantities, it is convenient to define an effective angle  $\bar{s}_f^2 \equiv \sin^2 \bar{\theta}_{Wf} \equiv \hat{\kappa}_f \hat{s}_Z^2 = \kappa_f s_W^2$ , in terms of which  $\bar{g}_V^f$  and  $\bar{g}_A^f$  are given by  $\sqrt{\rho_f}$  times their tree-level formulae. One finds that the  $\hat{\kappa}_f$  ( $f \neq b$ ) are almost independent of  $(m_t, M_H)$ , and thus one can write

$$\bar{s}_\ell^2 = \hat{s}_Z^2 + 0.00029, \quad (10.34)$$

while the  $\kappa$ 's for the other schemes are  $m_t$  dependent.

### 10.4.1. $e^+e^-$ scattering below the $Z$ pole :

Experiments at PEP, PETRA and TRISTAN have measured the unpolarized forward-backward asymmetry,  $A_{FB}$ , and the total cross-section relative to pure QED,  $R$ , for  $e^+e^- \rightarrow \ell^+\ell^-$ ,  $\ell = \mu$  or  $\tau$  at CM energies  $\sqrt{s} < M_Z$ . They are defined as

$$A_{FB} \equiv \frac{\sigma_F - \sigma_B}{\sigma_F + \sigma_B}, \quad R = \frac{\sigma}{\mathcal{R}_{\text{ini}} 4\pi\alpha^2/3s}, \quad (10.35)$$

where  $\sigma_F$  ( $\sigma_B$ ) is the cross-section for  $\ell^-$  to travel forward (backward) with respect to the  $e^-$  direction. Neglecting box graph contribution, they are given by

$$A_{FB} = \frac{3}{4} \frac{F_2}{F_1}, \quad R = F_1. \quad (10.36)$$

For the available data, it is sufficient to approximate the EW corrections through the leading running  $\alpha(s)$  and quadratic  $m_t$  contributions [149,150] as described above. Reviews and formulae for  $e^+e^- \rightarrow$  hadrons may be found in Ref. 151.

### 10.4.2. $Z$ pole physics :

High-precision measurements of various  $Z$  pole ( $\sqrt{s} \approx M_Z$ ) observables have been performed at LEP 1 and SLC [11,152–157], as summarized in Table 10.5. These include the  $Z$  mass and total width,  $\Gamma_Z$ , and partial widths  $\Gamma(f\bar{f})$  for  $Z \rightarrow f\bar{f}$ , where  $f = e, \mu, \tau$ , light hadrons,  $b$ , or  $c$ . It is convenient to use the variables  $M_Z$ ,  $\Gamma_Z$ ,  $R_\ell \equiv \Gamma(\text{had})/\Gamma(\ell^+\ell^-)$  ( $\ell = e, \mu, \tau$ ),  $\sigma_{\text{had}} \equiv 12\pi\Gamma(e^+e^-)\Gamma(\text{had})/M_Z^2\Gamma_Z^2$ <sup>††</sup>,  $R_b \equiv \Gamma(b\bar{b})/\Gamma(\text{had})$ , and  $R_c \equiv \Gamma(c\bar{c})/\Gamma(\text{had})$ , most of which are weakly correlated experimentally. ( $\Gamma(\text{had})$  is the partial width into hadrons.) The three values for  $R_\ell$  are consistent with lepton universality (although  $R_\tau$  is somewhat low compared to  $R_e$  and  $R_\mu$ ), but we use the general analysis in which the three observables are treated as independent. Similar remarks apply to  $A_{FB}^{0,\ell}$  defined through Eq. (10.39) with  $P_e = 0$ . ( $A_{FB}^{0,\tau}$  is somewhat high).  $\mathcal{O}(\alpha^3)$  QED corrections introduce a large anti-correlation ( $-30\%$ ) between  $\Gamma_Z$  and  $\sigma_{\text{had}}$ . The anti-correlation between  $R_b$  and  $R_c$  is  $-18\%$  [11]. The  $R_\ell$  are insensitive to  $m_t$  except for the  $Z \rightarrow b\bar{b}$  vertex and final state corrections and the implicit dependence through  $\sin^2\theta_W$ . Thus, they are especially useful for constraining  $\alpha_s$ . The invisible decay width [11],  $\Gamma(\text{inv}) = \Gamma_Z - 3\Gamma(\ell^+\ell^-) - \Gamma(\text{had}) = 499.0 \pm 1.5$  MeV, can be used to determine the number of neutrino flavors,  $N_\nu = \Gamma(\text{inv})/\Gamma^{\text{theory}}(\nu\bar{\nu})$ , much lighter than  $M_Z/2$ . In practice, we determine  $N_\nu$  by allowing it as an additional fit parameter and obtain,

$$N_\nu = 2.990 \pm 0.007. \quad (10.37)$$

Additional constraints follow from measurements of various  $Z$ -pole asymmetries. These include the forward-backward asymmetry  $A_{FB}$  and the polarization or left-right asymmetry,

$$A_{LR} \equiv \frac{\sigma_L - \sigma_R}{\sigma_L + \sigma_R}, \quad (10.38)$$

---

<sup>††</sup> Note that in general  $\sigma_{\text{had}}$  receives additional EW corrections that are not captured in the partial widths [158], but they only become relevant in a full two-loop calculation.

where  $\sigma_L(\sigma_R)$  is the cross-section for a left-(right-)handed incident electron.  $A_{LR}$  was measured precisely by the SLD collaboration at the SLC [154], and has the advantages of being very sensitive to  $\sin^2 \theta_W$  and that systematic uncertainties largely cancel. After removing initial state QED corrections and contributions from photon exchange,  $\gamma$ - $Z$  interference and EW boxes, see Eq. (10.31), one can use the effective tree-level expressions

$$A_{LR} = A_e P_e, \quad A_{FB} = \frac{3}{4} A_f \frac{A_e + P_e}{1 + P_e A_e}, \quad (10.39)$$

where

$$A_f \equiv \frac{2\bar{g}_V^f \bar{g}_A^f}{\bar{g}_V^{f2} + \bar{g}_A^{f2}} = \frac{1 - 4|Q_f|\bar{s}_f^2}{1 - 4|Q_f|\bar{s}_f^2 + 8(|Q_f|\bar{s}_f^2)^2}. \quad (10.40)$$

$P_e$  is the initial  $e^-$  polarization, so that the second equality in Eq. (10.41) is reproduced for  $P_e = 1$ , and the  $Z$  pole forward-backward asymmetries at LEP 1 ( $P_e = 0$ ) are given by  $A_{FB}^{(0,f)} = \frac{3}{4} A_e A_f$  where  $f = e, \mu, \tau, b, c, s$  [11], and  $q$ , and where  $A_{FB}^{(0,q)}$  refers to the hadronic charge asymmetry. Corrections for  $t$ -channel exchange and  $s/t$ -channel interference cause  $A_{FB}^{(0,e)}$  to be strongly anti-correlated with  $R_e$  ( $-37\%$ ). The correlation between  $A_{FB}^{(0,b)}$  and  $A_{FB}^{(0,c)}$  amounts to 15%.

In addition, SLD extracted the final-state couplings  $A_b, A_c$  [11],  $A_s$  [155],  $A_\tau$ , and  $A_\mu$  [156], from left-right forward-backward asymmetries, using

$$A_{LR}^{FB}(f) = \frac{\sigma_{LF}^f - \sigma_{LB}^f - \sigma_{RF}^f + \sigma_{RB}^f}{\sigma_{LF}^f + \sigma_{LB}^f + \sigma_{RF}^f + \sigma_{RB}^f} = \frac{3}{4} A_f, \quad (10.41)$$

where, for example,  $\sigma_{LF}^f$  is the cross-section for a left-handed incident electron to produce a fermion  $f$  traveling in the forward hemisphere. Similarly,  $A_\tau$  and  $A_e$  were measured at LEP 1 [11] through the negative total  $\tau$  polarization,  $\mathcal{P}_\tau$ , as a function of the scattering angle  $\theta$ , which can be written as

$$\mathcal{P}_\tau = -\frac{A_\tau(1 + \cos^2 \theta) + 2A_e \cos \theta}{(1 + \cos^2 \theta) + 2A_\tau A_e \cos \theta} \quad (10.42)$$

The average polarization,  $\langle \mathcal{P}_\tau \rangle$ , obtained by integrating over  $\cos \theta$  in the numerator and denominator of Eq. (10.42), yields  $\langle \mathcal{P}_\tau \rangle = -A_\tau$ , while  $A_e$  can be extracted from the angular distribution of  $\mathcal{P}_\tau$ .

The initial state coupling,  $A_e$ , was also determined through the left-right charge asymmetry [157] and in polarized Bhabba scattering [156] at SLC. Because  $\bar{g}_V^\ell$  is very small, not only  $A_{LR}^0 = A_e$ ,  $A_{FB}^{(0,\ell)}$ , and  $\mathcal{P}_\tau$ , but also  $A_{FB}^{(0,b)}$ ,  $A_{FB}^{(0,c)}$ ,  $A_{FB}^{(0,s)}$ , and the hadronic asymmetries are mainly sensitive to  $\bar{s}_\ell^2$ .

As mentioned in Sec. 10.2, radiative corrections to  $\bar{s}_\ell^2$  have been computed with full two-loop and partial higher-order corrections. Moreover, fermionic two-loop EW corrections

to  $\bar{s}_q^2$  ( $q = b, c, s$ ) have been obtained [74,148], but the purely bosonic contributions of this order are still missing. For the partial widths,  $\Gamma(f\bar{f})$ , and the hadronic peak cross-section,  $\sigma_{\text{had}}$ , currently only approximate EW two-loop corrections based on a large- $m_t$  expansion [59,60,159,160] are known. Non-factorizable  $\mathcal{O}(\alpha\alpha_s)$  corrections for the  $Z \rightarrow q\bar{q}$  vertex are also available [147]. They add coherently, resulting in a sizable effect and shift  $\alpha_s(M_Z)$  when extracted from  $Z$  lineshape observables by  $\approx +0.0007$ . Very recently, complete fermionic two-loop EW contributions to  $R_b$  [161] and to  $\Gamma_Z$  [162] have been calculated, but their numerical impact is relatively small, and they have not been included in the fits in this *Review*.

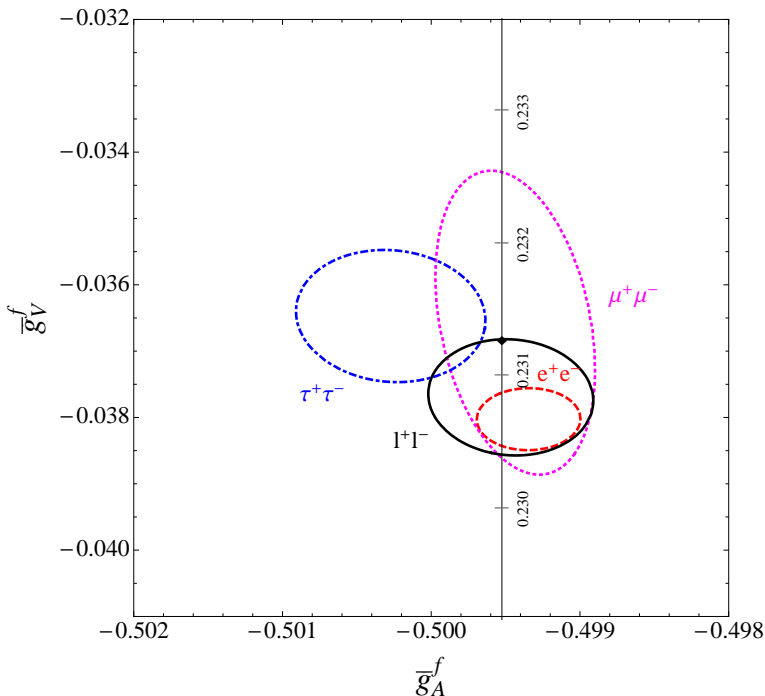


**Figure 10.3:**  $1\sigma$  (39.35% C.L.) contours for the  $Z$ -pole observables  $\bar{g}_A^f$  and  $\bar{g}_V^f$ ,  $f = e, \mu, \tau$  obtained at LEP and SLC [11], compared to the SM expectation as a function of  $\hat{s}_Z^2$ . (The SM best fit value  $\hat{s}_Z^2 = 0.23126$  is also indicated.) Also shown is the 90% CL allowed region in  $\bar{g}_{A,V}^\ell$  obtained assuming lepton universality.

As an example of the precision of the  $Z$ -pole observables, the values of  $\bar{g}_A^f$  and  $\bar{g}_V^f$ ,  $f = e, \mu, \tau, \ell$ , extracted from the LEP and SLC lineshape and asymmetry data, are shown in Fig. 10.3, which should be compared with Fig. 10.1. (The two sets of parameters coincide in the SM at tree-level.)

As for hadron colliders, the forward-backward asymmetry,  $A_{FB}$ , for  $e^+e^-$  and  $\mu^+\mu^-$  final states (with invariant masses restricted to or dominated by values around  $M_Z$ ) in  $p\bar{p}$  collisions has been measured by the DØ [163] (only  $e^+e^-$ ) and CDF [164,165] collaborations, and values for  $\bar{s}_\ell^2$  were extracted. Assuming lepton universality and that the smallest systematic uncertainty ( $\pm 0.0003$  from the  $e^+e^-$  analysis at CDF [164])

is common to both final states and experiments, these measurements combine to  $\bar{s}_\ell^2 = 0.23176 \pm 0.00060$ . By varying the invariant mass and the scattering angle (and assuming the electron couplings), information on the effective  $Z$  couplings to light quarks,  $\bar{g}_{V,A}^{u,d}$ , could also be obtained [163,166], but with large uncertainties and mutual correlations and not independently of  $\bar{s}_\ell^2$  above. Similar analyses have also been reported by the H1 and ZEUS collaborations at HERA [167] and by the LEP collaborations [11]. This kind of measurement is harder in the  $pp$  environment due to the difficulty to assign the initial quark and antiquark in the underlying Drell-Yan process to the protons. Nevertheless, measurements of  $A_{FB}$  have been reported by the CMS [168] (only  $\mu^+\mu^-$ ) and ATLAS [169] collaborations. Again assuming lepton universality and that the  $\pm 0.0007$  PDF uncertainty from ATLAS [169] is common to both experiments, these measurements combine to give the value,  $\bar{s}_\ell^2 = 0.2297 \pm 0.0010$ , which is driven by the more precise ATLAS results.

### 10.4.3. LEP 2 :

LEP 2 [170,171] ran at several energies above the  $Z$  pole up to  $\sim 209$  GeV. Measurements were made of a number of observables, including the cross-sections for  $e^+e^- \rightarrow f\bar{f}$  for  $f = q, \mu, \tau$ ; the differential cross-sections for  $f = e, \mu, \tau$ ;  $R_q$  for  $q = b, c$ ;  $A_{FB}(f)$  for  $f = \mu, \tau, b, c$ ;  $W$  branching ratios; and  $\gamma\gamma$ ,  $WW$ ,  $WW\gamma$ ,  $ZZ$ , single  $W$ , and single  $Z$  cross-sections. They are in good agreement with the SM predictions, with the exceptions of  $R_b$  (2.1  $\sigma$  low),  $A_{FB}(b)$  (1.6  $\sigma$  low), and the  $W \rightarrow \tau\nu_\tau$  branching fraction (2.6  $\sigma$  high).

The  $Z$  boson properties are extracted assuming the SM expressions for the  $\gamma$ - $Z$  interference terms. These have also been tested experimentally by performing more general fits [170,172] to the LEP 1 and LEP 2 data. Assuming family universality this approach introduces three additional parameters relative to the standard fit [11], describing the  $\gamma$ - $Z$  interference contribution to the total hadronic and leptonic cross-sections,  $j_{\text{had}}^{\text{tot}}$  and  $j_\ell^{\text{tot}}$ , and to the leptonic forward-backward asymmetry,  $j_\ell^{\text{fb}}$ . *E.g.*,

$$j_{\text{had}}^{\text{tot}} \sim g_V^\ell g_V^{\text{had}} = 0.277 \pm 0.065, \quad (10.43)$$

which is in agreement with the SM expectation [11] of  $0.21 \pm 0.01$ . These are valuable tests of the SM; but it should be cautioned that new physics is not expected to be described by this set of parameters, since (i) they do not account for extra interactions beyond the standard weak neutral current, and (ii) the photonic amplitude remains fixed to its SM value.

Strong constraints on anomalous triple and quartic gauge couplings have been obtained at LEP 2 and the Tevatron as described in the Gauge & Higgs Bosons Particle Listings.

**10.4.4.  $W$  and  $Z$  decays :**

The partial decay widths for gauge bosons to decay into massless fermions  $f_1\bar{f}_2$  (the numerical values include the small EW radiative corrections and final state mass effects) are given by

$$\Gamma(W^+ \rightarrow e^+\nu_e) = \frac{G_F M_W^3}{6\sqrt{2}\pi} \approx 226.32 \pm 0.05 \text{ MeV} , \quad (10.44a)$$

$$\Gamma(W^+ \rightarrow u_i\bar{d}_j) = \frac{\mathcal{R}_V^q G_F M_W^3}{6\sqrt{2}\pi} |V_{ij}|^2 \approx 705.5 \pm 0.4 \text{ MeV} |V_{ij}|^2, \quad (10.44b)$$

$$\Gamma(Z \rightarrow f\bar{f}) = \frac{G_F M_Z^3}{6\sqrt{2}\pi} \left[ \mathcal{R}_V^f \bar{g}_V^{f2} + \mathcal{R}_A^f \bar{g}_A^{f2} \right] \approx \begin{cases} 167.22 \pm 0.02 \text{ MeV} (\nu\bar{\nu}), \\ 84.00 \pm 0.01 \text{ MeV} (e^+e^-), \\ 300.15 \pm 0.20 \text{ MeV} (u\bar{u}), \\ 382.96 \pm 0.14 \text{ MeV} (d\bar{d}), \\ 375.87 \mp 0.17 \text{ MeV} (b\bar{b}). \end{cases} \quad (10.44c)$$

Final-state QED and QCD corrections to the vector and axial-vector form factors are given by

$$\mathcal{R}_{V,A}^f = N_C \left[ 1 + \frac{3}{4} (Q_f^2 \frac{\alpha(s)}{\pi} + \frac{N_C^2 - 1}{2N_C} \frac{\alpha_s(s)}{\pi}) + \dots \right], \quad (10.45)$$

where  $N_C = 3$  (1) is the color factor for quarks (leptons) and the dots indicate finite fermion mass effects proportional to  $m_f^2/s$  which are different for  $\mathcal{R}_V^f$  and  $\mathcal{R}_A^f$ , as well as higher-order QCD corrections, which are known to  $\mathcal{O}(\alpha_s^4)$  [173–175]. These include singlet contributions starting from two-loop order which are large, strongly top quark mass dependent, family universal, and flavor non-universal [176]. Also the  $\mathcal{O}(\alpha^2)$  self-energy corrections from Ref. 177 are taken into account.

For the  $W$  decay into quarks, Eq. (10.44b), only the universal massless part (non-singlet and  $m_q = 0$ ) of the final-state QCD radiator function in  $\mathcal{R}_V$  from Eq. (10.45) is used, and the QED corrections are modified. Expressing the widths in terms of  $G_F M_{W,Z}^3$  incorporates the largest radiative corrections from the running QED coupling [52,178]. EW corrections to the  $Z$  widths are then taken into account through the effective couplings  $\bar{g}_{V,A}^{i2}$ . Hence, in the on-shell scheme the  $Z$  widths are proportional to  $\rho_i \sim 1 + \rho_t$ . There is additional (negative) quadratic  $m_t$  dependence in the  $Z \rightarrow b\bar{b}$  vertex corrections [179] which causes  $\Gamma(b\bar{b})$  to decrease with  $m_t$ . The dominant effect is to multiply  $\Gamma(b\bar{b})$  by the vertex correction  $1 + \delta\rho_{b\bar{b}}$ , where  $\delta\rho_{b\bar{b}} \sim 10^{-2}(-\frac{1}{2}m_t^2/M_Z^2 + \frac{1}{5})$ . In practice, the corrections are included in  $\rho_b$  and  $\kappa_b$ , as discussed in Sec. 10.4.

For three fermion families the total widths are predicted to be

$$\Gamma_Z \approx 2.4955 \pm 0.0009 \text{ GeV} , \quad \Gamma_W \approx 2.0897 \pm 0.0008 \text{ GeV} . \quad (10.46)$$

The uncertainties in these predictions are almost entirely induced from the fit error in  $\alpha_s(M_Z) = 0.1193 \pm 0.0016$ . These predictions are to be compared with the experimental results,  $\Gamma_Z = 2.4952 \pm 0.0023 \text{ GeV}$  [11] and  $\Gamma_W = 2.085 \pm 0.042 \text{ GeV}$  (see the Gauge & Higgs Boson Particle Listings for more details).

10.4.5. *H decays* :

The ATLAS and CMS collaborations at LHC observed a Higgs boson [180] with properties appearing well consistent with the SM Higgs (see the note on “The Higgs Boson  $H^0$ ” in the Gauge & Higgs Boson Particle Listings). The kinematically reconstructed masses from ATLAS and CMS of the Higgs boson [181,182] average to

$$M_H = 125.6 \pm 0.4 \text{ GeV}. \quad (10.47)$$

In analogy to the  $W$  and  $Z$  decays discussed in the previous subsection, we can include some of the Higgs decay properties into the global analysis of Sec. 10.6. However, the total Higgs decay width, which in the SM amounts to

$$\Gamma_H = 4.20 \pm 0.08 \text{ MeV}, \quad (10.48)$$

is too small to be resolved at the LHC. Furthermore, it is difficult (and has not been attempted yet by the experimental collaborations) to form branching ratios when the Higgs production mechanisms differ strongly for different final states. On the other hand, Higgs decay rates into  $WW^*$  and  $ZZ^*$  (with at least one gauge boson off-shell), as well as  $\gamma\gamma$  have been deduced predominantly from gluon-gluon fusion (ggF), so that theoretical production uncertainties mostly cancel in ratios of branching fractions. Thus, we can employ the results on the signal strength parameters,  $\mu_{XX}$ , quantifying the yields of Higgs production and decay into  $XX$ , normalized to the SM expectation, to define

$$\rho_{XY} \equiv \ln \frac{\mu_{XX}}{\mu_{YY}}. \quad (10.49)$$

These quantities are constructed to have a SM expectation of zero (for  $M_H = 125.5$  GeV for ATLAS and  $M_H = 125.7$  GeV for CMS), and their physical range is over all real numbers, which allows one to straightforwardly use Gaussian error propagation (in view of the fairly large errors). Moreover, possible effects of new physics on Higgs production rates would also cancel and one may focus on the decay side of the processes. Presently, one often combines Higgs production in association with  $t\bar{t}$ -pairs (ttH) into one category with ggF since they are subject to similar theory uncertainties. Higgs production through vector boson fusion (VBF) and Higgs-strahlung (VH) are important for decays into  $f\bar{f}$ , but at the moment there is clear evidence for VH production only for the  $b\bar{b}$  final state [182,183], while the measurement of  $\tau\tau$  receives contributions from both ggF and VBF [184]. As a result, one cannot form a meaningful ratio where the dependence on the production mechanism drops out.

For each of the two LHC experiments, we consider the ratios with the smallest mutual correlations. Assuming that theory errors cancel in the  $\rho_{XY}$  while experimental systematics does not, we find for ATLAS [185],

$$\rho_{\gamma W} = 0.45 \pm 0.31, \quad \rho_{\gamma Z} = 0.08 \pm 0.28,$$

with a correlation of 25% (induced by the 15% uncertainty in the common  $\mu_{\gamma\gamma}$ ), while for CMS [182] (using the same relative theory errors as ATLAS) we obtain,

$$\rho_{\gamma W} = 0.12 \pm 0.43, \quad \rho_{ZW} = 0.30 \pm 0.39,$$

with a correlation of 43% (due to the 27% uncertainty in  $\mu_{WW}$ ). We evaluate the decay rates with the package HDECAY [186].



## 10.5. Precision flavor physics

In addition to cross-sections, asymmetries, parity violation,  $W$  and  $Z$  decays, there is a large number of experiments and observables testing the flavor structure of the SM. These are addressed elsewhere in this *Review*, and are generally not included in this Section. However, we identify three precision observables with sensitivity to similar types of new physics as the other processes discussed here. The branching fraction of the flavor changing transition  $b \rightarrow s\gamma$  is of comparatively low precision, but since it is a loop-level process (in the SM) its sensitivity to new physics (and SM parameters, such as heavy quark masses) is enhanced. A discussion can be found in the 2010 edition of this *Review*. The  $\tau$ -lepton lifetime and leptonic branching ratios are primarily sensitive to  $\alpha_s$  and not affected significantly by many types of new physics. However, having an independent and reliable low energy measurement of  $\alpha_s$  in a global analysis allows the comparison with the  $Z$  lineshape determination of  $\alpha_s$  which shifts easily in the presence of new physics contributions. By far the most precise observable discussed here is the anomalous magnetic moment of the muon (the electron magnetic moment is measured to even greater precision and can be used to determine  $\alpha$ , but its new physics sensitivity is suppressed by an additional factor of  $m_e^2/m_\mu^2$ , unless there is a new light degree of freedom such as a dark  $Z$  [187] boson). Its combined experimental and theoretical uncertainty is comparable to typical new physics contributions.

The extraction of  $\alpha_s$  from the  $\tau$  lifetime [188] is standing out from other determinations because of a variety of independent reasons: (i) the  $\tau$ -scale is low, so that upon extrapolation to the  $Z$  scale (where it can be compared to the theoretically clean  $Z$  lineshape determinations) the  $\alpha_s$  error shrinks by about an order of magnitude; (ii) yet, this scale is high enough that perturbation theory and the operator product expansion (OPE) can be applied; (iii) these observables are fully inclusive and thus free of fragmentation and hadronization effects that would have to be modeled or measured; (iv) duality violation (DV) effects are most problematic near the branch cut but there they are suppressed by a double zero at  $s = m_\tau^2$ ; (v) there are data [34] to constrain non-perturbative effects both within ( $\delta_{D=6,8}$ ) and breaking ( $\delta_{DV}$ ) the OPE; (vi) a complete four-loop order QCD calculation is available [175]; (vii) large effects associated with the QCD  $\beta$ -function can be re-summed [189] in what has become known as contour improved perturbation theory (CIPT). However, while there is no doubt that CIPT shows faster convergence in the lower (calculable) orders, doubts have been cast on the method by the observation that at least in a specific model [190], which includes the exactly known coefficients and theoretical constraints on the large-order behavior, ordinary fixed order perturbation theory (FOPT) may nevertheless give a better approximation to the full result. We therefore use the expressions [45,174,175,191],

$$\tau_\tau = \hbar \frac{1 - \mathcal{B}_\tau^s}{\Gamma_\tau^e + \Gamma_\tau^\mu + \Gamma_\tau^{ud}} = 291.13 \pm 0.43 \text{ fs}, \quad (10.50)$$

$$\Gamma_\tau^{ud} = \frac{G_F^2 m_\tau^5 |V_{ud}|^2}{64\pi^3} S(m_\tau, M_Z) \left( 1 + \frac{3}{5} \frac{m_\tau^2 - m_\mu^2}{M_W^2} \right) \times$$

$$\left[1 + \frac{\alpha_s(m_\tau)}{\pi} + 5.202 \frac{\alpha_s^2}{\pi^2} + 26.37 \frac{\alpha_s^3}{\pi^3} + 127.1 \frac{\alpha_s^4}{\pi^4} + \frac{\hat{\alpha}}{\pi} \left(\frac{85}{24} - \frac{\pi^2}{2}\right) + \delta_q\right], \quad (10.51)$$

and  $\Gamma_\tau^e$  and  $\Gamma_\tau^\mu$  can be taken from Eq. (10.6) with obvious replacements. The relative fraction of decays with  $\Delta S = -1$ ,  $\mathcal{B}_\tau^s = 0.0286 \pm 0.0007$ , is based on experimental data since the value for the strange quark mass,  $\hat{m}_s(m_\tau)$ , is not well known and the QCD expansion proportional to  $\hat{m}_s^2$  converges poorly and cannot be trusted.  $S(m_\tau, M_Z) = 1.01907 \pm 0.0003$  is a logarithmically enhanced EW correction factor with higher orders re-summed [192].  $\delta_q$  contains the dimension six and eight terms in the OPE, as well as DV effects,  $\delta_{D=6,8} + \delta_{DV} = -0.004 \pm 0.012$  [193]. Depending on how  $\delta_{D=6}$ ,  $\delta_{D=8}$ , and  $\delta_{DV}$  are extracted, there are strong correlations not only between them, but also with the gluon condensate ( $D = 4$ ) and possibly  $D > 8$  terms. These latter are suppressed in Eq. (10.51) by additional factors of  $\alpha_s$ , but not so for more general weight functions. A simultaneous fit to all non-perturbative terms [193] (as is necessary if one wants to avoid *ad hoc* assumptions) indicates that the  $\alpha_s$  errors may have been underestimated in the past. Higher statistics  $\tau$  decay data [36] and spectral functions from  $e^+e^-$  annihilation (providing a larger fit window and thus more discriminatory power and smaller correlations) are likely to reduce the  $\delta_q$  error in the future. Also included in  $\delta_q$  are quark mass effects and the  $D = 4$  condensate contributions. An uncertainty of similar size arises from the truncation of the FOPT series and is conservatively taken as the  $\alpha_s^4$  term (this is re-calculated in each call of the fits, leading to an  $\alpha_s$ -dependent and thus asymmetric error) until a better understanding of the numerical differences between FOPT and CIPT has been gained. Our perturbative error covers almost the entire range from using CIPT to assuming that the nearly geometric series in Eq. (10.51) continues to higher orders. The experimental uncertainty in Eq. (10.50), is from the combination of the two leptonic branching ratios with the direct  $\tau_\tau$ . Included are also various smaller uncertainties ( $\pm 0.5$  fs) from other sources which are dominated by the evolution from the  $Z$  scale. In total we obtain a  $\sim 2\%$  determination of  $\alpha_s(M_Z) = 0.1193_{-0.0020}^{+0.0022}$ , which corresponds to  $\alpha_s(m_\tau) = 0.327_{-0.016}^{+0.019}$ , and updates the result of Refs. 45 and 194. For more details, see Refs. 193 and 195 where the  $\tau$  spectral functions are used as additional input.

The world average of the muon anomalous magnetic moment<sup>‡</sup>,

$$a_\mu^{\text{exp}} = \frac{g_\mu - 2}{2} = (1165920.80 \pm 0.63) \times 10^{-9}, \quad (10.52)$$

---

<sup>‡</sup> In what follows, we summarize the most important aspects of  $g_\mu - 2$ , and give some details on the evaluation in our fits. For more details see the dedicated contribution on “The Muon Anomalous Magnetic Moment” in this *Review*. There are some small numerical differences (at the level of 0.1 standard deviations), which are well understood and mostly arise because internal consistency of the fits requires the calculation of all observables from analytical expressions and common inputs and fit parameters, so that an independent evaluation is necessary for this Section. Note, that in the spirit of a global analysis based on all available information we have chosen here to average in the  $\tau$  decay data, as well.

is dominated by the final result of the E821 collaboration at BNL [196]. The QED contribution has been calculated to five loops [197] (fully analytic to three loops [198,199]). The estimated SM EW contribution [200–202],  $a_\mu^{\text{EW}} = (1.52 \pm 0.03) \times 10^{-9}$ , which includes leading two-loop [201] and three-loop [202] corrections, is at the level of twice the current uncertainty.

The limiting factor in the interpretation of the result are the uncertainties from the two- and three-loop hadronic contribution [203]. *E.g.*, Ref. 20 obtained the value  $a_\mu^{\text{had}} = (69.23 \pm 0.42) \times 10^{-9}$  which combines CMD-2 [38] and SND [39]  $e^+e^- \rightarrow$  hadrons cross-section data with radiative return results from BaBar [41] and KLOE [42]. This value suggests a  $3.6 \sigma$  discrepancy between Eq. (10.52) and the SM prediction. An alternative analysis [20] using  $\tau$  decay data and isospin symmetry (CVC) yields  $a_\mu^{\text{had}} = (70.15 \pm 0.47) \times 10^{-9}$ . This result implies a smaller conflict ( $2.4 \sigma$ ) with Eq. (10.52). Thus, there is also a discrepancy between the spectral functions obtained from the two methods. For example, the channel that is relevant for the determination of  $a_\mu^{\text{had}}$  from  $\tau$  data,  $\tau^- \rightarrow \nu_\tau \pi^- \pi^0$ , has been measured to have a branching ratio of  $25.51 \pm 0.09$  (global average), while if one uses the  $e^+e^-$  data and CVC to predict the branching ratio [20] we obtain an average of  $\mathcal{B}_{\text{CVC}} = 24.93 \pm 0.13 \pm 0.22_{\text{CVC}}$ , which is  $2.3 \sigma$  lower. It is important to understand the origin of this difference, but two observations point to the conclusion that at least some of it is experimental: (i) There is also a direct discrepancy of  $1.9 \sigma$  between  $\mathcal{B}_{\text{CVC}}$  derived from BaBar (which is not inconsistent with  $\tau$  decays) and KLOE. (ii) Isospin violating corrections have been studied in detail in Ref. 204 and found to be largely under control. The largest effect is due to higher-order EW corrections [205] but introduces a negligible uncertainty [192]. Nevertheless,  $a_\mu^{\text{had}}$  is often evaluated excluding the  $\tau$  decay data arguing [206] that CVC breaking effects (*e.g.*, through a relatively large mass difference between the  $\rho^\pm$  and  $\rho^0$  vector mesons) may be larger than expected. (This may also be relevant [206] in the context of the NuTeV result discussed above.) Experimentally [36], this mass difference is indeed larger than expected, but then one would also expect a significant width difference which is contrary to observation [36] <sup>#</sup>. Fortunately, due to the suppression at large  $s$  (from where the conflicts originate) these problems are less pronounced as far as  $a_\mu^{\text{had}}$  is concerned. In the following we view all differences in spectral functions as (systematic) fluctuations and average the results.

An additional uncertainty is induced by the hadronic three-loop light-by-light scattering contribution. Several recent independent model calculations yield compatible results:  $a_\mu^{\text{LBLS}} = (+1.36 \pm 0.25) \times 10^{-9}$  [209],  $a_\mu^{\text{LBLS}} = +1.37_{-0.27}^{+0.15} \times 10^{-9}$  [210],  $a_\mu^{\text{LBLS}} = (+1.16 \pm 0.40) \times 10^{-9}$  [211], and  $a_\mu^{\text{LBLS}} = (+1.05 \pm 0.26) \times 10^{-9}$  [212]. The sign of this effect is opposite [213] to the one quoted in the 2002 edition of this *Review*, and its magnitude is larger than previous evaluations [213,214]. There is also an upper bound  $a_\mu^{\text{LBLS}} < 1.59 \times 10^{-9}$  [210] but this requires an *ad hoc* assumption, too. Very recently, first results from lattice simulations have been obtained, finding agreement with the model calculations, although with large errors [215]. For the fits, we take the

---

<sup>#</sup> In the model of Ref. 207 an additional isospin correction due to  $\gamma$ - $\rho$  mixing leads to a  $\rho^\pm$ - $\rho^0$  mass splitting that is large enough to reconcile the discrepancy between  $\tau$  and  $e^+e^-$  data, but there is some debate about the magnitude of this effect [208].

result from Ref. 212, shifted by  $2 \times 10^{-11}$  to account for the more accurate charm quark treatment of Ref. 210, and with increased error to cover all recent evaluations, resulting in  $a_\mu^{\text{LBLS}} = (+1.07 \pm 0.32) \times 10^{-9}$ .

Other hadronic effects at three-loop order contribute [216]  $a_\mu^{\text{had}}(\alpha^3) = (-1.00 \pm 0.06) \times 10^{-9}$ . Correlations with the two-loop hadronic contribution and with  $\Delta\alpha(M_Z)$  (see Sec. 10.2) were considered in Ref. 199 which also contains analytic results for the perturbative QCD contribution.

Altogether, the SM prediction is

$$a_\mu^{\text{theory}} = (1165918.41 \pm 0.48) \times 10^{-9}, \quad (10.53)$$

where the error is from the hadronic uncertainties excluding parametric ones such as from  $\alpha_s$  and the heavy quark masses. Using a correlation of about 84% from the data input to the vacuum polarization integrals [20], we estimate the correlation of the total (experimental plus theoretical) uncertainty in  $a_\mu$  with  $\Delta\alpha(M_Z)$  as 24%. The overall  $3.0 \sigma$  discrepancy between the experimental and theoretical  $a_\mu$  values could be due to fluctuations (the E821 result is statistics dominated) or underestimates of the theoretical uncertainties. On the other hand, the deviation could also arise from physics beyond the SM, such as supersymmetric models with large  $\tan\beta$  and moderately light superparticle masses [217], or a dark  $Z$  boson [187].

## 10.6. Global fit results

In this section we present the results of global fits to the experimental data discussed in Sec. 10.3–Sec. 10.5. For earlier analyses see Refs. [11,113,218]

The values for  $m_t$  [48,49],  $M_W$  [170,219],  $\Gamma_W$  [170,220],  $M_H$  [181,182] and the ratios of Higgs branching fractions discussed in Sec. 10.4.5,  $\nu$ -lepton scattering [79–84], the weak charges of the electron [117], the proton [122], cesium [125,126] and thallium [127], the weak mixing angle extracted from eDIS [109], the muon anomalous magnetic moment [196], and the  $\tau$  lifetime are listed in Table 10.4. Likewise, the principal  $Z$  pole observables can be found in Table 10.5 where the LEP 1 averages of the ALEPH, DELPHI, L3, and OPAL results include common systematic errors and correlations [11]. The heavy flavor results of LEP 1 and SLD are based on common inputs and correlated, as well [11].

Note that the values of  $\Gamma(\ell^+\ell^-)$ ,  $\Gamma(\text{had})$ , and  $\Gamma(\text{inv})$  are not independent of  $\Gamma_Z$ , the  $R_\ell$ , and  $\sigma_{\text{had}}$  and that the SM errors in those latter are largely dominated by the uncertainty in  $\alpha_s$ . Also shown in both Tables are the SM predictions for the values of  $M_Z$ ,  $M_H$ ,  $\alpha_s(M_Z)$ ,  $\Delta\alpha_{\text{had}}^{(3)}$  and the heavy quark masses shown in Table 10.6. The predictions result from a global least-square ( $\chi^2$ ) fit to all data using the minimization package MINUIT [221] and the EW library GAPP [21]. In most cases, we treat all input errors (the uncertainties of the values) as Gaussian. The reason is not that we assume that theoretical and systematic errors are intrinsically bell-shaped (which they are not) but because in most cases the input errors are either dominated by the statistical components or they are combinations of many different (including statistical) error sources, which

**Table 10.4:** Principal non- $Z$  pole observables, compared with the SM best fit predictions. The first  $M_W$  and  $\Gamma_W$  values are from the Tevatron [219,220] and the second ones from LEP 2 [170]. The value of  $m_t$  differs from the one in the Particle Listings since it includes recent preliminary results. The world averages for  $g_{V,A}^{\nu e}$  are dominated by the CHARM II [82] results,  $g_V^{\nu e} = -0.035 \pm 0.017$  and  $g_A^{\nu e} = -0.503 \pm 0.017$ . The errors are the total (experimental plus theoretical) uncertainties. The  $\tau_\tau$  value is the  $\tau$  lifetime world average computed by combining the direct measurements with values derived from the leptonic branching ratios [45]; in this case, the theory uncertainty is included in the SM prediction. In all other SM predictions, the uncertainty is from  $M_Z$ ,  $M_H$ ,  $m_t$ ,  $m_b$ ,  $m_c$ ,  $\hat{\alpha}(M_Z)$ , and  $\alpha_s$ , and their correlations have been accounted for. The column denoted Pull gives the standard deviations.

Quantity	Value	Standard Model	Pull
$m_t$ [GeV]	$173.24 \pm 0.95$	$173.87 \pm 0.87$	-0.7
$M_W$ [GeV]	$80.387 \pm 0.016$	$80.363 \pm 0.006$	1.5
	$80.376 \pm 0.033$		0.4
$\Gamma_W$ [GeV]	$2.046 \pm 0.049$	$2.090 \pm 0.001$	-0.9
	$2.196 \pm 0.083$		1.3
$M_H$ [GeV]	$125.6 \pm 0.4$	$125.5 \pm 0.4$	0.1
$\rho_{\gamma W}$	$0.45 \pm 0.31$	$0.01 \pm 0.03$	1.4
	$0.12 \pm 0.43$	$0.00 \pm 0.03$	0.3
$\rho_{\gamma Z}$	$0.08 \pm 0.28$	$0.01 \pm 0.04$	0.2
$\rho_{ZW}$	$0.30 \pm 0.39$	$0.00 \pm 0.01$	0.8
$g_V^{\nu e}$	$-0.040 \pm 0.015$	$-0.0397 \pm 0.0001$	0.0
$g_A^{\nu e}$	$-0.507 \pm 0.014$	$-0.5064$	0.0
$Q_W(e)$	$-0.0403 \pm 0.0053$	$-0.0473 \pm 0.0003$	1.3
$Q_W(p)$	$0.064 \pm 0.012$	$0.0708 \pm 0.0003$	-0.6
$Q_W(\text{Cs})$	$-72.62 \pm 0.43$	$-73.25 \pm 0.01$	1.5
$Q_W(\text{Tl})$	$-116.4 \pm 3.6$	$-116.90 \pm 0.02$	0.1
$\hat{s}_Z^2(\text{eDIS})$	$0.2299 \pm 0.0043$	$0.23126 \pm 0.00005$	-0.3
$\tau_\tau$ [fs]	$291.13 \pm 0.43$	$291.19 \pm 2.41$	0.0
$\frac{1}{2}(g_\mu - 2 - \frac{\alpha}{\pi})$	$(4511.07 \pm 0.79) \times 10^{-9}$	$(4508.68 \pm 0.08) \times 10^{-9}$	3.0

should yield approximately Gaussian *combined* errors by the large number theorem. An exception is the theory dominated error on the  $\tau$  lifetime, which we recalculate in each  $\chi^2$ -function call since it depends itself on  $\alpha_s$ . Sizes and shapes of the output errors (the uncertainties of the predictions and the SM fit parameters) are fully determined by the fit, and  $1 \sigma$  errors are defined to correspond to  $\Delta\chi^2 = \chi^2 - \chi_{\min}^2 = 1$ , and do not necessarily correspond to the 68.3% probability range or the 39.3% probability contour

**Table 10.5:** Principal  $Z$  pole observables and their SM predictions (*cf.* Table 10.4). The first  $\bar{s}_\ell^2$  is the effective weak mixing angle extracted from the hadronic charge asymmetry, the second is the combined value from the Tevatron [163,164,165], and the third from the LHC [168,169]. The values of  $A_e$  are (i) from  $A_{LR}$  for hadronic final states [154]; (ii) from  $A_{LR}$  for leptonic final states and from polarized Bhabba scattering [156]; and (iii) from the angular distribution of the  $\tau$  polarization at LEP 1. The  $A_\tau$  values are from SLD and the total  $\tau$  polarization, respectively.

Quantity	Value	Standard Model	Pull
$M_Z$ [GeV]	$91.1876 \pm 0.0021$	$91.1880 \pm 0.0020$	-0.2
$\Gamma_Z$ [GeV]	$2.4952 \pm 0.0023$	$2.4955 \pm 0.0009$	-0.1
$\Gamma(\text{had})$ [GeV]	$1.7444 \pm 0.0020$	$1.7420 \pm 0.0008$	—
$\Gamma(\text{inv})$ [MeV]	$499.0 \pm 1.5$	$501.66 \pm 0.05$	—
$\Gamma(\ell^+\ell^-)$ [MeV]	$83.984 \pm 0.086$	$83.995 \pm 0.010$	—
$\sigma_{\text{had}}$ [nb]	$41.541 \pm 0.037$	$41.479 \pm 0.008$	1.7
$R_e$	$20.804 \pm 0.050$	$20.740 \pm 0.010$	1.3
$R_\mu$	$20.785 \pm 0.033$	$20.740 \pm 0.010$	1.4
$R_\tau$	$20.764 \pm 0.045$	$20.785 \pm 0.010$	-0.5
$R_b$	$0.21629 \pm 0.00066$	$0.21576 \pm 0.00003$	0.8
$R_c$	$0.1721 \pm 0.0030$	$0.17226 \pm 0.00003$	-0.1
$A_{FB}^{(0,e)}$	$0.0145 \pm 0.0025$	$0.01616 \pm 0.00008$	-0.7
$A_{FB}^{(0,\mu)}$	$0.0169 \pm 0.0013$		0.6
$A_{FB}^{(0,\tau)}$	$0.0188 \pm 0.0017$		1.6
$A_{FB}^{(0,b)}$	$0.0992 \pm 0.0016$	$0.1029 \pm 0.0003$	-2.3
$A_{FB}^{(0,c)}$	$0.0707 \pm 0.0035$	$0.0735 \pm 0.0002$	-0.8
$A_{FB}^{(0,s)}$	$0.0976 \pm 0.0114$	$0.1030 \pm 0.0003$	-0.5
$\bar{s}_\ell^2$	$0.2324 \pm 0.0012$	$0.23155 \pm 0.00005$	0.7
	$0.23176 \pm 0.00060$		0.3
	$0.2297 \pm 0.0010$		-1.9
$A_e$	$0.15138 \pm 0.00216$	$0.1468 \pm 0.0004$	2.1
	$0.1544 \pm 0.0060$		1.3
	$0.1498 \pm 0.0049$		0.6
$A_\mu$	$0.142 \pm 0.015$		-0.3
$A_\tau$	$0.136 \pm 0.015$		-0.7
	$0.1439 \pm 0.0043$		-0.7
$A_b$	$0.923 \pm 0.020$	0.9347	-0.6
$A_c$	$0.670 \pm 0.027$	$0.6676 \pm 0.0002$	0.1
$A_s$	$0.895 \pm 0.091$	0.9356	-0.4

**Table 10.6:** Principal SM fit result including mutual correlations (all masses in GeV). Note that  $\widehat{m}_c(\widehat{m}_c)$  induces a significant uncertainty in the running of  $\alpha$  beyond  $\Delta\alpha_{\text{had}}^{(3)}(1.8 \text{ GeV})$  resulting in a relatively large correlation with  $M_H$ . Since this effect is proportional to the quark's electric charge squared it is much smaller for  $\widehat{m}_b(\widehat{m}_b)$ .

$M_Z$	$91.1880 \pm 0.0020$	1.00	-0.08	0.01	-0.01	0.02	0.04	0.01
$\widehat{m}_t(\widehat{m}_t)$	$164.09 \pm 0.83$	-0.08	1.00	0.00	-0.06	-0.16	0.08	0.06
$\widehat{m}_b(\widehat{m}_b)$	$4.199 \pm 0.024$	0.01	0.00	1.00	0.26	-0.02	0.05	0.02
$\widehat{m}_c(\widehat{m}_c)$	$1.274^{+0.030}_{-0.035}$	-0.01	-0.06	0.26	1.00	0.15	0.08	0.01
$\alpha_s(M_Z)$	$0.1193 \pm 0.0016$	0.02	-0.16	-0.02	0.15	1.00	-0.05	-0.03
$\Delta\alpha_{\text{had}}^{(3)}(1.8 \text{ GeV})$	$0.00559 \pm 0.00008$	0.04	0.08	0.05	0.08	-0.05	1.00	0.05
$M_H$	$125.5 \pm 0.4$	0.01	0.06	0.02	0.01	-0.03	0.05	1.00

(for 2 parameters).

The agreement is generally very good. Despite the few discrepancies discussed in the following, the fit describes the data well, with a  $\chi^2/\text{d.o.f.} = 48.3/44$ . The probability of a larger  $\chi^2$  is 30%. Only the final result for  $g_\mu - 2$  from BNL is currently showing a large ( $3.0 \sigma$ ) deviation. In addition,  $A_{FB}^{(0,b)}$  from LEP 1 and  $A_{LR}^0$  (SLD) from hadronic final states differ by more than  $2 \sigma$ .  $g_L^2$  from NuTeV is nominally in conflict with the SM, as well, but the precise status is under investigation (see Sec. 10.3).

$A_b$  can be extracted from  $A_{FB}^{(0,b)}$  when  $A_e = 0.1501 \pm 0.0016$  is taken from a fit to leptonic asymmetries (using lepton universality). The result,  $A_b = 0.881 \pm 0.017$ , is  $3.2 \sigma$  below the SM prediction<sup>§</sup> and also  $1.6 \sigma$  below  $A_b = 0.923 \pm 0.020$  obtained from  $A_{LR}^{FB}(b)$  at SLD. Thus, it appears that at least some of the problem in  $A_b$  is due to a statistical fluctuation or other experimental effect in one of the asymmetries. Note, however, that the uncertainty in  $A_{FB}^{(0,b)}$  is strongly statistics dominated. The combined value,  $A_b = 0.899 \pm 0.013$  deviates by  $2.8 \sigma$ . It would be difficult to account for this 4.0% deviation by new physics that enters only at the level of radiative corrections since about a 20% correction to  $\widehat{\kappa}_b$  would be necessary to account for the central value of  $A_b$  [222]. If this deviation is due to new physics, it is most likely of tree-level type affecting preferentially the third generation. Examples include the decay of a scalar neutrino resonance [223], mixing of the  $b$  quark with heavy exotics [224], and a heavy  $Z'$  with family non-universal couplings [225,226]. It is difficult, however, to simultaneously

<sup>§</sup> Alternatively, one can use  $A_\ell = 0.1481 \pm 0.0027$ , which is from LEP 1 alone and in excellent agreement with the SM, and obtain  $A_b = 0.893 \pm 0.022$  which is  $1.9 \sigma$  low. This illustrates that some of the discrepancy is related to the one in  $A_{LR}$ .

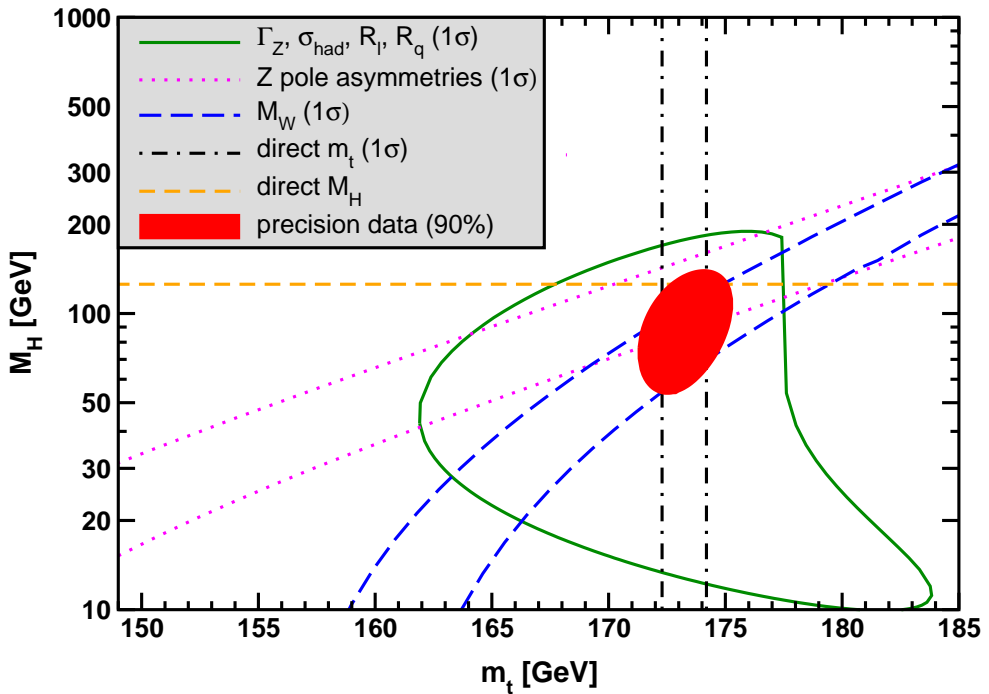


**Figure 10.4:** Fit result and one-standard-deviation (39.35% for the closed contours and 68% for the others) uncertainties in  $M_H$  as a function of  $m_t$  for various inputs, and the 90% CL region ( $\Delta\chi^2 = 4.605$ ) allowed by all data.  $\alpha_s(M_Z) = 0.1185$  is assumed except for the fits including the  $Z$  lineshape. The width of the horizontal dashed (yellow) band is not visible on the scale of the plot.

account for  $R_b$ , which has been measured on the  $Z$  peak and off-peak [227] at LEP 1. An average of  $R_b$  measurements at LEP 2 at energies between 133 and 207 GeV is  $2.1 \sigma$  below the SM prediction, while  $A_{FB}^{(b)}$  (LEP 2) is  $1.6 \sigma$  low [171].

The left-right asymmetry,  $A_{LR}^0 = 0.15138 \pm 0.00216$  [154], based on all hadronic data from 1992–1998 differs  $2.1 \sigma$  from the SM expectation of  $0.1468 \pm 0.0004$ . The combined value of  $A_\ell = 0.1513 \pm 0.0021$  from SLD (using lepton-family universality and including correlations) is also  $2.1 \sigma$  above the SM prediction; but there is experimental agreement between this SLD value and the LEP 1 value,  $A_\ell = 0.1481 \pm 0.0027$ , obtained from a fit to  $A_{FB}^{(0,\ell)}$ ,  $A_e(\mathcal{P}_\tau)$ , and  $A_\tau(\mathcal{P}_\tau)$ , again assuming universality.

The observables in Table 10.4 and Table 10.5, as well as some other less precise observables, are used in the global fits described below. In all fits, the errors include full statistical, systematic, and theoretical uncertainties. The correlations on the LEP 1 lineshape and  $\tau$  polarization, the LEP/SLD heavy flavor observables, the SLD lepton asymmetries, and the  $\nu$ - $e$  scattering observables, are included. The theoretical correlations between  $\Delta\alpha_{\text{had}}^{(5)}$  and  $g_\mu - 2$ , and between the charm and bottom quark masses, are also accounted for.

The data allow a simultaneous determination of  $M_Z$ ,  $M_H$ ,  $m_t$ , and the strong coupling  $\alpha_s(M_Z)$ . ( $\hat{m}_c$ ,  $\hat{m}_b$ , and  $\Delta\alpha_{\text{had}}^{(3)}$  are also allowed to float in the fits, subject to the



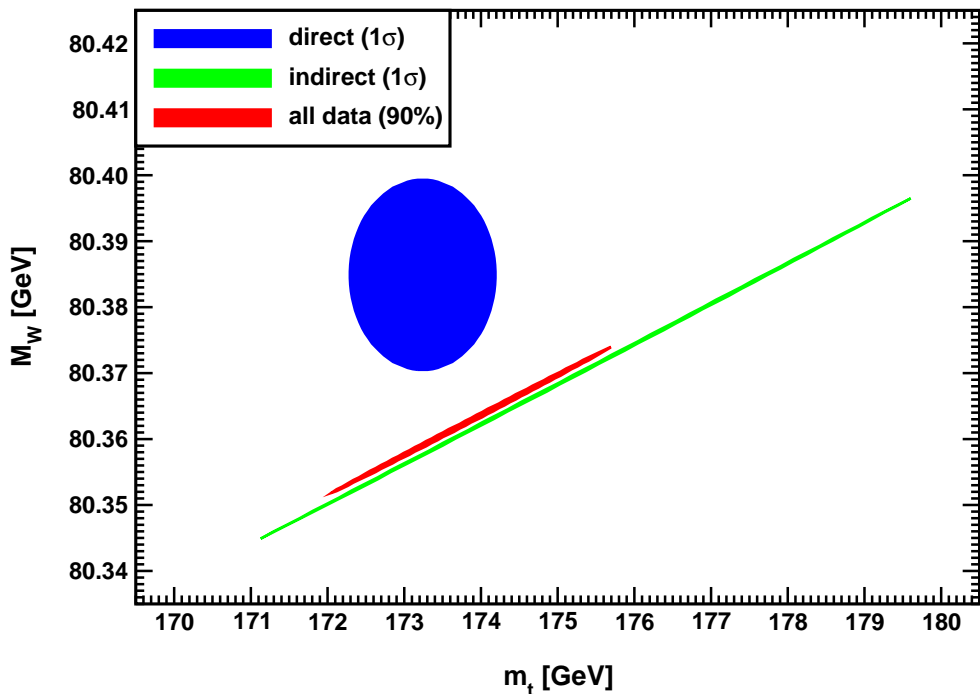


**Figure 10.5:** One-standard-deviation (39.35%) region in  $M_W$  as a function of  $m_t$  for the direct and indirect data, and the 90% CL region ( $\Delta\chi^2 = 4.605$ ) allowed by all data.

theoretical constraints [19,45] described in Sec. 10.2. These are correlated with  $\alpha_s$ .)  $\alpha_s$  is determined mainly from  $R_\ell$ ,  $\Gamma_Z$ ,  $\sigma_{\text{had}}$ , and  $\tau_\tau$ . The global fit to all data, including the hadron collider average  $m_t = 173.24 \pm 0.95$  GeV, yields the result in Table 10.6 (the  $\overline{\text{MS}}$  top quark mass given there corresponds to  $m_t = 173.87 \pm 0.87$  GeV). The weak mixing angle, see Table 10.2, is determined to

$$\hat{s}_Z^2 = 0.23126 \pm 0.00005, \quad s_W^2 = 0.22333 \pm 0.00011,$$

while the corresponding effective angle is  $\overline{s}_\ell^2 = 0.23155 \pm 0.00005$ .

One can also perform a fit without the direct mass constraint,  $M_H = 125.6 \pm 0.4$  GeV, in Eq. (10.47). In this case we obtain a 2% indirect mass determination,

$$M_H = 123.7 \pm 2.3 \text{ GeV} , \quad (10.54)$$

arising predominantly from the quantities in Eq. (10.49), since the branching ratio for  $H \rightarrow ZZ^*$  varies very rapidly as a function of  $M_H$  for Higgs masses near 125 GeV. It is interesting to note that this value is closer to the ATLAS Higgs mass measurement in the  $ZZ^*$  channel,  $M_H = 124.3_{-0.5}^{+0.6}(\text{stat.})_{-0.3}^{+0.5}(\text{syst.})$  GeV, which differs by more than  $2\sigma$  from their  $\gamma\gamma$  result,  $M_H = 126.8 \pm 0.2_{\text{stat.}} \pm 0.7_{\text{syst.}}$  GeV. Removing also the branching ratio constraints gives the loop-level determination from the precision data alone,

$$M_H = 89_{-18}^{+22} \text{ GeV} , \quad (10.55)$$

**Table 10.7:** Values of  $\hat{s}_Z^2$ ,  $s_W^2$ ,  $\alpha_s$ ,  $m_t$  and  $M_H$  [both in GeV] for various data sets. The  $M_H$  constraint refers collectively to the kinematical and decay information from Sec. 10.4.5. In the fit to the LHC (Tevatron) data the  $\alpha_s$  constraint is from the  $t\bar{t}$  production [228] (inclusive jet [229]) cross section.

Data	$\hat{s}_Z^2$	$s_W^2$	$\alpha_s(M_Z)$	$m_t$	$M_H$
All data	0.23126(5)	0.22333(11)	0.1193(16)	$173.9 \pm 0.9$	$125.5 \pm 0.4$
All data except $M_H$	0.23112(10)	0.22304(22)	0.1195(17)	$173.3 \pm 0.9$	$89_{-18}^{+22}$
All data except $M_Z$	0.23119(7)	0.22330(11)	0.1192(16)	$173.4 \pm 0.9$	$125.6 \pm 0.4$
All data except $M_W$	0.23129(5)	0.22341(12)	0.1196(17)	$173.3 \pm 0.9$	$125.6 \pm 0.4$
All data except $m_t$	0.23118(7)	0.22298(25)	0.1196(17)	$177.0 \pm 2.1$	$125.6 \pm 0.4$
$M_H, M_Z, \Gamma_Z, m_t$	0.23126(9)	0.22339(17)	0.1190(45)	$173.2 \pm 0.9$	$125.6 \pm 0.4$
LHC	0.2294(10)	0.2215(10)	0.1151(46)	$173.3 \pm 1.1$	$125.6 \pm 0.4$
Tevatron + $M_Z$	0.23106(15)	0.22295(32)	0.1160(44)	$173.2 \pm 1.0$	$90_{-26}^{+32}$
LEP	0.23143(18)	0.22348(46)	0.1214(31)	$180 \pm 11$	$240_{-134}^{+333}$
SLD + $M_Z, \Gamma_Z, m_t$	0.23067(28)	0.22220(55)	0.1162(46)	$173.2 \pm 0.9$	$40_{-22}^{+31}$
$A_{FB}^{(b,c)}, M_Z, \Gamma_Z, m_t$	0.23193(29)	0.22497(70)	0.1261(50)	$173.2 \pm 0.9$	$363_{-132}^{+206}$
$M_{W,Z}, \Gamma_{W,Z}, m_t$	0.23105(14)	0.22292(29)	0.1173(43)	$173.2 \pm 0.9$	$86_{-23}^{+27}$
low energy + $M_{H,Z}$	0.2327(14)	0.2289(54)	0.1195(21)	$123 \pm 44$	$125.6 \pm 0.4$

which is  $1.5 \sigma$  below the kinematical constraint. This is mostly a reflection of the Tevatron determination of  $M_W$ , which is  $1.5 \sigma$  higher than the SM best fit value in Table 10.4. Another consequence is that the 90% central confidence range determined from the precision data,

$$60 \text{ GeV} < M_H < 127 \text{ GeV} , \quad (10.56)$$

is only marginally consistent with Eq. (10.47). This is illustrated in Fig. 10.4 where one sees that the precision data together with  $M_H$  from the LHC prefer that  $m_t$  is closer to the upper end of its  $1\sigma$  allowed range. Conversely, one can remove the direct  $M_W$  and  $\Gamma_W$  constraints from the fits and use Eq. (10.47) to obtain  $M_W = 80.358 \pm 0.007 \text{ GeV}$ . This is  $1.7 \sigma$  below the Tevatron/LEP 2 average,  $M_W = 80.385 \pm 0.015 \text{ GeV}$ .

Finally, one can carry out a fit without including the constraint,  $m_t = 173.24 \pm 0.95 \text{ GeV}$ , from the hadron colliders. (The indirect prediction is for the  $\overline{\text{MS}}$  mass,  $\hat{m}_t(\hat{m}_t) = 167.1 \pm 2.0 \text{ GeV}$ , which is in the end converted to the pole mass.) One obtains  $m_t = 177.0 \pm 2.1 \text{ GeV}$ , which is  $1.6 \sigma$  higher than the direct Tevatron/LHC average. The situation is summarized in Fig. 10.5 showing the  $1 \sigma$  contours in the  $M_W$ - $m_t$  plane from the direct and indirect determinations, as well as the combined 90% CL region.

As described in Sec. 10.2 and the paragraph following Eq. (10.52) in Sec. 10.5, there is considerable stress in the experimental  $e^+e^-$  spectral functions and also conflict when these are compared with  $\tau$  decay spectral functions. These are below or above the  $2\sigma$  level (depending on what is actually compared) but not larger than the deviations of some other quantities entering our analyses. The number and size of these deviations are not inconsistent with what one would expect to happen as a result of random fluctuations. It is nevertheless instructive to study the effect of doubling the uncertainty in  $\Delta\alpha_{\text{had}}^{(3)}(1.8 \text{ GeV}) = (55.50 \pm 0.78) \times 10^{-4}$  (see Sec. 10.2) on the loop-level determination. The result,  $M_H = 86_{-18}^{+22} \text{ GeV}$ , deviates even slightly *more* ( $1.6 \sigma$ ) than Eq. (10.55), and demonstrates that the uncertainty in  $\Delta\alpha_{\text{had}}$  is currently of only secondary importance. Note also that a shift of  $\pm 10^{-4}$  in  $\Delta\alpha_{\text{had}}^{(3)}(1.8 \text{ GeV})$  corresponds to a shift of  $\mp 4.3 \text{ GeV}$  in  $M_H$ . The hadronic contribution to  $\alpha(M_Z)$  is correlated with  $g_\mu - 2$  (see Sec. 10.5). The measurement of the latter is higher than the SM prediction, and its inclusion in the fit favors a larger  $\alpha(M_Z)$  and a lower  $M_H$  from the precision data (currently by  $3.4 \text{ GeV}$ ).

The weak mixing angle can be determined from  $Z$  pole observables,  $M_W$ , and from a variety of neutral-current processes spanning a very wide  $Q^2$  range. The results (for the older low energy neutral-current data see Refs. 113 and 218, as well as earlier editions of this *Review*) shown in Table 10.7 are in reasonable agreement with each other, indicating the quantitative success of the SM. The largest discrepancy is the value  $\hat{s}_Z^2 = 0.23193 \pm 0.00029$  from the forward-backward asymmetries into bottom and charm quarks, which is  $2.3 \sigma$  above the value  $0.23126 \pm 0.00005$  from the global fit to all data, see Table 10.5. Similarly,  $\hat{s}_Z^2 = 0.23067 \pm 0.00028$  from the SLD asymmetries (in both cases when combined with  $M_Z$ ) is  $2.1 \sigma$  low. The SLD result has the additional difficulty (within the SM) of implying very low and excluded [230] Higgs masses. This is also true for  $\hat{s}_Z^2 = 0.23105 \pm 0.00014$  from  $M_W$  and  $M_Z$  and, as a consequence, for the global fit.

The extracted  $Z$  pole value of  $\alpha_s(M_Z)$  is based on a formula with negligible theoretical uncertainty if one assumes the exact validity of the SM. One should keep in mind, however, that this value,  $\alpha_s(M_Z) = 0.1197 \pm 0.0027$ , is very sensitive to certain types of new physics such as non-universal vertex corrections. In contrast, the value derived from  $\tau$  decays,  $\alpha_s(M_Z) = 0.1193_{-0.0020}^{+0.0022}$ , is theory dominated but less sensitive to new physics. The two values are in remarkable agreement with each other. They are also in perfect agreement with the averages from jet-event shapes in  $e^+e^-$  annihilation ( $0.1177 \pm 0.0046$ ) and lattice simulations ( $0.1185 \pm 0.0005$ ), whereas the DIS average ( $0.1154 \pm 0.0020$ ) is somewhat lower. For more details, other determinations, and references, see Section 9 on “Quantum Chromodynamics” in this *Review*.

Using  $\alpha(M_Z)$  and  $\hat{s}_Z^2$  as inputs, one can predict  $\alpha_s(M_Z)$  assuming grand unification. One finds [231]  $\alpha_s(M_Z) = 0.130 \pm 0.001 \pm 0.01$  for the simplest theories based on the minimal supersymmetric extension of the SM, where the first (second) uncertainty is from the inputs (thresholds). This is slightly larger, but consistent with  $\alpha_s(M_Z) = 0.1193 \pm 0.0016$  from our fit, as well as with most other determinations. Non-supersymmetric unified theories predict the low value  $\alpha_s(M_Z) = 0.073 \pm 0.001 \pm 0.001$ . See also the note on “Supersymmetry” in the Searches Particle Listings.

Most of the parameters relevant to  $\nu$ -hadron,  $\nu$ - $e$ ,  $e$ -hadron, and  $e^-e^\pm$  processes are

**Table 10.8:** Values of the model-independent neutral-current parameters, compared with the SM predictions. There is a second  $g_{LV,LA}^{\nu e}$  solution, given approximately by  $g_{LV}^{\nu e} \leftrightarrow g_{LA}^{\nu e}$ , which is eliminated by  $e^+e^-$  data under the assumption that the neutral current is dominated by the exchange of a single  $Z$  boson. The  $g_{LL}^{\nu q}$ , as well as the  $g_{LR}^{\nu q}$ , are strongly correlated and non-Gaussian, so that for implementations we recommend the parametrization using  $g_i^2$  and  $\tan \theta_i = g_{Li}^{\nu u}/g_{Li}^{\nu d}$  where  $i = L, R$ . In the SM predictions, the parametric uncertainties from  $M_Z$ ,  $M_H$ ,  $m_t$ ,  $m_b$ ,  $m_c$ ,  $\hat{\alpha}(M_Z)$ , and  $\alpha_s$  are negligible.

Quantity	Experimental Value	Standard Model	Correlation	
$g_{LL}^{\nu u}$	$0.328 \pm 0.016$	0.3457		
$g_{LL}^{\nu d}$	$-0.440 \pm 0.011$	-0.4288	non-	
$g_{LR}^{\nu u}$	$-0.179 \pm 0.013$	-0.1553	Gaussian	
$g_{LR}^{\nu d}$	$-0.027^{+0.077}_{-0.048}$	0.0777		
$g_L^2$	$0.3005 \pm 0.0028$	0.3034		
$g_R^2$	$0.0329 \pm 0.0030$	0.0301	small	
$\tan \theta_L$	$2.50 \pm 0.035$	2.4630		
$\tan \theta_R$	$4.56^{+0.42}_{-0.27}$	5.1765		
$g_{LV}^{\nu e}$	$-0.040 \pm 0.015$	-0.0396	-0.05	
$g_{LA}^{\nu e}$	$-0.507 \pm 0.014$	-0.5064		
$g_{AV}^{eu} + 2g_{AV}^{ed}$	$0.489 \pm 0.005$	0.4951	-0.94	0.42
$2g_{AV}^{eu} - g_{AV}^{ed}$	$-0.708 \pm 0.016$	-0.7192	-0.45	
$2g_{VA}^{eu} - g_{VA}^{ed}$	$-0.144 \pm 0.068$	-0.0950		
$g_{VA}^{ee}$	$0.0190 \pm 0.0027$	0.0225		

determined uniquely and precisely from the data in “model-independent” fits (*i.e.*, fits which allow for an arbitrary EW gauge theory). The values for the parameters defined in Eqs. (10.16)–(10.17) are given in Table 10.8 along with the predictions of the SM. The agreement is very good. (The  $\nu$ -hadron results including the original NuTeV data can be found in the 2006 edition of this *Review*, and fits with modified NuTeV constraints in the 2008 and 2010 editions.) The off  $Z$  pole  $e^+e^-$  results are difficult to present in a model-independent way because  $Z$  propagator effects are non-negligible at TRISTAN, PETRA, PEP, and LEP 2 energies. However, assuming  $e$ - $\mu$ - $\tau$  universality, the low energy lepton asymmetries imply [151]  $4(g_A^e)^2 = 0.99 \pm 0.05$ , in good agreement with the SM prediction  $\simeq 1$ .

## 10.7. Constraints on new physics

The masses and decay properties of the electroweak bosons and low energy data can be used to search for and set limits on deviations from the SM. We will mainly discuss the effects of exotic particles (with heavy masses  $M_{\text{new}} \gg M_Z$  in an expansion in  $M_Z/M_{\text{new}}$ ) on the gauge boson self-energies. (Brief remarks are made on new physics which is not of this type.) Most of the effects on precision measurements can be described by three gauge self-energy parameters  $S$ ,  $T$ , and  $U$ . We will define these, as well as the related parameters  $\rho_0$ ,  $\epsilon_i$ , and  $\hat{\epsilon}_i$ , to arise from new physics only. In other words, they are equal to zero ( $\rho_0 = 1$ ) exactly in the SM, and do not include any (loop induced) contributions that depend on  $m_t$  or  $M_H$ , which are treated separately. Our treatment differs from most of the original papers.

The dominant effect of many extensions of the SM can be described by the  $\rho_0$  parameter,

$$\rho_0 \equiv \frac{M_W^2}{M_Z^2 \hat{c}_Z^2 \hat{\rho}}, \quad (10.57)$$

which describes new sources of SU(2) breaking that cannot be accounted for by the SM Higgs doublet or  $m_t$  effects.  $\hat{\rho}$  is calculated as in Eq. (10.12) assuming the validity of the SM. In the presence of  $\rho_0 \neq 1$ , Eq. (10.57) generalizes the second Eq. (10.12) while the first remains unchanged. Provided that the new physics which yields  $\rho_0 \neq 1$  is a small perturbation which does not significantly affect other radiative corrections,  $\rho_0$  can be regarded as a phenomenological parameter which multiplies  $G_F$  in Eqs. (10.16)–(10.17), (10.32), and  $\Gamma_Z$  in Eq. (10.44c). There are enough data to determine  $\rho_0$ ,  $M_H$ ,  $m_t$ , and  $\alpha_s$ , simultaneously. From the global fit,

$$\rho_0 = 1.00040 \pm 0.00024, \quad (10.58)$$

$$\alpha_s(M_Z) = 0.1194 \pm 0.0017, \quad (10.59)$$

and  $M_H$  and  $m_t$  are as given in Table 10.6 and Table 10.5. The result in Eq. (10.58) is 1.7  $\sigma$  above the SM expectation,  $\rho_0 = 1$ . It can be used to constrain higher-dimensional Higgs representations to have vacuum expectation values of less than a few percent of those of the doublets. Indeed, the relation between  $M_W$  and  $M_Z$  is modified if there are Higgs multiplets with weak isospin  $> 1/2$  with significant vacuum expectation values. For a general (charge-conserving) Higgs structure,

$$\rho_0 = \frac{\sum_i [t(i)(t(i) + 1) - t_3(i)^2] |v_i|^2}{2 \sum_i t_3(i)^2 |v_i|^2}, \quad (10.60)$$

where  $v_i$  is the expectation value of the neutral component of a Higgs multiplet with weak isospin  $t(i)$  and third component  $t_3(i)$ . In order to calculate to higher orders in such theories one must define a set of four fundamental renormalized parameters which one may conveniently choose to be  $\alpha$ ,  $G_F$ ,  $M_Z$ , and  $M_W$ , since  $M_W$  and  $M_Z$  are directly measurable. Then  $\hat{s}_Z^2$  and  $\rho_0$  can be considered dependent parameters.

Eq. (10.58) can also be used to constrain other types of new physics. For example, non-degenerate multiplets of heavy fermions or scalars break the vector part of weak SU(2) and lead to a decrease in the value of  $M_Z/M_W$ . Each non-degenerate SU(2) doublet  $\begin{pmatrix} f_1 \\ f_2 \end{pmatrix}$  yields a positive contribution to  $\rho_0$  [232] of

$$\frac{C G_F}{8\sqrt{2}\pi^2} \Delta m^2, \quad (10.61)$$

where

$$\Delta m^2 \equiv m_1^2 + m_2^2 - \frac{4m_1^2 m_2^2}{m_1^2 - m_2^2} \ln \frac{m_1}{m_2} \geq (m_1 - m_2)^2, \quad (10.62)$$

and  $C = 1$  (3) for color singlets (triplets). Eq. (10.58) taken together with Eq. (10.61) implies the following constraint on the mass splitting at the 95% CL,

$$\sum_i \frac{C_i}{3} \Delta m_i^2 \leq (50 \text{ GeV})^2. \quad (10.63)$$

where the sum runs over all new-physics doublets, for example fourth-family quarks or leptons,  $\begin{pmatrix} t' \\ b' \end{pmatrix}$  or  $\begin{pmatrix} \nu' \\ \ell' \end{pmatrix}$ , vector-like fermion doublets (which contribute to the sum in Eq. (10.63) with an extra factor of 2), and scalar doublets such as  $\begin{pmatrix} \tilde{t} \\ \tilde{b} \end{pmatrix}$  in Supersymmetry (in the absence of  $L$ - $R$  mixing).

Non-degenerate multiplets usually imply  $\rho_0 > 1$ . Similarly, heavy  $Z'$  bosons decrease the prediction for  $M_Z$  due to mixing and generally lead to  $\rho_0 > 1$  [233]. On the other hand, additional Higgs doublets which participate in spontaneous symmetry breaking [234] or heavy lepton doublets involving Majorana neutrinos [235], both of which have more complicated expressions, as well as the vacuum expectation values of Higgs triplets or higher-dimensional representations can contribute to  $\rho_0$  with either sign. Allowing for the presence of heavy degenerate chiral multiplets (the  $S$  parameter, to be discussed below) affects the determination of  $\rho_0$  from the data, at present leading to a slightly larger value.

A number of authors [236–241] have considered the general effects on neutral-current and  $Z$  and  $W$  boson observables of various types of heavy (*i.e.*,  $M_{\text{new}} \gg M_Z$ ) physics which contribute to the  $W$  and  $Z$  self-energies but which do not have any direct coupling to the ordinary fermions. In addition to non-degenerate multiplets, which break the vector part of weak SU(2), these include heavy degenerate multiplets of chiral fermions which break the axial generators.

Such effects can be described by just three parameters,  $S$ ,  $T$ , and  $U$ , at the (EW) one-loop level. (Three additional parameters are needed if the new physics scale is comparable to  $M_Z$  [242]. Further generalizations, including effects relevant to LEP 2, are described in Ref. 243.)  $T$  is proportional to the difference between the  $W$  and  $Z$  self-energies at  $Q^2 = 0$  (*i.e.*, vector SU(2)-breaking), while  $S$  ( $S + U$ ) is associated with the difference between the  $Z$  ( $W$ ) self-energy at  $Q^2 = M_{Z,W}^2$  and  $Q^2 = 0$  (axial

SU(2)-breaking). Denoting the contributions of new physics to the various self-energies by  $\Pi_{ij}^{\text{new}}$ , we have

$$\widehat{\alpha}(M_Z)T \equiv \frac{\Pi_{WW}^{\text{new}}(0)}{M_W^2} - \frac{\Pi_{ZZ}^{\text{new}}(0)}{M_Z^2}, \quad (10.64a)$$

$$\frac{\widehat{\alpha}(M_Z)}{4\widehat{s}_Z^2\widehat{c}_Z^2}S \equiv \frac{\Pi_{ZZ}^{\text{new}}(M_Z^2) - \Pi_{ZZ}^{\text{new}}(0)}{M_Z^2} - \frac{\widehat{c}_Z^2 - \widehat{s}_Z^2}{\widehat{c}_Z\widehat{s}_Z} \frac{\Pi_{Z\gamma}^{\text{new}}(M_Z^2)}{M_Z^2} - \frac{\Pi_{\gamma\gamma}^{\text{new}}(M_Z^2)}{M_Z^2}, \quad (10.64b)$$

$$\frac{\widehat{\alpha}(M_Z)}{4\widehat{s}_Z^2}(S+U) \equiv \frac{\Pi_{WW}^{\text{new}}(M_W^2) - \Pi_{WW}^{\text{new}}(0)}{M_W^2} - \frac{\widehat{c}_Z}{\widehat{s}_Z} \frac{\Pi_{Z\gamma}^{\text{new}}(M_Z^2)}{M_Z^2} - \frac{\Pi_{\gamma\gamma}^{\text{new}}(M_Z^2)}{M_Z^2}. \quad (10.64c)$$

$S$ ,  $T$ , and  $U$  are defined with a factor proportional to  $\widehat{\alpha}$  removed, so that they are expected to be of order unity in the presence of new physics. In the  $\overline{\text{MS}}$  scheme as defined in Ref. 53, the last two terms in Eqs. (10.64b) and (10.64c) can be omitted (as was done in some earlier editions of this *Review*). These three parameters are related to other parameters ( $S_i$ ,  $h_i$ ,  $\widehat{\epsilon}_i$ ) defined in Refs. [53,237,238] by

$$\begin{aligned} T &= h_V = \widehat{\epsilon}_1/\widehat{\alpha}(M_Z), \\ S &= h_{AZ} = S_Z = 4\widehat{s}_Z^2\widehat{\epsilon}_3/\widehat{\alpha}(M_Z), \\ U &= h_{AW} - h_{AZ} = S_W - S_Z = -4\widehat{s}_Z^2\widehat{\epsilon}_2/\widehat{\alpha}(M_Z). \end{aligned} \quad (10.65)$$

A heavy non-degenerate multiplet of fermions or scalars contributes positively to  $T$  as

$$\rho_0 - 1 = \frac{1}{1 - \widehat{\alpha}(M_Z)T} - 1 \simeq \widehat{\alpha}(M_Z)T, \quad (10.66)$$

where  $\rho_0 - 1$  is given in Eq. (10.61). The effects of non-standard Higgs representations cannot be separated from heavy non-degenerate multiplets unless the new physics has other consequences, such as vertex corrections. Most of the original papers defined  $T$  to include the effects of loops only. However, we will redefine  $T$  to include all new sources of SU(2) breaking, including non-standard Higgs, so that  $T$  and  $\rho_0$  are equivalent by Eq. (10.66).

A multiplet of heavy degenerate chiral fermions yields

$$S = \frac{C}{3\pi} \sum_i \left( t_{3L}(i) - t_{3R}(i) \right)^2, \quad (10.67)$$

where  $t_{3L,R}(i)$  is the third component of weak isospin of the left-(right-)handed component of fermion  $i$  and  $C$  is the number of colors. For example, a heavy degenerate ordinary

or mirror family would contribute  $2/3\pi$  to  $S$ . In models with warped extra dimensions, sizeable correction to the  $S$  parameter are generated by mixing effects between the SM gauge bosons and their Kaluza-Klein (KK) excitations. One finds  $S \approx 30v^2/M_{KK}^2$ , where  $M_{KK}$  is the mass of the KK gauge bosons [244]. Large positive values  $S > 0$  can also be generated in Technicolor models with QCD-like dynamics, where one expects [236]  $S \sim 0.45$  for an iso-doublet of techni-fermions, assuming  $N_{TC} = 4$  techni-colors, while  $S \sim 1.62$  for a full techni-generation with  $N_{TC} = 4$ . However, the QCD-like models are excluded on other grounds (flavor changing neutral currents, too-light quarks and pseudo-Goldstone bosons [245], and absence of a Higgs-like scalar).

On the other hand, negative values  $S < 0$  are possible, for example, for models of walking Technicolor [246] or loops involving scalars or Majorana particles [247]. The simplest origin of  $S < 0$  would probably be an additional heavy  $Z'$  boson [233]. Supersymmetric extensions of the SM generally give very small effects. See Refs. 248 and 249 and the note on ‘‘Supersymmetry’’ in the Searches Particle Listings for a complete set of references.

Most simple types of new physics yield  $U = 0$ , although there are counter-examples, such as the effects of anomalous triple gauge vertices [238].

The SM expressions for observables are replaced by

$$\begin{aligned} M_Z^2 &= M_{Z0}^2 \frac{1 - \widehat{\alpha}(M_Z)T}{1 - G_F M_{Z0}^2 S / 2\sqrt{2}\pi}, \\ M_W^2 &= M_{W0}^2 \frac{1}{1 - G_F M_{W0}^2 (S + U) / 2\sqrt{2}\pi}, \end{aligned} \quad (10.68)$$

where  $M_{Z0}$  and  $M_{W0}$  are the SM expressions (as functions of  $m_t$  and  $M_H$ ) in the  $\overline{\text{MS}}$  scheme. Furthermore,

$$\Gamma_Z = \frac{M_Z^3 \beta_Z}{1 - \widehat{\alpha}(M_Z)T}, \quad \Gamma_W = M_W^3 \beta_W, \quad A_i = \frac{A_{i0}}{1 - \widehat{\alpha}(M_Z)T}, \quad (10.69)$$

where  $\beta_Z$  and  $\beta_W$  are the SM expressions for the reduced widths  $\Gamma_{Z0}/M_{Z0}^3$  and  $\Gamma_{W0}/M_{W0}^3$ ,  $M_Z$  and  $M_W$  are the physical masses, and  $A_i$  ( $A_{i0}$ ) is a neutral-current amplitude (in the SM).

The data allow a simultaneous determination of  $\widehat{s}_Z^2$  (from the  $Z$  pole asymmetries),  $S$  (from  $M_Z$ ),  $U$  (from  $M_W$ ),  $T$  (mainly from  $\Gamma_Z$ ),  $\alpha_s$  (from  $R_\ell$ ,  $\sigma_{\text{had}}$ , and  $\tau_\tau$ ),  $M_H$  and  $m_t$  (from the hadron colliders), with little correlation among the SM parameters:

$$\begin{aligned} S &= -0.03 \pm 0.10, \\ T &= 0.01 \pm 0.12, \\ U &= 0.05 \pm 0.10, \end{aligned} \quad (10.70)$$

$\widehat{s}_Z^2 = 0.23119 \pm 0.00016$ , and  $\alpha_s(M_Z) = 0.1196 \pm 0.0017$ , where the uncertainties are from the inputs. The parameters in Eqs. (10.70), which by definition are due to new physics



only, are in excellent agreement with the SM values of zero. Fixing  $U = 0$  (as is also done in Fig. 10.6) moves  $S$  and  $T$  slightly upwards,

$$\begin{aligned} S &= 0.00 \pm 0.08, \\ T &= 0.05 \pm 0.07. \end{aligned} \tag{10.71}$$

Again, good agreement with the SM is observed. If only any one of the three parameters is allowed, then this parameter would deviate at the 1.5 to 1.7  $\sigma$  level, reflecting the deviation in  $M_W$ . Using Eq. (10.66), the value of  $\rho_0$  corresponding to  $T$  in Eq. (10.70) is  $1.0000 \pm 0.0009$ , while the one corresponding to Eq. (10.71) is  $1.0004 \pm 0.0005$ .

There is a strong correlation (90%) between the  $S$  and  $T$  parameters. The  $U$  parameter is  $-59\%$  ( $-81\%$ ) anti-correlated with  $S$  ( $T$ ). The allowed regions in  $S$ - $T$  are shown in Fig. 10.6. From Eqs. (10.70) one obtains  $S \leq 0.14$  and  $T \leq 0.20$  at 95% CL, where the former puts the constraint  $M_{KK} \gtrsim 3.5$  TeV on the masses of KK gauge bosons in warped extra dimensions.

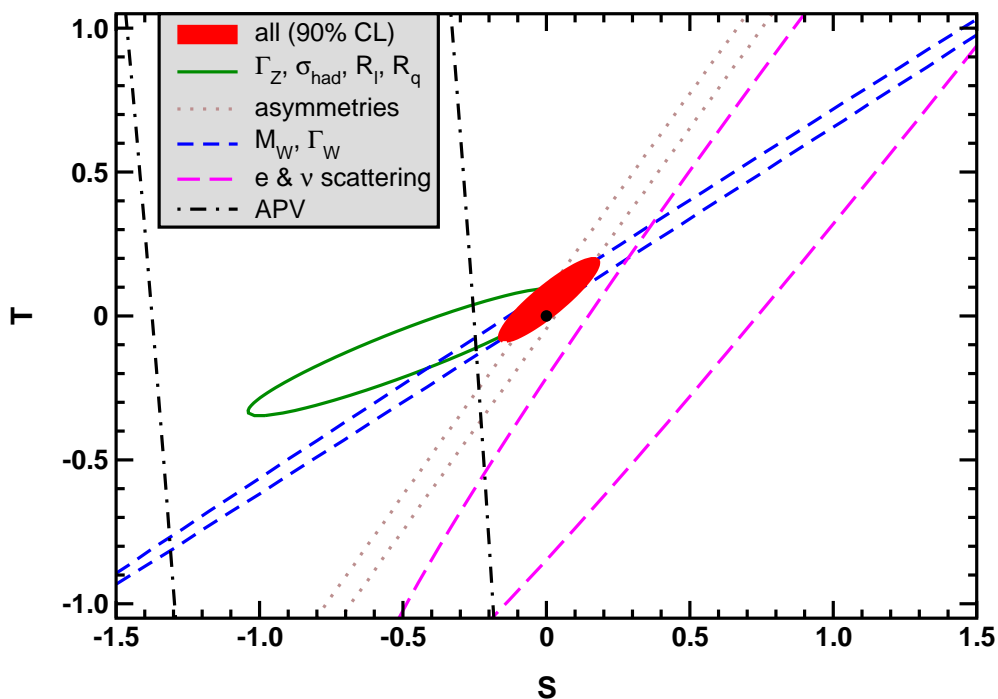


**Figure 10.6:**  $1 \sigma$  constraints (39.35%) on  $S$  and  $T$  (for  $U = 0$ ) from various inputs combined with  $M_Z$ .  $S$  and  $T$  represent the contributions of new physics only. Data sets not involving  $M_W$  or  $\Gamma_W$  are insensitive to  $U$ . With the exception of the fit to all data, we fix  $\alpha_s = 0.1185$ . The black dot indicates the Standard Model values  $S = T = 0$ .

The  $S$  parameter can also be used to constrain the number of fermion families, *under the assumption* that there are no new contributions to  $T$  or  $U$  and therefore that any new families are degenerate; then an extra generation of SM fermions is excluded at

the  $7\sigma$  level corresponding to  $N_F = 2.75 \pm 0.17$ . This can be compared to the fit to the number of light neutrinos given in Eq. (10.37),  $N_\nu = 2.990 \pm 0.007$ . However, the  $S$  parameter fits are valid even for a very heavy fourth family neutrino. Allowing  $T$  to vary as well, the constraint on a fourth family is weaker [250]. However, a heavy fourth family would increase the Higgs production cross section through gluon fusion by a factor  $\sim 9$ , which is in considerable tension with the observed Higgs signal at LHC. Combining the limits from electroweak precision data with the measured Higgs production rate and limits from direct searches for heavy quarks [251], a fourth family of chiral fermions is now excluded by more than five standard deviations [252]. Similar remarks apply to a heavy mirror family [253] involving right-handed SU(2) doublets and left-handed singlets. In contrast, new doublets that receive most of their mass from a different source than the Higgs vacuum expectation value, such as vector-like fermion doublets or scalar doublets in Supersymmetry, give small or no contribution to  $S$ ,  $T$ ,  $U$  and the Higgs production cross section and thus are still allowed. Partial or complete vector-like fermion families are predicted in many grand unified theories [254].

There is no simple parametrization to describe the effects of every type of new physics on every possible observable. The  $S$ ,  $T$ , and  $U$  formalism describes many types of heavy physics which affect only the gauge self-energies, and it can be applied to all precision observables. However, new physics which couples directly to ordinary fermions, such as heavy  $Z'$  bosons [233], mixing with exotic fermions [255], or leptoquark exchange [170,256] cannot be fully parametrized in the  $S$ ,  $T$ , and  $U$  framework. It is convenient to treat these types of new physics by parameterizations that are specialized to that particular class of theories (*e.g.*, extra  $Z'$  bosons), or to consider specific models (which might contain, *e.g.*,  $Z'$  bosons and exotic fermions with correlated parameters). Fits to Supersymmetric models are described in Ref. 249. Models involving strong dynamics (such as (extended) Technicolor) for EW breaking are considered in Ref. 257. The effects of compactified extra spatial dimensions at the TeV scale are reviewed in Ref. 258, and constraints on Little Higgs models in Ref. 259. The implications of non-standard Higgs sectors, *e.g.*, involving Higgs singlets or triplets, are discussed in Ref. 260, while additional Higgs doublets are considered in Refs. 234 and 261. Limits on new four-Fermi operators and on leptoquarks using LEP 2 and lower energy data are given in Refs. 170 and 262. Constraints on various types of new physics are reviewed in Refs. [7,75,113,138,153,263,264], and implications for the LHC in Ref. 265.

An alternate formalism [266] defines parameters,  $\epsilon_1$ ,  $\epsilon_2$ ,  $\epsilon_3$ , and  $\epsilon_b$  in terms of the specific observables  $M_W/M_Z$ ,  $\Gamma_{\ell\ell}$ ,  $A_{FB}^{(0,\ell)}$ , and  $R_b$ . The definitions coincide with those for  $\hat{\epsilon}_i$  in Eqs. (10.64) and (10.65) for physics which affects gauge self-energies only, but the  $\epsilon$ 's now parametrize arbitrary types of new physics. However, the  $\epsilon$ 's are not related to other observables unless additional model-dependent assumptions are made. Another approach [267] parametrizes new physics in terms of gauge-invariant sets of operators. It is especially powerful in studying the effects of new physics on non-Abelian gauge vertices. The most general approach introduces deviation vectors [263]. Each type of new physics defines a deviation vector, the components of which are the deviations of each observable from its SM prediction, normalized to the experimental uncertainty. The length (direction) of the vector represents the strength (type) of new physics.

**Table 10.9:** 95% CL lower mass limits (in GeV) on various extra  $Z'$  gauge bosons, appearing in models of unification. More general parametrizations are described in Refs. 268 and 271. The EW results [272] from low energy and  $W$  and  $Z$  boson data are for Higgs sectors consisting of doublets and singlets only ( $\rho_0 = 1$ ) with unspecified  $U(1)'$  charges. The next two columns show the limits from ATLAS [273] and CMS [274] from the combination of both lepton channels. The CDF [275] and DØ [276] bounds from searches in  $\bar{p}p \rightarrow \mu^+\mu^-$  and  $e^+e^-$ , respectively, are listed in the next two columns, followed by the LEP 2  $e^+e^- \rightarrow f\bar{f}$  bounds [170] (assuming  $\theta = 0$ ). The hadron collider bounds would be moderately weakened if there are open exotic decay channels [277]. The last column shows the  $1\sigma$  ranges for  $M_H$  when it is left unconstrained in the EW fits.

$Z'$	EW	ATLAS	CMS	CDF	DØ	LEP 2	$M_H$
$Z_\chi$	1,141	2,540	–	930	903	785	$171_{-89}^{+493}$
$Z_\psi$	147	2,380	2,600	917	891	500	$97_{-25}^{+31}$
$Z_\eta$	427	2,440	–	938	923	500	$423_{-350}^{+577}$
$Z_{LR}$	998	–	–	–	–	825	$804_{-35}^{+174}$
$Z_S$	1,257	2,470	–	858	822	–	$149_{-68}^{+353}$
$Z_{SM}$	1,403	2,860	2,960	1,071	1,023	1,760	$331_{-246}^{+669}$

One well explored type of physics beyond the SM are extra  $Z'$  bosons [268]. They do not spoil the observed approximate gauge coupling unification, and appear in many Grand Unified Theories (GUTs), models with extra dimensions [258], as well as in dynamical symmetry breaking [257] and Little Higgs models [259]. For example, the SO(10) GUT contains an extra U(1) as can be seen from its maximal subgroup,  $SU(5) \times U(1)_\chi$ . Similarly, the  $E_6$  GUT contains the subgroup  $SO(10) \times U(1)_\psi$ . The  $Z_\psi$  possesses only axial-vector couplings to the ordinary fermions, and its mass is generally less constrained. The  $Z_\eta$  boson is the linear combination  $\sqrt{3/8}Z_\chi - \sqrt{5/8}Z_\psi$ . The  $Z_{LR}$  boson occurs in left-right models with gauge group  $SU(3)_C \times SU(2)_L \times SU(2)_R \times U(1)_{B-L} \subset SO(10)$ , and the secluded  $Z_S$  emerges in a supersymmetric bottom-up scenario [269]. The sequential  $Z_{SM}$  boson is defined to have the same couplings to fermions as the SM  $Z$  boson. Such a boson is not expected in the context of gauge theories unless it has different couplings to exotic fermions than the ordinary  $Z$  boson. However, it serves as a useful reference case when comparing constraints from various sources. The physical  $Z'$  boson is in general a superposition of the SM  $Z$  and the new boson associated with the extra U(1). The mixing angle  $\theta$  satisfies,

$$\tan^2 \theta = \frac{M_{Z_1}^2 - M_Z^2}{M_{Z'}^2 - M_{Z_1}^2},$$

where  $M_{Z_1}^2$  is the SM value for  $M_Z$  in the absence of mixing. Note that  $M_Z < M_{Z_1}$ , and that the SM  $Z$  couplings are changed by the mixing. The couplings of the heavier  $Z'$

may also be modified by kinetic mixing [268,270]. If the Higgs  $U(1)'$  quantum numbers are known, there will be an extra constraint,

$$\theta = C \frac{g_2}{g_1} \frac{M_Z^2}{M_{Z'}^2},$$

where  $g_{1,2}$  are the  $U(1)$  and  $U(1)'$  gauge couplings with  $g_2 = \sqrt{\frac{5}{3}} \sin \theta_W \sqrt{\lambda} g_1$  and  $g_1 = \sqrt{g^2 + g'^2}$ . We assume that  $\lambda \sim 1$ , which happens if the GUT group breaks directly to  $SU(3) \times SU(2) \times U(1) \times U(1)'$ .  $C$  is a function of vacuum expectation values. For minimal Higgs sectors it can be found in Ref. 233. Table 10.9 shows the 95% CL lower mass limits [272] for  $\rho_0 = 1$  and  $114.4 \text{ GeV} \leq M_H \leq 1 \text{ TeV}$ . The last column shows the  $1 \sigma$  ranges for  $M_H$  when it is left unconstrained. In cases of specific minimal Higgs sectors where  $C$  is known, the  $Z'$  mass limits from the EW precision data are generally pushed into the TeV region. The limits on  $|\theta|$  are typically smaller than a few  $\times 10^{-3}$ . The mass bounds from direct searches at the LHC [273,274], however, exceed the EW precision constraints by a factor two or more for the models considered here. While the latter can be slightly improved by fixing  $M_H$  to the value measured at LHC, this general conclusion will not change. Also listed in Table 10.9 are the direct lower limits on  $Z'$  production from the Tevatron [275,276], as well as the LEP 2 bounds [170]. For more details see [268,272,278,279] and the note on “The  $Z'$  Searches” in the Gauge & Higgs Boson Particle Listings.

### Acknowledgments:

We are indebted to M. Davier, B. Malaescu, and K. Maltman for providing us with additional information about their work in a form suitable to be included in our fits. We also thank R. H. Bernstein, K. S. McFarland, H. Schellman, and G. P. Zeller for discussions on the NuTeV analysis, and M. Spira for details about HDECAY. J.E. was supported by PAPIIT (DGAPA–UNAM) project IN106913 and CONACyT (México) project 151234, and gratefully acknowledges the hospitality and support by the Mainz Institute for Theoretical Physics (MITP) where part of this work was completed. A.F. is supported in part by the National Science Foundation under grant no. PHY-1212635.

### References:

1. S. L. Glashow, Nucl. Phys. **22**, 579 (1961);  
S. Weinberg, Phys. Rev. Lett. **19**, 1264 (1967);  
A. Salam, p. 367 of *Elementary Particle Theory*, ed. N. Svartholm (Almqvist and Wiksells, Stockholm, 1969);  
S.L. Glashow, J. Iliopoulos, and L. Maiani, Phys. Rev. **D2**, 1285 (1970).
2. CKMfitter Group: J. Charles *et al.*, Eur. Phys. J. **C41**, 1 (2005); updated results and plots are available at <http://ckmfitter.in2p3.fr>.
3. For reviews, see the Section on “Higgs Bosons: Theory and Searches” in this *Review*;  
J. Gunion *et al.*, *The Higgs Hunter’s Guide*, (Addison-Wesley, Redwood City, 1990);

- M. Carena and H.E. Haber, Prog. in Part. Nucl. Phys. **50**, 63 (2003);  
A. Djouadi, Phys. Reports **457**, 1 (2008).
4. For reviews, see E.D. Commins and P.H. Bucksbaum, *Weak Interactions of Leptons and Quarks*, (Cambridge Univ. Press, 1983);  
G. Barbiellini and C. Santoni, Riv. Nuovo Cimento **9(2)**, 1 (1986);  
N. Severijns, M. Beck, and O. Naviliat-Cuncic, Rev. Mod. Phys. **78**, 991 (2006);  
W. Fetscher and H.J. Gerber, p. 657 of Ref. 5;  
J. Deutsch and P. Quin, p. 706 of Ref. 5;  
P. Herczeg, p. 786 of Ref. 5;  
P. Herczeg, Prog. in Part. Nucl. Phys. **46**, 413 (2001).
  5. *Precision Tests of the Standard Electroweak Model*, ed. P. Langacker (World Scientific, Singapore, 1995).
  6. J. Erler and M.J. Ramsey-Musolf, Prog. in Part. Nucl. Phys. **54**, 351 (2005).
  7. P. Langacker, *The Standard Model and Beyond*, (CRC Press, New York, 2009).
  8. T. Kinoshita, *Quantum Electrodynamics*, (World Scientific, Singapore, 1990).
  9. S. G. Karshenboim, Phys. Reports **422**, 1 (2005).
  10. P.J. Mohr, B.N. Taylor, and D.B. Newell, Rev. Mod. Phys. **80**, 633 (2008); for updates see <http://physics.nist.gov/cuu/Constants/>.
  11. ALEPH, DELPHI, L3, OPAL, SLD, LEP Electroweak Working Group, SLD Electroweak and Heavy Flavour Groups: S. Schael *et al.*, Phys. Reports **427**, 257 (2006); for updates see <http://lepewwg.web.cern.ch/LEPEWWG/>.
  12. MuLan: D. M. Webber *et al.*, Phys. Rev. Lett. **106**, 041803 (2011).
  13. T. Kinoshita and A. Sirlin, Phys. Rev. **113**, 1652 (1959).
  14. T. van Ritbergen and R.G. Stuart, Nucl. Phys. **B564**, 343 (2000);  
M. Steinhauser and T. Seidensticker, Phys. Lett. **B467**, 271 (1999).
  15. Y. Nir, Phys. Lett. **B221**, 184 (1989).
  16. A. Pak and A. Czarnecki, Phys. Rev. Lett. **100**, 241807 (2008).
  17. For a review, see S. Mele, [arXiv:hep-ex/0610037](https://arxiv.org/abs/hep-ex/0610037).
  18. S. Fanchiotti, B. Kniehl, and A. Sirlin, Phys. Rev. **D48**, 307 (1993) and references therein.
  19. J. Erler, Phys. Rev. **D59**, 054008 (1999).
  20. M. Davier *et al.*, Eur. Phys. J. **C71**, 1515 (2011);  
the quoted value uses additional information thankfully provided to us by the authors in a private communication.
  21. J. Erler, [hep-ph/0005084](https://arxiv.org/abs/hep-ph/0005084).
  22. P. A. Baikov *et al.*, JHEP **1207**, 017 (2012).
  23. M. Steinhauser, Phys. Lett. **B429**, 158 (1998).
  24. B.V. Geshkenbein and V.L. Morgunov, Phys. Lett. **B352**, 456 (1995).
  25. M.L. Swartz, Phys. Rev. **D53**, 5268 (1996).
  26. N.V. Krasnikov and R. Rodenber, Nuovo Cimento **111A**, 217 (1998).
  27. J.H. Kühn and M. Steinhauser, Phys. Lett. **B437**, 425 (1998).
  28. S. Groote *et al.*, Phys. Lett. **B440**, 375 (1998).
  29. A.D. Martin, J. Outhwaite, and M.G. Ryskin, Phys. Lett. **B492**, 69 (2000).
  30. J.F. de Troconiz and F.J. Yndurain, Phys. Rev. **D65**, 093002 (2002).

31. F. Jegerlehner, Nucl. Phys. Proc. Suppl. **181**, 135 (2008).
32. H. Burkhardt and B. Pietrzyk, Phys. Rev. **D84**, 037502 (2011).
33. K. Hagiwara *et al.*, J. Phys. **G38**, 085003 (2011).
34. OPAL: K. Ackerstaff *et al.*, Eur. Phys. J. **C7**, 571 (1999).
35. CLEO: S. Anderson *et al.*, Phys. Rev. **D61**, 112002 (2000).
36. ALEPH: S. Schael *et al.*, Phys. Reports **421**, 191 (2005).
37. Belle: M. Fujikawa *et al.*: Phys. Rev. **D78**, 072006 (2008).
38. CMD-2: R.R. Akhmetshin *et al.*, Phys. Lett. **B578**, 285 (2004);  
CMD-2: V.M. Aulchenko *et al.*, JETP Lett. **82**, 743 (2005);  
CMD-2: R.R. Akhmetshin *et al.*, JETP Lett. **84**, 413 (2006);  
CMD-2: R.R. Akhmetshin *et al.*, Phys. Lett. **B648**, 28 (2007).
39. SND: M.N. Achasov *et al.*, Sov. Phys. JETP **103**, 380 (2006).
40. A.B. Arbuzov *et al.*, JHEP **9812**, 009 (1998);  
S. Binner, J.H. Kühn, and K. Melnikov, Phys. Lett. **B459**, 279 (1999).
41. BaBar: B. Aubert *et al.*, Phys. Rev. **D70**, 072004 (2004);  
BaBar: B. Aubert *et al.*, Phys. Rev. **D71**, 052001 (2005);  
BaBar: B. Aubert *et al.*, Phys. Rev. **D73**, 052003 (2006);  
BaBar: B. Aubert *et al.*, Phys. Rev. **D76**, 092005 (2007);  
BaBar: B. Aubert *et al.*, Phys. Rev. Lett. **103**, 231801 (2009).
42. KLOE: F. Ambrosino *et al.*, Phys. Lett. **B670**, 285 (2009);  
KLOE: F. Ambrosino *et al.*, Phys. Lett. **B700**, 102 (2011).
43. See *e.g.*, CMD and OLYA: L.M. Barkov *et al.*, Nucl. Phys. **B256**, 365 (1985).
44. V.A. Novikov *et al.*, Phys. Reports **41**, 1 (1978).
45. J. Erler and M. Luo, Phys. Lett. **B558**, 125 (2003).
46. K. G. Chetyrkin *et al.*, Theor. Math. Phys. **170**, 217 (2012).
47. B. Dehnadi *et al.*, JHEP **1309**, 103 (2013).
48. Tevatron Electroweak Working Group, CDF and DØ: arXiv:1305.3929 [hep-ex].
49. ATLAS and CMS: [cds.cern.ch/record/1601811/files/ATLAS-CONF-2013-102.pdf](https://cds.cern.ch/record/1601811/files/ATLAS-CONF-2013-102.pdf).
50. M. Beneke, Phys. Reports **317**, 1 (1999).
51. K. G. Chetyrkin and M. Steinhauser, Nucl. Phys. **B573**, 617 (2000);  
K. Melnikov and T. van Ritbergen, Phys. Lett. **B482**, 99 (2000).
52. A. Sirlin, Phys. Rev. **D22**, 971 (1980);  
D.C. Kennedy *et al.*, Nucl. Phys. **B321**, 83 (1989);  
D.Yu. Bardin *et al.*, Z. Phys. **C44**, 493 (1989);  
W. Hollik, Fortsch. Phys. **38**, 165 (1990);  
for reviews, see W. Hollik, pp. 37 and 117, and W. Marciano, p. 170 of Ref. 5.
53. W.J. Marciano and J.L. Rosner, Phys. Rev. Lett. **65**, 2963 (1990).
54. G. Degrossi, S. Fanchiotti, and A. Sirlin, Nucl. Phys. **B351**, 49 (1991).
55. K.S. Kumar *et al.*, Ann. Rev. Nucl. and Part. Sci. **63**, 237 (2013).
56. G. Degrossi and A. Sirlin, Nucl. Phys. **B352**, 342 (1991).
57. P. Gambino and A. Sirlin, Phys. Rev. **D49**, 1160 (1994).
58. ZFITTER: A.B. Arbuzov *et al.*, Comput. Phys. Commun. **174**, 728 (2006) and references therein.

59. R. Barbieri *et al.*, Nucl. Phys. **B409**, 105 (1993);  
J. Fleischer, O.V. Tarasov, and F. Jegerlehner, Phys. Lett. **B319**, 249 (1993).
60. G. Degrassi, P. Gambino, and A. Vicini, Phys. Lett. **B383**, 219 (1996);  
G. Degrassi, P. Gambino, and A. Sirlin, Phys. Lett. **B394**, 188 (1997).
61. A. Freitas *et al.*, Phys. Lett. **B495**, 338 (2000) and *ibid.* **570**, 260(E) (2003);  
M. Awramik and M. Czakon, Phys. Lett. **B568**, 48 (2003).
62. A. Freitas *et al.*, Nucl. Phys. **B632**, 189 (2002) and *ibid.* **666**, 305(E) (2003);  
M. Awramik and M. Czakon, Phys. Rev. Lett. **89**, 241801 (2002);  
A. Onishchenko and O. Veretin, Phys. Lett. **B551**, 111 (2003).
63. M. Awramik *et al.*, Phys. Rev. Lett. **93**, 201805 (2004);  
W. Hollik, U. Meier, and S. Uccirati, Nucl. Phys. **B731**, 213 (2005).
64. M. Awramik, M. Czakon, and A. Freitas, Phys. Lett. **B642**, 563 (2006);  
W. Hollik, U. Meier, and S. Uccirati, Nucl. Phys. **B765**, 154 (2007).
65. A. Djouadi and C. Verzegnassi, Phys. Lett. **B195**, 265 (1987);  
A. Djouadi, Nuovo Cimento **100A**, 357 (1988).
66. K.G. Chetyrkin, J.H. Kühn, and M. Steinhauser, Phys. Lett. **B351**, 331 (1995).
67. Y. Schröder and M. Steinhauser, Phys. Lett. **B622**, 124 (2005);  
K.G. Chetyrkin *et al.*, Phys. Rev. Lett. **97**, 102003 (2006);  
R. Boughezal and M. Czakon, Nucl. Phys. **B755**, 221 (2006);  
L. Avdeev *et al.*, Phys. Lett. **B336**, 560 (1994) and *ibid.* **B349**, 597(E) (1995).
68. B.A. Kniehl, J.H. Kühn, and R.G. Stuart, Phys. Lett. **B214**, 621 (1988);  
B.A. Kniehl, Nucl. Phys. **B347**, 86 (1990);  
F. Halzen and B.A. Kniehl, Nucl. Phys. **B353**, 567 (1991);  
A. Djouadi and P. Gambino, Phys. Rev. **D49**, 3499 (1994) and *ibid.* **53**, 4111(E) (1996).
69. A. Anselm, N. Dombey, and E. Leader, Phys. Lett. **B312**, 232 (1993).
70. K.G. Chetyrkin, J.H. Kühn, and M. Steinhauser, Phys. Rev. Lett. **75**, 3394 (1995).
71. J.J. van der Bij *et al.*, Phys. Lett. **B498**, 156 (2001);  
M. Faisst *et al.*, Nucl. Phys. **B665**, 649 (2003).
72. R. Boughezal, J.B. Tausk, and J.J. van der Bij, Nucl. Phys. **B725**, 3 (2005).
73. M. Awramik *et al.*, Phys. Rev. **D69**, 053006 (2004).
74. M. Awramik, M. Czakon, and A. Freitas, JHEP **0611**, 048 (2006).
75. M. Baak *et al.*, Eur. Phys. J. **C72**, 2003 (2012).
76. J. Erler and S. Su, Prog. in Part. Nucl. Phys. **71**, 119 (2013).
77. J.M. Conrad, M.H. Shaevitz, and T. Bolton, Rev. Mod. Phys. **70**, 1341 (1998).
78. Z. Berezhiani and A. Rossi, Phys. Lett. **B535**, 207 (2002);  
S. Davidson *et al.*, JHEP **0303**, 011 (2003);  
A. Friedland, C. Lunardini and C. Pena-Garay, Phys. Lett. **B594**, 347 (2004).
79. J. Panman, p. 504 of Ref. 5.
80. CHARM: J. Dorenbosch *et al.*, Z. Phys. **C41**, 567 (1989).
81. CALO: L.A. Ahrens *et al.*, Phys. Rev. **D41**, 3297 (1990).
82. CHARM II: P. Vilain *et al.*, Phys. Lett. **B335**, 246 (1994).
83. ILM: R.C. Allen *et al.*, Phys. Rev. **D47**, 11 (1993);  
LSND: L.B. Auerbach *et al.*, Phys. Rev. **D63**, 112001 (2001).

84. TEXONO: M. Deniz *et al.*, Phys. Rev. **D81**, 072001 (2010).
85. For reviews, see G.L. Fogli and D. Haidt, Z. Phys. **C40**, 379 (1988); F. Perrier, p. 385 of Ref. 5.
86. CDHS: A. Blondel *et al.*, Z. Phys. **C45**, 361 (1990).
87. CHARM: J.V. Allaby *et al.*, Z. Phys. **C36**, 611 (1987).
88. CCFR: K.S. McFarland *et al.*, Eur. Phys. J. **C1**, 509 (1998).
89. R.M. Barnett, Phys. Rev. **D14**, 70 (1976);  
H. Georgi and H.D. Politzer, Phys. Rev. **D14**, 1829 (1976).
90. LAB-E: S.A. Rabinowitz *et al.*, Phys. Rev. Lett. **70**, 134 (1993).
91. E.A. Paschos and L. Wolfenstein, Phys. Rev. **D7**, 91 (1973).
92. NuTeV: G.P. Zeller *et al.*, Phys. Rev. Lett. **88**, 091802 (2002).
93. D. Mason *et al.*, Phys. Rev. Lett. **99**, 192001 (2007).
94. S. Kretzer, D. Mason, and F. Olness, Phys. Rev. **D65**, 074010 (2002).
95. J. Pumplin *et al.*, JHEP **0207**, 012 (2002);  
S. Kretzer *et al.*, Phys. Rev. Lett. **93**, 041802 (2004).
96. S. Alekhin, S.A. Kulagin, and R. Petti, Phys. Lett. **B675**, 433 (2009).
97. W. Bentz *et al.*, Phys. Lett. **B693**, 462 (2010).
98. E. Sather, Phys. Lett. **B274**, 433 (1992);  
E.N. Rodionov, A.W. Thomas, and J.T. Londergan, Mod. Phys. Lett. **A9**, 1799 (1994).
99. A.D. Martin *et al.*, Eur. Phys. J. **C35**, 325 (2004).
100. J.T. Londergan and A.W. Thomas, Phys. Rev. **D67**, 111901 (2003).
101. M. Glück, P. Jimenez-Delgado, and E. Reya, Phys. Rev. Lett. **95**, 022002 (2005).
102. S. Kumano, Phys. Rev. **D66**, 111301 (2002);  
S.A. Kulagin, Phys. Rev. **D67**, 091301 (2003);  
S.J. Brodsky, I. Schmidt, and J.J. Yang, Phys. Rev. **D70**, 116003 (2004);  
M. Hirai, S. Kumano, and T. H. Nagai, Phys. Rev. **D71**, 113007 (2005);  
G.A. Miller and A.W. Thomas, Int. J. Mod. Phys. A **20**, 95 (2005).
103. I.C. Cloet, W. Bentz, and A.W. Thomas, Phys. Rev. Lett. **102**, 252301 (2009).
104. K.P.O. Diener, S. Dittmaier, and W. Hollik, Phys. Rev. **D69**, 073005 (2004);  
A.B. Arbuzov, D.Y. Bardin, and L.V. Kalinovskaya, JHEP **0506**, 078 (2005);  
K. Park, U. Baur, and D. Wackerath, [arXiv:0910.5013](https://arxiv.org/abs/0910.5013) [hep-ph].
105. K.P.O. Diener, S. Dittmaier, and W. Hollik, Phys. Rev. **D72**, 093002 (2005).
106. B.A. Dobrescu and R.K. Ellis, Phys. Rev. **D69**, 114014 (2004).
107. For a review, see S. Davidson *et al.*, JHEP **0202**, 037 (2002).
108. SSF: C.Y. Prescott *et al.*, Phys. Lett. **B84**, 524 (1979).
109. JLab Hall A: X. Zheng *et al.*, to be published.
110. E.J. Beise, M.L. Pitt, and D.T. Spayde, Prog. in Part. Nucl. Phys. **54**, 289 (2005).
111. S.L. Zhu *et al.*, Phys. Rev. **D62**, 033008 (2000).
112. P. Souder, p. 599 of Ref. 5.
113. P. Langacker, p. 883 of Ref. 5.
114. R.D. Young *et al.*, Phys. Rev. Lett. **99**, 122003 (2007).
115. D.S. Armstrong and R.D. McKeown, Ann. Rev. Nucl. and Part. Sci. **62**, 337 (2012).
116. E. Derman and W.J. Marciano, Annals Phys. **121**, 147 (1979).



117. E158: P.L. Anthony *et al.*, Phys. Rev. Lett. **95**, 081601 (2005).
118. J. Erler and M.J. Ramsey-Musolf, Phys. Rev. **D72**, 073003 (2005).
119. A. Czarnecki and W.J. Marciano, Int. J. Mod. Phys. A **15**, 2365 (2000).
120. K.S. McFarland, in the *Proceedings of DIS* 2008.
121. C. Bouchiat and C.A. Piketty, Phys. Lett. **B128**, 73 (1983).
122. Qweak: M.T. Gericke *et al.*, AIP Conf. Proc. **1149**, 237 (2009).
123. Qweak: D. Androic *et al.*, Phys. Rev. Lett. **111**, 141803 (2013); the implications are discussed in Ref. 138.
124. For reviews and references to earlier work, see M.A. Bouchiat and L. Pottier, Science **234**, 1203 (1986); B.P. Masterson and C.E. Wieman, p. 545 of Ref. 5.
125. Cesium (Boulder): C.S. Wood *et al.*, Science **275**, 1759 (1997).
126. Cesium (Paris): J. Guéna, M. Lintz, and M.A. Bouchiat, Phys. Rev. **A71**, 042108 (2005).
127. Thallium (Oxford): N.H. Edwards *et al.*, Phys. Rev. Lett. **74**, 2654 (1995); Thallium (Seattle): P.A. Vetter *et al.*, Phys. Rev. Lett. **74**, 2658 (1995).
128. Lead (Seattle): D.M. Meekhof *et al.*, Phys. Rev. Lett. **71**, 3442 (1993).
129. Bismuth (Oxford): M.J.D. MacPherson *et al.*, Phys. Rev. Lett. **67**, 2784 (1991).
130. P.G. Blunden, W. Melnitchouk and A.W. Thomas, Phys. Rev. Lett. **109**, 262301 (2012).
131. V.A. Dzuba, V.V. Flambaum, and O.P. Sushkov, Phys. Lett. **141A**, 147 (1989); S.A. Blundell, J. Sapirstein, and W.R. Johnson, Phys. Rev. **D45**, 1602 (1992); For reviews, see S.A. Blundell, W.R. Johnson, and J. Sapirstein, p. 577 of Ref. 5; J.S.M. Ginges and V.V. Flambaum, Phys. Reports **397**, 63 (2004); J. Guéna, M. Lintz, and M. A. Bouchiat, Mod. Phys. Lett. **A20**, 375 (2005); A. Derevianko and S.G. Porsev, Eur. Phys. J. A **32**, 517 (2007).
132. V.A. Dzuba, V.V. Flambaum, and O.P. Sushkov, Phys. Rev. **A56**, R4357 (1997).
133. S.C. Bennett and C.E. Wieman, Phys. Rev. Lett. **82**, 2484 (1999).
134. M.A. Bouchiat and J. Guéna, J. Phys. (France) **49**, 2037 (1988).
135. S. G. Porsev, K. Beloy, and A. Derevianko, Phys. Rev. Lett. **102**, 181601 (2009).
136. V.A. Dzuba *et al.*, Phys. Rev. Lett. **109**, 203003 (2012).
137. A. Derevianko, Phys. Rev. Lett. **85**, 1618 (2000); V.A. Dzuba, C. Harabati, and W.R. Johnson, Phys. Rev. **A63**, 044103 (2001); M.G. Kozlov, S.G. Porsev, and I.I. Tupitsyn, Phys. Rev. Lett. **86**, 3260 (2001); W.R. Johnson, I. Bednyakov, and G. Soff, Phys. Rev. Lett. **87**, 233001 (2001); A.I. Milstein and O.P. Sushkov, Phys. Rev. **A66**, 022108 (2002); V.A. Dzuba, V.V. Flambaum, and J.S. Ginges, Phys. Rev. **D66**, 076013 (2002); M.Y. Kuchiev and V.V. Flambaum, Phys. Rev. Lett. **89**, 283002 (2002); A.I. Milstein, O.P. Sushkov, and I.S. Terekhov, Phys. Rev. Lett. **89**, 283003 (2002); V.V. Flambaum and J.S.M. Ginges, Phys. Rev. **A72**, 052115 (2005).
138. J. Erler, A. Kurylov, and M.J. Ramsey-Musolf, Phys. Rev. **D68**, 016006 (2003).
139. V.A. Dzuba *et al.*, J. Phys. **B20**, 3297 (1987).

140. Ya.B. Zel'dovich, Sov. Phys. JETP **6**, 1184 (1958);  
V.V. Flambaum and D.W. Murray, Phys. Rev. **C56**, 1641 (1997);  
W.C. Haxton and C.E. Wieman, Ann. Rev. Nucl. Part. Sci. **51**, 261 (2001).
141. J.L. Rosner, Phys. Rev. **D53**, 2724 (1996).
142. S.J. Pollock, E.N. Fortson, and L. Willets, Phys. Rev. **C46**, 2587 (1992);  
B.Q. Chen and P. Vogel, Phys. Rev. **C48**, 1392 (1993).
143. R.W. Dunford and R.J. Holt, J. Phys. **G34**, 2099 (2007).
144. O.O. Versolato *et al.*, Hyperfine Interact. **199**, 9 (2011).
145. W. Hollik and G. Duckeck, *Electroweak Precision Tests at LEP*, Springer Tracts Mod. Phys. **162**, 1 (2000).
146. D.Yu. Bardin *et al.*, *Electroweak Working Group Report*, hep-ph/9709229.
147. A. Czarnecki and J.H. Kühn, Phys. Rev. Lett. **77**, 3955 (1996);  
R. Harlander, T. Seidensticker, and M. Steinhauser, Phys. Lett. **B426**, 125 (1998);  
J. Fleischer *et al.*, Phys. Lett. **B459**, 625 (1999).
148. M. Awramik *et al.*, Nucl. Phys. **B813**, 174 (2009).
149. B.W. Lynn and R.G. Stuart, Nucl. Phys. **B253**, 216 (1985).
150. *Physics at LEP*, ed. J. Ellis and R. Peccei, CERN 86-02, Vol. 1.
151. PETRA: S.L. Wu, Phys. Reports **107**, 59 (1984);  
C. Kiesling, *Tests of the Standard Theory of Electroweak Interactions*, (Springer-Verlag, New York, 1988);  
R. Marshall, Z. Phys. **C43**, 607 (1989);  
Y. Mori *et al.*, Phys. Lett. **B218**, 499 (1989);  
D. Haidt, p. 203 of Ref. 5.
152. For reviews, see D. Schaile, p. 215, and A. Blondel, p. 277 of Ref. 5; P. Langacker [7];  
and S. Riemann [153].
153. S. Riemann, Rept. on Prog. in Phys. **73**, 126201 (2010).
154. SLD: K. Abe *et al.*, Phys. Rev. Lett. **84**, 5945 (2000).
155. SLD: K. Abe *et al.*, Phys. Rev. Lett. **85**, 5059 (2000).
156. SLD: K. Abe *et al.*, Phys. Rev. Lett. **86**, 1162 (2001).
157. SLD: K. Abe *et al.*, Phys. Rev. Lett. **78**, 17 (1997).
158. P.A. Grassi, B.A. Kniehl, and A. Sirlin, Phys. Rev. Lett. **86**, 389 (2001).
159. G. Degrassi and P. Gambino, Nucl. Phys. **B567**, 3 (2000).
160. J. Fleischer *et al.*, Phys. Lett. **B293**, 437 (1992);  
K.G. Chetyrkin, A. Kwiatkowski, and M. Steinhauser, Mod. Phys. Lett. **A8**, 2785 (1993).
161. A. Freitas and Y.-C. Huang, JHEP **1208**, 050 (2012) and *ibid.* **1310**, 044(E) (2013).
162. A. Freitas, Phys. Lett. **B730**, 50 (2014);  
A. Freitas, arXiv:1401.2447 [hep-ph].
163. DØ: V.M. Abazov *et al.*, Phys. Rev. **D84**, 012007 (2011).
164. CDF: T. Aaltonen *et al.*, Phys. Rev. **D88**, 072002 (2013).
165. CDF: [www-cdf.fnal.gov/physics/ewk/2013/zAfb9mm/](http://www-cdf.fnal.gov/physics/ewk/2013/zAfb9mm/).
166. CDF: D. Acosta *et al.*, Phys. Rev. **D71**, 052002 (2005).

167. H1: A. Aktas *et al.*, Phys. Lett. **B632**, 35 (2006);  
H1 and ZEUS: Z. Zhang, Nucl. Phys. Proc. Suppl. **191**, 271 (2009).
168. CMS: S. Chatrchyan *et al.*, Phys. Rev. **D84**, 112002 (2011).
169. ATLAS: [cds.cern.ch/record/1544035/files/ATLAS-CONF-2013-043.pdf](https://cds.cern.ch/record/1544035/files/ATLAS-CONF-2013-043.pdf).
170. ALEPH, DELPHI, L3, OPAL, and LEP Electroweak Working Group: S. Schael *et al.*, Phys. Reports **532**, 119 (2013).
171. ALEPH, DELPHI, L3, OPAL, and LEP Electroweak Working Group: J. Alcaraz *et al.*, [hep-ex/0612034](https://arxiv.org/abs/hep-ex/0612034).
172. A. Leike, T. Riemann, and J. Rose, Phys. Lett. **B273**, 513 (1991);  
T. Riemann, Phys. Lett. **B293**, 451 (1992).
173. A comprehensive report and further references can be found in K.G. Chetyrkin, J.H. Kühn, and A. Kwiatkowski, Phys. Reports **277**, 189 (1996).
174. J. Schwinger, *Particles, Sources, and Fields*, Vol. II, (Addison-Wesley, New York, 1973);  
K.G. Chetyrkin, A.L. Kataev, and F.V. Tkachev, Phys. Lett. **B85**, 277 (1979);  
M. Dine and J. Sapirstein, Phys. Rev. Lett. **43**, 668 (1979);  
W. Celmaster and R.J. Gonsalves, Phys. Rev. Lett. **44**, 560 (1980);  
S.G. Gorishnii, A.L. Kataev, and S.A. Larin, Phys. Lett. **B259**, 144 (1991);  
L.R. Surguladze, M.A. Samuel, Phys. Rev. Lett. **66**, 560 (1991) and *ibid.* 2416(E).
175. P.A. Baikov, K.G. Chetyrkin, and J.H. Kühn, Phys. Rev. Lett. **101**, 012002 (2008).
176. B.A. Kniehl and J.H. Kühn, Nucl. Phys. **B329**, 547 (1990);  
K.G. Chetyrkin and A. Kwiatkowski, Phys. Lett. **B319**, 307 (1993);  
S.A. Larin, T. van Ritbergen, and J.A.M. Vermaseren, Phys. Lett. **B320**, 159 (1994);  
K.G. Chetyrkin and O.V. Tarasov, Phys. Lett. **B327**, 114 (1994).
177. A.L. Kataev, Phys. Lett. **B287**, 209 (1992).
178. D. Albert *et al.*, Nucl. Phys. **B166**, 460 (1980);  
F. Jegerlehner, Z. Phys. **C32**, 425 (1986);  
A. Djouadi, J.H. Kühn, and P.M. Zerwas, Z. Phys. **C46**, 411 (1990);  
A. Borrelli *et al.*, Nucl. Phys. **B333**, 357 (1990).
179. A.A. Akhundov, D.Yu. Bardin, and T. Riemann, Nucl. Phys. **B276**, 1 (1986);  
W. Beenakker and W. Hollik, Z. Phys. **C40**, 141 (1988);  
B.W. Lynn and R.G. Stuart, Phys. Lett. **B352**, 676 (1990);  
J. Bernabeu, A. Pich, and A. Santamaria, Phys. Lett. **B200**, 569 (1988) and Nucl. Phys. **B363**, 326 (1991).
180. ATLAS: G. Aad *et al.*, Phys. Lett. **B716**, 1 (2012);  
CMS: S. Chatrchyan *et al.*, Phys. Lett. **B716**, 30 (2012);  
CMS: S. Chatrchyan *et al.*, JHEP **1306**, 081 (2013).
181. ATLAS: G. Aad *et al.*, Phys. Lett. **B726**, 88 (2013).
182. CMS: [cds.cern.ch/record/1542387/files/HIG-13-005-pas.pdf](https://cds.cern.ch/record/1542387/files/HIG-13-005-pas.pdf).
183. CDF and DØ: T. Aaltonen *et al.*, Phys. Rev. **D88**, 052014 (2013).
184. ATLAS: [cds.cern.ch/record/1632191/files/ATLAS-CONF-2013-108.pdf](https://cds.cern.ch/record/1632191/files/ATLAS-CONF-2013-108.pdf);  
CMS: S. Chatrchyan *et al.*, [arXiv:1401.5041](https://arxiv.org/abs/1401.5041).
185. ATLAS: G. Aad *et al.*, Phys. Lett. **B726**, 88 (2013).

186. A. Djouadi, J. Kalinowski, and M. Spira, *Comp. Phys. Comm.* **108**, 56 (1998).
187. H. Davoudiasl, H.-S. Lee, and W.J. Marciano, *Phys. Rev.* **D86**, 095009 (2012).
188. E. Braaten, S. Narison, and A. Pich, *Nucl. Phys.* **B373**, 581 (1992).
189. F. Le Diberder and A. Pich, *Phys. Lett.* **B286**, 147 (1992).
190. M. Beneke and M. Jamin, *JHEP* **0809**, 044 (2008).
191. E. Braaten and C.S. Li, *Phys. Rev.* **D42**, 3888 (1990).
192. J. Erler, *Rev. Mex. Fis.* **50**, 200 (2004).
193. D. Boito *et al.*, *Phys. Rev.* **D85**, 093015 (2012).
194. J. Erler, [arXiv:1102.5520](https://arxiv.org/abs/1102.5520) [hep-ph].
195. M. Davier *et al.*, *Eur. Phys. J.* **C56**, 305 (2008);  
K. Maltman and T. Yavin, *Phys. Rev.* **D78**, 094020 (2008).
196. E821: G.W. Bennett *et al.*, *Phys. Rev. Lett.* **92**, 161802 (2004).
197. T. Aoyama *et al.*, *Phys. Rev. Lett.* **109**, 111808 (2012);  
T. Aoyama *et al.*, *PTEP* **2012**, 01A107 (2012);  
P. Baikov, A. Maier and P. Marquard, *Nucl. Phys.* **B877**, 647 (2013).
198. G. Li, R. Mendel, and M.A. Samuel, *Phys. Rev.* **D47**, 1723 (1993);  
S. Laporta and E. Remiddi, *Phys. Lett.* **B301**, 440 (1993);  
S. Laporta and E. Remiddi, *Phys. Lett.* **B379**, 283 (1996);  
A. Czarnecki and M. Skrzypek, *Phys. Lett.* **B449**, 354 (1999).
199. J. Erler and M. Luo, *Phys. Rev. Lett.* **87**, 071804 (2001).
200. S.J. Brodsky and J.D. Sullivan, *Phys. Rev.* **D156**, 1644 (1967);  
T. Burnett and M.J. Levine, *Phys. Lett.* **B24**, 467 (1967);  
R. Jackiw and S. Weinberg, *Phys. Rev.* **D5**, 2473 (1972);  
I. Bars and M. Yoshimura, *Phys. Rev.* **D6**, 374 (1972);  
K. Fujikawa, B.W. Lee, and A.I. Sanda, *Phys. Rev.* **D6**, 2923 (1972);  
G. Altarelli, N. Cabibbo, and L. Maiani, *Phys. Lett.* **B40**, 415 (1972);  
W.A. Bardeen, R. Gastmans, and B.E. Laurup, *Nucl. Phys.* **B46**, 315 (1972).
201. T.V. Kukhto *et al.*, *Nucl. Phys.* **B371**, 567 (1992);  
S. Peris, M. Perrottet, and E. de Rafael, *Phys. Lett.* **B355**, 523 (1995);  
A. Czarnecki, B. Krause, and W.J. Marciano, *Phys. Rev.* **D52**, 2619 (1995);  
A. Czarnecki, B. Krause, and W.J. Marciano, *Phys. Rev. Lett.* **76**, 3267 (1996).
202. G. Degrassi and G. Giudice, *Phys. Rev.* **D58**, 053007 (1998);  
A. Czarnecki, W.J. Marciano and A. Vainshtein, *Phys. Rev.* **D67**, 073006 (2003)  
and *ibid.*, **D73**, 119901(E) (2006).
203. For reviews, see M. Davier and W.J. Marciano, *Ann. Rev. Nucl. Part. Sci.* **54**, 115 (2004);  
J.P. Miller, E. de Rafael, and B.L. Roberts, *Rept. Prog. Phys.* **70**, 795 (2007);  
F. Jegerlehner and A. Nyffeler, *Phys. Reports* **477**, 1 (2009).
204. V. Cirigliano, G. Ecker, and H. Neufeld, *JHEP* **0208**, 002 (2002);  
K. Maltman and C.E. Wolfe, *Phys. Rev.* **D73**, 013004 (2006);  
M. Davier *et al.*, *Eur. Phys. J.* **C66**, 127 (2010).
205. W.J. Marciano and A. Sirlin, *Phys. Rev. Lett.* **61**, 1815 (1988).
206. S. Ghozzi and F. Jegerlehner, *Phys. Lett.* **B583**, 222 (2004).
207. F. Jegerlehner and R. Szafron, *Eur. Phys. J.* **C71**, 1632 (2011).

208. M. Davier and B. Malaescu, *Eur. Phys. J.* **C73**, 2597 (2013).
209. K. Melnikov and A. Vainshtein, *Phys. Rev.* **D70**, 113006 (2004).
210. J. Erler and G. Toledo Sánchez, *Phys. Rev. Lett.* **97**, 161801 (2006).
211. A. Nyffeler, *Phys. Rev.* **D79**, 073012 (2009).
212. J. Prades, E. de Rafael, and A. Vainshtein, [arXiv:0901.0306 \[hep-ph\]](https://arxiv.org/abs/0901.0306).
213. M. Knecht and A. Nyffeler, *Phys. Rev.* **D65**, 073034 (2002).
214. M. Hayakawa and T. Kinoshita, [hep-ph/0112102](https://arxiv.org/abs/hep-ph/0112102);  
J. Bijnens, E. Pallante, and J. Prades, *Nucl. Phys.* **B626**, 410 (2002);  
A recent discussion is in J. Bijnens and J. Prades, *Mod. Phys. Lett.* **A22**, 767 (2007).
215. T. Blum, M. Hayakawa and T. Izubuchi, *PoS LATTICE 2012*, 022 (2012).
216. B. Krause, *Phys. Lett.* **B390**, 392 (1997).
217. J.L. Lopez, D.V. Nanopoulos, and X. Wang, *Phys. Rev.* **D49**, 366 (1994);  
for recent reviews, see Ref. 203.
218. U. Amaldi *et al.*, *Phys. Rev.* **D36**, 1385 (1987);  
G. Costa *et al.*, *Nucl. Phys.* **B297**, 244 (1988);  
P. Langacker and M. Luo, *Phys. Rev.* **D44**, 817 (1991);  
J. Erler and P. Langacker, *Phys. Rev.* **D52**, 441 (1995).
219. CDF and DØ: T. Aaltonen *et al.*, *Phys. Rev.* **D88**, 052018 (2013).
220. Tevatron Electroweak Working Group, CDF and DØ: [arXiv:1003.2826 \[hep-ex\]](https://arxiv.org/abs/1003.2826).
221. F. James and M. Roos, *Comput. Phys. Commun.* **10**, 343 (1975).
222. For a more recent study, see J. Cao and J.M. Yang, *JHEP* **0812**, 006 (2008).
223. J. Erler, J.L. Feng, and N. Polonsky, *Phys. Rev. Lett.* **78**, 3063 (1997).
224. D. Choudhury, T.M.P. Tait, and C.E.M. Wagner, *Phys. Rev.* **D65**, 053002 (2002).
225. J. Erler and P. Langacker, *Phys. Rev. Lett.* **84**, 212 (2000).
226. P. Langacker and M. Plümacher, *Phys. Rev.* **D62**, 013006 (2000).
227. DELPHI: P. Abreu *et al.*, *Eur. Phys. J.* **C10**, 415 (1999).
228. CMS: S. Chatrchyan *et al.*, *Phys. Lett.* **B728**, 496 (2014).
229. DØ: V.M. Abazov *et al.*, *Phys. Rev.* **D80**, 111107 (2009).
230. ALEPH, DELPHI, L3, OPAL, and the LEP Working Group for Higgs Boson Searches: D. Abbaneo *et al.*, *Phys. Lett.* **B565**, 61 (2003).
231. P. Langacker and N. Polonsky, *Phys. Rev.* **D52**, 3081 (1995);  
J. Bagger, K.T. Matchev, and D. Pierce, *Phys. Lett.* **B348**, 443 (1995).
232. M. Veltman, *Nucl. Phys.* **B123**, 89 (1977);  
M. Chanowitz, M.A. Furman, and I. Hinchliffe, *Phys. Lett.* **B78**, 285 (1978);  
The two-loop correction has been obtained by J.J. van der Bij and F. Hoogeveen,  
*Nucl. Phys.* **B283**, 477 (1987).
233. P. Langacker and M. Luo, *Phys. Rev.* **D45**, 278 (1992) and refs. therein.
234. A. Denner, R.J. Guth, and J.H. Kühn, *Phys. Lett.* **B240**, 438 (1990);  
W. Grimus *et al.*, *J. Phys. G* **35**, 075001 (2008);  
H. E. Haber and D. O’Neil, *Phys. Rev.* **D83**, 055017 (2011).
235. S. Bertolini and A. Sirlin, *Phys. Lett.* **B257**, 179 (1991).

236. M. Peskin and T. Takeuchi, Phys. Rev. Lett. **65**, 964 (1990);  
M. Peskin and T. Takeuchi, Phys. Rev. **D46**, 381 (1992);  
M. Golden and L. Randall, Nucl. Phys. **B361**, 3 (1991).
237. D. Kennedy and P. Langacker, Phys. Rev. **D44**, 1591 (1991).
238. G. Altarelli and R. Barbieri, Phys. Lett. **B253**, 161 (1991).
239. B. Holdom and J. Terning, Phys. Lett. **B247**, 88 (1990).
240. B.W. Lynn, M.E. Peskin, and R.G. Stuart, p. 90 of Ref. 150.
241. An alternative formulation is given by K. Hagiwara *et al.*, Z. Phys. **C64**, 559 (1994), and *ibid.* **68**, 352(E) (1995);  
K. Hagiwara, D. Haidt, and S. Matsumoto, Eur. Phys. J. **C2**, 95 (1998).
242. I. Maksymyk, C.P. Burgess, and D. London, Phys. Rev. **D50**, 529 (1994);  
C.P. Burgess *et al.*, Phys. Lett. **B326**, 276 (1994);  
R. Barbieri, M. Frigeni, and F. Caravaglios, Phys. Lett. **B279**, 169 (1992).
243. R. Barbieri *et al.*, Nucl. Phys. **B703**, 127 (2004).
244. M.S. Carena *et al.*, Nucl. Phys. **B759**, 202 (2006).
245. K. Lane, hep-ph/0202255.
246. E. Gates and J. Terning, Phys. Rev. Lett. **67**, 1840 (1991);  
R. Sundrum and S.D.H. Hsu, Nucl. Phys. **B391**, 127 (1993);  
R. Sundrum, Nucl. Phys. **B395**, 60 (1993);  
M. Luty and R. Sundrum, Phys. Rev. Lett. **70**, 529 (1993);  
T. Appelquist and J. Terning, Phys. Lett. **B315**, 139 (1993);  
D.D. Dietrich, F. Sannino, and K. Tuominen, Phys. Rev. **D72**, 055001 (2005);  
N.D. Christensen and R. Shrock, Phys. Lett. **B632**, 92 (2006);  
M. Harada, M. Kurachi, and K. Yamawaki, Prog. Theor. Phys. **115**, 765 (2006).
247. H. Georgi, Nucl. Phys. **B363**, 301 (1991);  
M.J. Dugan and L. Randall, Phys. Lett. **B264**, 154 (1991).
248. R. Barbieri *et al.*, Nucl. Phys. **B341**, 309 (1990).
249. J. Erler and D.M. Pierce, Nucl. Phys. **B526**, 53 (1998);  
G.C. Cho and K. Hagiwara, Nucl. Phys. **B574**, 623 (2000);  
G. Altarelli *et al.*, JHEP **0106**, 018 (2001);  
S. Heinemeyer, W. Hollik, and G. Weiglein, Phys. Reports **425**, 265 (2006);  
S.P. Martin, K. Tobe, and J.D. Wells, Phys. Rev. **D71**, 073014 (2005);  
G. Marandella, C. Schappacher, and A. Strumia, Nucl. Phys. **B715**, 173 (2005);  
M.J. Ramsey-Musolf and S. Su, Phys. Reports **456**, 1 (2008);  
A. Djouadi, Phys. Reports **459**, 1 (2008);  
S. Heinemeyer *et al.*, JHEP **0804**, 039 (2008);  
O. Buchmueller *et al.*, Eur. Phys. J. **C72**, 2020 (2012).
250. J. Erler and P. Langacker, Phys. Rev. Lett. **105**, 031801 (2010).
251. CMS: S. Chatrchyan *et al.*, Phys. Rev. **D86**, 112003 (2012).
252. O. Eberhardt *et al.*, Phys. Rev. Lett. **109**, 241802 (2012);  
A. Djouadi and A. Lenz, Phys. Lett. **B715**, 310 (2012).
253. J. Maalampi and M. Roos, Phys. Reports **186**, 53 (1990).
254. For reviews, see the Section on “Grand Unified Theories” in this *Review*;  
P. Langacker, Phys. Reports **72**, 185 (1981);

- J.L. Hewett and T.G. Rizzo, Phys. Reports **183**, 193 (1989);  
 J. Kang, P. Langacker and B.D. Nelson, Phys. Rev. **D77**, 035003 (2008);  
 S.P. Martin, Phys. Rev. **D81**, 035004 (2010);  
 P.W. Graham *et al.*, Phys. Rev. **D81**, 055016 (2010).
255. P. Langacker and D. London, Phys. Rev. **D38**, 886 (1988);  
 D. London, p. 951 of Ref. 5;  
 a recent analysis is F. del Aguila, J. de Blas and M. Perez-Victoria, Phys. Rev. **D78**, 013010 (2008).
256. M. Chemtob, Prog. in Part. Nucl. Phys. **54**, 71 (2005);  
 R. Barbier *et al.*, Phys. Reports **420**, 1 (2005).
257. R.S. Chivukula and E.H. Simmons, Phys. Rev. **D66**, 015006 (2002);  
 C.T. Hill and E.H. Simmons, Phys. Reports **381**, 235 (2003);  
 R.S. Chivukula *et al.*, Phys. Rev. **D70**, 075008 (2004).
258. K. Agashe *et al.*, JHEP **0308**, 050 (2003);  
 M. Carena *et al.*, Phys. Rev. **D68**, 035010 (2003);  
 I. Gogoladze and C. Macesanu, Phys. Rev. **D74**, 093012 (2006);  
 I. Antoniadis, hep-th/0102202 see also the note on “Extra Dimensions” in the Searches Particle Listings.
259. T. Han, H.E. Logan, and L.T. Wang, JHEP **0601**, 099 (2006);  
 M. Perelstein, Prog. in Part. Nucl. Phys. **58**, 247 (2007).
260. E. Accomando *et al.*, arXiv:hep-ph/0608079;  
 V. Barger *et al.*, Phys. Rev. **D77**, 035005 (2008);  
 W. Grimus *et al.*, Nucl. Phys. **B801**, 81 (2008);  
 M. Maniatis, Int. J. Mod. Phys. **A25**, 3505 (2010);  
 U. Ellwanger, C. Hugonie, and A.M. Teixeira, Phys. Reports **496**, 1 (2010);  
 M.C. Chen, S. Dawson, and C.B. Jackson, Phys. Rev. **D78**, 093001 (2008).
261. A. Barroso *et al.*, arXiv:1304.5225 [hep-ph];  
 B. Grinstein and P. Uttayarat, JHEP **1306**, 094 (2013) and *ibid.* **1309**, 110(E) (2013);  
 O. Eberhardt, U. Nierste and M. Wiebusch, JHEP **1307**, 118 (2013).
262. G.C. Cho, K. Hagiwara, and S. Matsumoto, Eur. Phys. J. **C5**, 155 (1998);  
 K. Cheung, Phys. Lett. **B517**, 167 (2001);  
 Z. Han and W. Skiba, Phys. Rev. **D71**, 075009 (2005).
263. P. Langacker, M. Luo, and A.K. Mann, Rev. Mod. Phys. **64**, 87 (1992);  
 M. Luo, p. 977 of Ref. 5.
264. F.S. Merritt *et al.*, p. 19 of *Particle Physics: Perspectives and Opportunities: Report of the DPF Committee on Long Term Planning*, ed. R. Peccei *et al.* (World Scientific, Singapore, 1995).
265. D.E. Morrissey, T. Plehn, and T.M.P. Tait, Phys. Reports **515**, 1 (2012).
266. G. Altarelli, R. Barbieri, and S. Jadach, Nucl. Phys. **B369**, 3 (1992) and *ibid.* **B376**, 444(E) (1992).
267. A. De Rújula *et al.*, Nucl. Phys. **B384**, 3 (1992);  
 K. Hagiwara *et al.*, Phys. Rev. **D48**, 2182 (1993);  
 C.P. Burgess *et al.*, Phys. Rev. **D49**, 6115 (1994);

- Z. Han and W. Skiba, Phys. Rev. **D71**, 075009 (2005);  
G. Cacciapaglia *et al.*, Phys. Rev. **D74**, 033011 (2006);  
V. Bernard *et al.*, JHEP **0801**, 015 (2008);  
Z. Han, Int. J. Mod. Phys. A **23**, 2653 (2008).
268. For reviews, see A. Leike, Phys. Reports **317**, 143 (1999);  
P. Langacker, Rev. Mod. Phys. **81**, 1199 (2009).
269. J. Erler, P. Langacker, and T. Li, Phys. Rev. **D66**, 015002 (2002);  
G. Cleaver *et al.*, Phys. Rev. **D59**, 055005 (1999).
270. B. Holdom, Phys. Lett. **B166**, 196 (1986).
271. M. Carena *et al.*, Phys. Rev. **D70**, 093009 (2004).
272. J. Erler, P. Langacker, S. Munir and E. Rojas, JHEP **0908**, 017 (2009).
273. ATLAS: [cds.cern.ch/record/1525524/files/ATLAS-CONF-2013-017.pdf](https://cds.cern.ch/record/1525524/files/ATLAS-CONF-2013-017.pdf).
274. CMS: [cds.cern.ch/record/1519132/files/EXO-12-061-pas.pdf](https://cds.cern.ch/record/1519132/files/EXO-12-061-pas.pdf).
275. CDF: T. Aaltonen *et al.*, Phys. Rev. Lett. **106**, 121801 (2011).
276. DØ: V.M. Abazov *et al.*, Phys. Lett. **B695**, 88 (2011).
277. J. Kang and P. Langacker, Phys. Rev. **D71**, 035014 (2005);  
C.-F. Chang, K. Cheung, and T.-C. Yuan, JHEP **1109**, 058 (2011).
278. F. del Aguila, J. de Blas, and M. Perez-Victoria, JHEP **1009**, 033 (2010).
279. T. Appelquist, B.A. Dobrescu, and A.R. Hopper, Phys. Rev. **D68**, 035012 (2003);  
R.S. Chivukula *et al.*, Phys. Rev. **D69**, 015009 (2004).